Liv Irene Korstad

Energy-efficient High Temperature Heat Pump Systems for a Spray-Dryer

Master's thesis in Mechanical Engineering
Supervisor: Trygve Eikevik
June 2019

Master's thesis

NTNU
Norwegian University of Science and Technology
Faculty of Engineering
Department of Energy and Process Engineering

NTNU
Kunnskap for en bedre verden

Preface

This master thesis was carried out at the Department of Energy and Process Engineering to conclude a five-year master's degree at the Norwegian University of Science and Technology (NTNU). The thesis studies the possibilities of high-temperature heat pumps to increase the energy efficiency of spray-dryers and was written the spring of 2019.

I would like to thank my supervisor Trygve M. Eikevik for the counsel and advise through the semester. Also, a special thanks to my co-supervisor Ignat Tolstorebrov for all the good advice and discussions on the topic, and for helping me structure my thesis. I would also like to thank my friends and family, for the love and support through my five years at NTNU.

Abstract

Industrial processes have a common energy-intensive heat demand, and a focus on heat recovery required for the industry to become more sustainable. High temperature heat pumps are showing good potential to utilize waste heat from industrial processes, and through heat exchange produce heat at higher temperatures by compression work.

The process of spray-drying is chosen for the study, as it is an industrial process utilizing air at temperatures around 200°C with waste heat temperatures between 70-115°C that is not yet utilized.

The theoretical study compares a supercritical heat pump cycle using CO_2 as the working fluid, a transcritical heat pump cycle using iso-butane as the working fluid and a compression-absorption heat pump cycle with an ammonia-water mixture as the working fluid, to study the potential of using a high-temperature heat pump solution to increase the energy efficiency of the spray-drying process. The calculations are done using EES.

The transcritical cycle achieves a maximum COP of 3.16 when the working fluid is overheated to 15K. It manages to utilize the excess air to cover the heat demand of 30% of the air flow with a gas cooler pressure of 18MPa. The constant evaporation temperature limits the transcritical cycle to be optimized in the thermodynamic sense, limiting the gas cooler effectiveness to around 30% for the given specifications.

The supercritical cycle has a higher heating capacity and a lower COP than the transcritical cycle, and the solutions vary more. By allowing a COP of 1.98, the gas heater is optimized at a pressure of 7.5MPa, and the supercritical cycle covers 45% of the air flow heat demand. However, by optimizing the gas cooler at 37MPa, the COP increases to 2.5 but the heat load only covers 35% of the airflow.

Both cycles are challenged by the lack of components found on today's market.

The compression-absorption heat pump cycles found in the literature achieves an average COP of 3 but differs from the transcritical and supercritical heat pump cycles by focusing on heating a larger flow rate of air with a lower temperature lift.

Sammendrag

Industrielle prosesser har en fellesnevner i å kreve store mengder varme, og et fokus på å resirkulere restvarmen dette slipper ut er nødvendig for at næringen skal bli mer bærekraftig. Høytemperatur varmepumper viser et godt potensial for å utnytte en slik restvarmen som varmekilde for å produsere høyere temperaturer ved hjelp av kompressorarbeid.

Spraytørkingsprosessen er valgt som fokusområdet for denne oppgaven, da det er en industriell prosess som krever luft ved temperaturer rundt 200°C og slipper ut en restvarme med en temperatur mellom 70-115°C, som pr dags dato ikke blir utnyttet.

En teoretisk studie er utført for å sammenlikne en superkritisk varmepumpes med CO_2 som arbeidsmedium, en transkritisk varmepumpe som bruker iso-butan og en kompresjons/absorbsjonsvarmepumpe med en blanding av ammoniakk og vann som arbeidsmedium. Målet med studiet er å analysere potensialet ved å bruke de forskjellige varmepumpene til å produsere høy-temperatur varme for å øke energieffektiviteten til en spraytørker. Beregningene er gjort ved bruk av EES.

Den transkritiske modellen oppnår en maksimal COP på 3.16 når arbeidsmediet overvarmes med 15K før kompresjonen. Den dekker 30% av energibehovet til spraytørkeren oppgaven er basert på og har et gass-kjøler trykk på 18MPa. Den konstante fordampningstemperaturen begrenser den transkritiske syklusen for å bli optimalisert i termodynamisk forstand, noe som begrenser gass-kjølerens effektivitet til rundt 30% for de oppgitte spesifikasjonene.

Den superkritiske syklusen har høyere varmekapasitet og lavere COP enn den transkritiske syklusen, og løsningene varierer mer. Ved å tillate en COP på 1,98 blir gassvarmeren optimalisert ved et trykk på 7,5 MPa, og den superkritiske syklusen dekker 45% av luftstrømmenes varmekrav. Ved å istede optimalisere gass kjøleren ved 37MPa, øker COP til 2,5, men varmekapasiteten dekker bare 35% av luftstrømmen.

Begge varmepumpeløsningene har utfordringer i mangel på komponenter som kan takle forholdene.

Den kompresjons/absorbsjonsvarmepumpen er analysert gjennom et litteratursøk, der en gjennomsnittlig COP på 3 er funnet for liknende scenarier. Analyser fra litteraturen skiller seg fra den transkritiske og superkritiske analysen ved å heller fokusere på å varme en større luftstrøm med en mindre temperatur-differanse.

Contents

List of Figures

List of Tables

Nomenclature

Abbreviations

CO_2	Carbon Dioxide
COP	Coefficient of Performance
DOE	Department of Energy
EES	Engineering Equation Solver
GWP	Global Warming Potential
HTHP	High temperature heat pump
IHX	Internal heat exchanger
ODP	Ozone Deception Potential
PHE	Plate Heat Exchanger
PHE	Plate heat exchanger
PR	Pressure ratio
RPM	Revolution per minute
SPP	Suspended Particle Processing

Greek letters

ϵ_i	Effectiveness sub-heat exchanger
η	Heater efficiency
η_t	Thermal efficiency
η_{comp}	Compressor efficiency
η_{IHX}	IHX efficiency
$\eta_{is,turbine}$	Isentropic turbine efficiency
λ_e	Latent heat of evaporation, J/kg
ρ_g	Gas Density, kg/m^3
ρ_v	Volumetric Efficiency
τ_f	Time constant for fouling
f	Recirculation ratio

Latin letters

ΔT_{lift}	Temperature lift, K
$\dot{m}$	Mass Flowrate, kg/s
$\dot{m}_F$	Feed flow rate, kg/s
$\dot{m}_{air}$	Air Flow Rate, kg/s
$\dot{m}_{R600a}$	Mass flow rate iso-butane, kg/s
$\dot{Q}$	Heat Load, W
$\dot{Q}_{air}$	Air heat Load, W
$\dot{Q}_{cond}$	Heating capacity in condenser, W
$\dot{Q}_{GC}$	Heating capacity in Gas Cooler, W
$\dot{V}$	Volumetric flow rate, m^3/s
$\dot{W}$	Work, W
$\dot{W}_t$	Turbine work, W
$\dot{W}_{comp}$	Compressor work, W
$\dot{W}_{TX}$	Turbine expander work, W
C_{PA}	Heat capacity of air, J/kgK
C_{PF}	Heat capacity of feed, J/kgK
h	Specific Enthalpy, J/kg
H_c	Condensate enthalpy, J/kg
H_s	Steam enthalpy, J/kg
P	Pressure, Pa or %
P_{GC}	Pressure in gas cooler, Pa

P_{GH}	Pressure in gas heater, Pa
s	Specific entropy, J/kg
T	Temperature, K
T_g	Glass transition temperature, K
T_{AI}	Inlet temperature of air, K
T_{AMB}	Ambient temperature of air, K
T_{AO}	Outlet temperature of air, K
T_A	Temperature of air, K
T_F	Temperature of feed, K
T_{WB}	Wet bulb temperature, K
V_s	Swept volume, kg/s
x_r	Ammonia mass fraction
a_w	Surface water activity, –

1 Introduction

1.1 Background

The world is experiencing an increase in the global energy demand. Industrial processes have a common energy-intensive heat demand, and a focus on heat recovery is required for the industry to become more sustainable. High temperature heat pumps (HTHP) are showing good potential to increase the energy efficiency of industrial processes. By utilizing the waste heat from industrial processes, the heat pump can produce heat at higher temperatures, which can reduce the energy demand in many industries.

One specific process with high energy demand is the spray-drying process. The process requires temperatures around 250ºC and has waste heat temperatures of around 100°C. Today, the heat is produced using oil-burners, and the waste heat is not utilized. Therefore, the process could benefit from utilizing a high-temperature heat pump solution, to produce the same temperatures in a more energy-efficient way and at the same time utilizing the waste heat.

As the heat requirement is very large, the spray-drying process is depended on having a heat pump cycle with a large temperature glide. Therefore, the thesis will focus on studying and comparing different heat pump solutions that can provide this.

Another focus area is the integration of natural working fluids. Synthetic working fluids are being phased out and the thesis focuses on finding high-temperature heat pump solutions utilizing natural working fluids only.

1.2 Objective

The objective of this thesis is to evaluate the possibility of using heat pump solutions to increase the energy efficiency of a spray-dryer. The calculations are done through simulation models designed in EES and are comparing one transcritical heat pump using iso-butane as a working fluid, one supercritical cycle using carbon dioxide and one compression-absorption cycle using ammonia-water as the working fluid.

The following tasks are to be considered

1. Literature review on high-temperature heat pumps with large temperature glide.
2. Determent more specific temperatures and requirements for a spray-drying process
3. Develop a simulation model for the transcritical and supercritical heat pump cycle

to compare different configurations to be able to deliver heat at 220ºC and find the best solutions for the spray-drying process. Losses for the different components shall be included in the calculations, corresponding to whats found in the literature

4. Compare the compression-absorption cycles found in the literature to the simulation model of the transcritical and supercritical heat pump cycle
5. Study and optimize the heat exchangers used in the heat pump cycles
6. Evaluate the potential of components found in other industries to be used in HTHP, especially heat exchangers
7. Make a draft scientific paper from the main results of the work
8. Make suggestion for the further work

The results should not necessarily be viewed as a strict conclusion, but rather an indication of performance and possibilities for the technology. The final results and recommendations will also be presented in a scientific paper.

1.3 Limitation of Scope

The thesis focuses on spray-drying for the production of milk powder and focuses only on the limitations of milk powder production, not other industries. The aim of the heat pump solution is to be added on to an existing spray-dryer, so the conditions within the spray-dryer are excluded. Within the design, the focus areas are the main components; compressor, evaporator, condenser, expander and internal heat exchanger.

1.4 Outline of Thesis

Chapter 2 presents the spray-drying process, including how it works, the energy requirements and the challenges with the technology becoming more energy efficient.
Chapter 3 presents the theoretical aspect of high temperature heat pumps, through a literature study of the transcritical cycle, supercritical cycle and the compression-absorption heat pump cycles. It aslo studies the components utilized in the heat pumps.
Chapter 4 describes the methodology used in the thesis, including the heat loads from the spray-dryer, the thermodynamic set-up and the heat exchanger simulation models
Chapter 5 presents the results found in the analysis, through a thermodynamic analysis, an heat exchanger optimization analysis and a compression-absorption literature study for spray-drying situations

Chapter 6 concludes the work

Chapter 7 presents suggestions for future work.

2 Theoretical Background on Spray Drying

Spray drying is an industrial process requiring very high temperatures and releases excess air at high temperatures. The principal uses evaporation to remove water or other solvents from a liquid, slurry or solid. It is based on the concept of creating droplets of the product to increase the surface area before using a hot, gaseous drying medium to dry the droplets into individual particles of a solid product. The drying medium is required to have an inlet temperature between 180-250 °C and produces waste temperatures between 70-115°C [1].

Spray dryers are used in many industries, including agrochemicals, biotechnology products, fine and heavy metals, dairy products, dyestuffs, mineral concentrates and pharmaceuticals. It has been used in the dairy industry since the 1800s and was possible to use on an industrial scale to produce milk powder already in the 1850s [1]. The technology has been growing and improving ever since, and today, around 25,000 spray driers are found in commercial use.

The process is very energy consuming regarding the high inlet temperature and has a high thermal pollution due to the high excess temperatures. Hence, there is great potential for becoming more energy efficient. The spray-drying process is, therefore considered to benefit from installing high-temperature heat pump systems. One important application of spray drying is the production of milk powder, thus the description if the spray-drying process will be discussed with respect to this process.

2.1 Basic Concept of Milk Powder Production

Raw milk moves through six stages before becoming milk powder, due to requirements both for the spray-dryer and the finished product. The processes requires energy, as presented in Figure 2.1 [2]. The fat to none-fat ratio of milk solids is a product specification and is achieved through the standardization processes. Evenly distributing the fat in the milk powder is accomplished in the homogenization stage and the reduction of bacteria concentration is conducted through pasteurization. The evaporation into a higher solid content is done in the concentration step, as the milk slurry entering the spray dryer is required to have a solid content of around 50% [2].

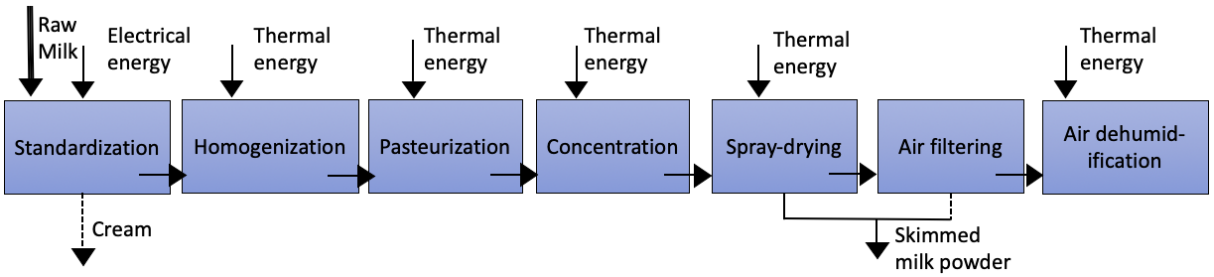

Figure 2.1: Production cycle of dry milk powder

The spray-drying process is illustrated in Figure 2.2. The slurry being dried, point 3, is pumped from the mixing tank to the atomizer device located at the top of the drying chamber. The atomizer device is rotating, breaking the liquid down to smaller droplets and disputes the droplets evenly throughout the drying chamber. Dry air, point 1, is commonly used as the gaseous drying medium. It is extracted from the surroundings and heated up to a high temperature via a heating unit, typically an oil furnace, electric heater, steam heater etc. The heated air is then introduced to the drying chamber through an air dispersal unit, point 5.

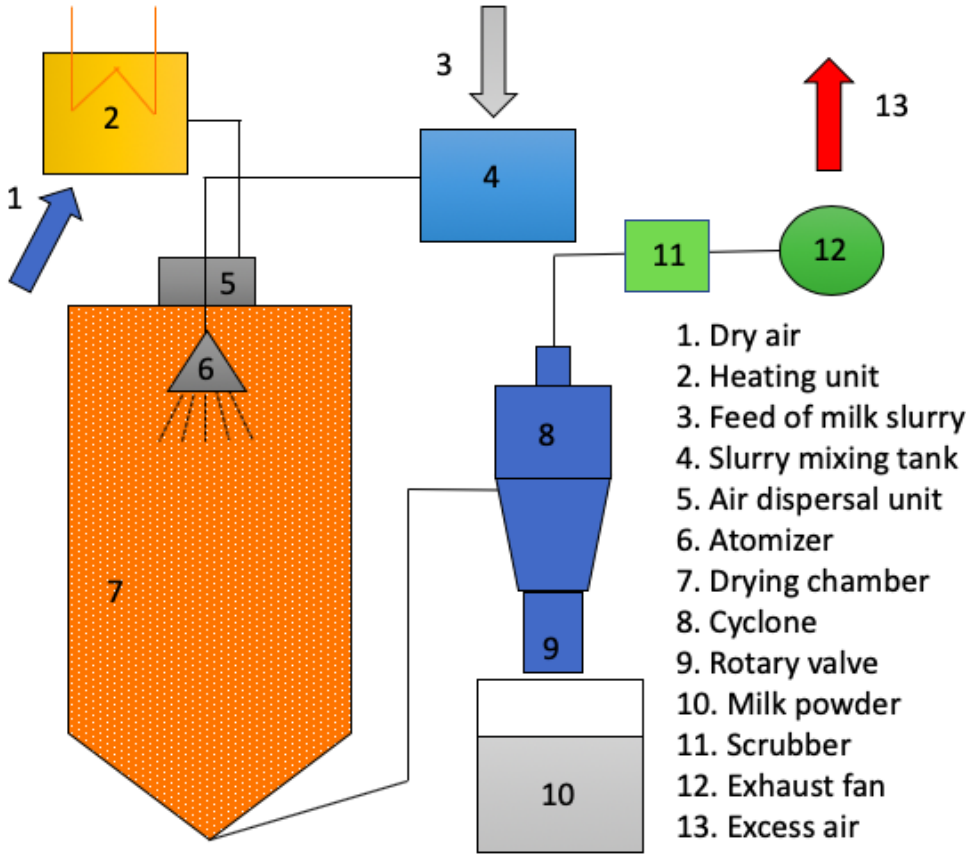

Figure 2.2: Illustration of a spray drying system for milk powder production

When the slurry is spread out as droplets in the drying chamber, the surface area increases to cause a maximum contact area between the hot air and the droplets. Evaporation of solvent begins when the hot air is in contact with the droplets, solids form and falls to the bottom of the chamber. The contact time between the air and the slurry is between 20-60seconds [3, 4], before the cooled air carries the solid powder out of the drying chamber to the cyclone, point 8. The powder leaves the cyclone at the bottom through a rotary valve and is collected as the finished milk powder product. The cooled air then continues through a scrubber, where traces of milk particles are removed, before the exhaust fan releases the air out into the atmosphere as excess air. At this point, the air is cooled down through the process but leaves the process at a temperature between 75°C and 115°C.

Advantages	**Disadvantages**
• The process is very easy to control, regarding particle size, shape, form and moisture content.	• The process has very low thermal efficiency
• It is suitable both for heat sensitive, non-sensitive and heat resistant fluids.	• The equipment has high installation costs
• The process has a wide range of production rates and short residence time.	• The equipment is bulky and is challenging to maintain

2.2 Thermal Efficiency of Spray Drying

Thermal efficiency,ρ_t, of the spray drying process in Figure 2.2 is defined by Equation 2.1.

$$\eta_t = \frac{\dot{m}_{CH}\lambda_e}{\dot{m}_{air}(T_A - T_{WB})C_{PA} + \dot{m}_F(T_F - T_{WB})C_{PF}} \tag{2.1}$$

Where $\dot{m}_{CH}$ is the chamber evaporation capacity, kg_{H_2O}/s, λ_e is the latent heat of evaporation, J/kg, $\dot{m}_{air}$ is the airflow rate, kg/s, $\dot{m}_F$ is the feed flow rate, kg/s, C_{PA} and C_{PF} are the heat capacity of the air and the feed, respectively, J/kgK, T_A, T_F and T_{WB} is the temperature of air, feed and wet-bulb temperature in °K.

Equation 2.2 represents the thermal efficiency if the process is defined as loss free.

$$\eta = \frac{T_{AI} - T_{AO}}{T_{AI} - T_{AMB}} \times 100(\%) \tag{2.2}$$

Where T_{AMB} is the ambient temperature of air, T_{AI} is the air inlet temperature and T_{AO} is the air outlet temperature, all in °K.

Equation 2.1 and 2.2 presents the importance of the temperature difference in the process regarding the thermal efficiency. The thermal efficiency would increase by either

increasing the inlet air temperature or decreasing the outlet temperature, as presented in Figure 2.3 [1].

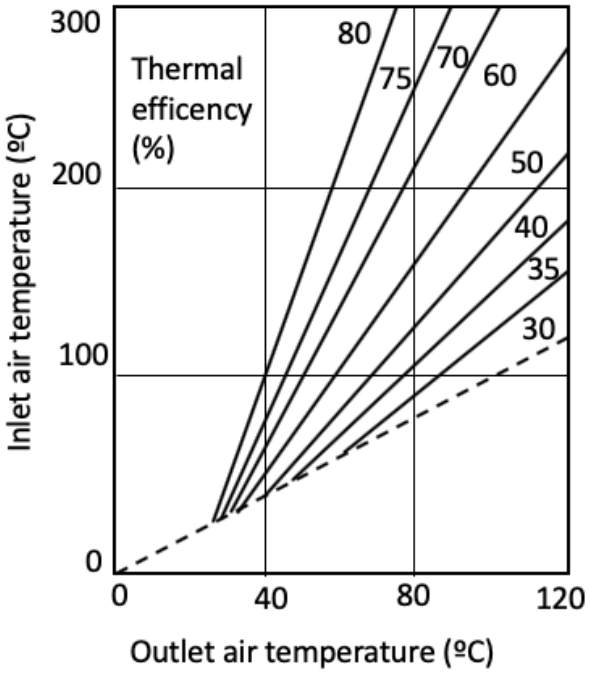

Figure 2.3: How inlet- and outlet temperature affect the thermal efficiency

The temperature difference between the inlet and outlet air is proportional to the capacity of the drying chamber [1], which is why it is desirable to have the highest possible temperature difference. The maximum inlet temperature is depended on the product being dried, as some products are more heat sensitive than others. By increasing the outlet temperature, the moisture content of the dried product increases. Therefore, the thermal efficiency is depended on both the spray-dryer design and the specifications of the product.

It is not an option to have to produce a different product to become more sustainable. Therefore, a more thermal efficient production of heat and heat recovery of the excess is the focus areas in making the process more sustainable.

2.3 Heat Requirement of spray drying

The spray-drying process has the highest heat consumption for evaporation of 1kg water, compared to any dehydrating equipment[1]. It is energy intensive due to the high temperature of the inlet air, the high temperature of the excess air and the low temperature difference across the chamber. Still, it is the most common one seen in the industry

because of all the benefits.

Table 2.1 presents the energy consumption of different spray drying set-ups. The single-stage dryer requires the highest amount of energy and is reduced by using more drying stages.

Table 2.1: Energy consumption for the skimmed milk powder production using 48% dry matter concentrate

Dryer type	Energy consumption
Single-stage dryer	6,777 kJ/kg
Two-stage dryer with vibrofluidizer	5,362 kJ/kg
Two-stage dryer with a static bed	4,602 kJ/kg
Multi-stage dryer with a static bed	4,020 kJ/kg

The one-stage spray drying unit has a short processing time, with an average of 20-60 seconds. It causes the outlet temperature of the air to be very high, decreasing the energy efficiency [3]. By changing the process into a two-step drying process, the drying time increases and a 20% decreased energy consumption is seen [1]. It is achieved by the first stage drying the matter down to a moisture content of 10%, before using a vibrofluidized bed or a static bed for the second stage to reach a moisture content between 3-5%. It causes the excess air temperature to decrease down to a temperature around 80°C, whereas the single stage has a temperature of around 100°C.

The heat requirement is also depended on the solid content of the slurry. Table 2.2 presents the decrease in heat requirement with the increase in solid content. Today, most spray-dryers utilize material with a solid content in the range between 40% and 50%.

Table 2.2: Heat consumption of various feed concentrations in a spray-dryer

Feed Solids (%)	**Approximate Heat Consumption (kJ/kg powder)**
10	$23{,}65\times10^3$
20	$10{,}46\times10^3$
30	$6{,}17\times10^3$
40	$3{,}97\times10^3$
50	$2{,}68\times10^3$

If the solid content could be higher than 50%, the energy consumption would decrease even further. The reason why it is not yet possible is the increasing viscosity with increasing solid content, and today's spray dryers are lacking the technology to handle such conditions [2].

2.4 Excess Air Heat Recovery

Dried milk powder is popular due to its ability to keep high quality without requiring any special storage conditions, it reduces mass and volume, it is a valuable food reserve for emergencies, and it is a needed component in many other productions such as chocolate and baby food [5]. Different usage areas require different compositions, microbiological and physical properties, which is produced differently with different heating demand. Therefore, the amount of heat that goes to waste as excess air is different for each product and each drying facility. Still, the losses through excess air are between 20-60% for all the processes [4]. This value has to be improved for the process to become more energy-efficient.

One possible solution is to recycle the excess air, as presented in Figure 2.4a. By using a semi-closed cycle, a reduction of 20% in fuel consumption can be achieved by recycling 50% of the excess air if the temperature is higher than 120°C[1]. Golman et al. (2014) presents a solution to recycling the excess air, an energy efficient solution that only requires energy to reheat the air. It can be used in the drying of ceramic materials because the slurry of material is concentrated and does not require the dehydration of the excess air [6].

Figure 2.4: Heat recovery solutions of excess air from a spray dryer

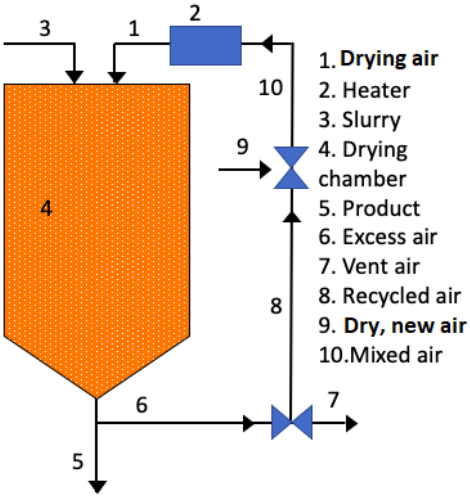

(a) The basis principle of recirculating the excess heat

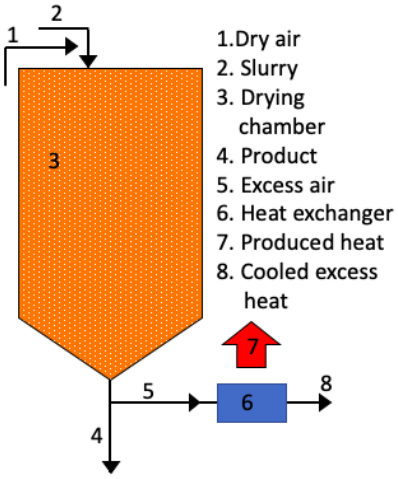

(b) The basis principle of utilizing the excess heat in a heat exchanger

However, for the production of milk powder, recirculation of excess air is not an option. The scrubber removes most of the milk powder particles from the excess air, but there will always be trace particles left. These trace particles can lead to bacteria growth in the spray-dryer and on the milk powder, a risk the producers can never accept [7].

A second way to make spray-dryers more energy efficient is to indirectly take advantage of the energy found in the excess air. The use of a heat exchanger is illustrated in Figure 2.4b. It is a challenging request, as the temperature is between 70-115°C, with high humidity and consist of a large amount of latent heat and smaller amounts of sensible heat. Also, milk powder particles are present in the excess air, and the dew point of the stream is quite low [8]. However, it is possible and is, therefore, the chosen excess heat recovery solution chosen for this thesis.

2.5 Fouling on Heat Recovery Systems

The biggest challenge in using the excess heat in a heat recovery system is the milk powder particles left in the air. The excess heat is used as the heat source of the heat pump cycle, but the powder particles cause fouling on the surfaces over time. Fouling leads to a reduction in the heat transfer rate and increases the pressure drop. It causes the saving potential to decrease and increases the costs of both electricity and maintenance. In New Zealand, a liquid coupled loop heat recovery system was tried introduced in 2014, but the program was shut down due to concerns that the fouling would cause too many problems

[9]. Still, there are design parameters that could be implicated to decrease fouling and foresee the reduction in heat transfer rate and the increasing pressure drop.

The stickiness of the milk powder intricately related to viscosity and glass transition temperature, and it is what determines the occurring amount of fouling. Milk powder is stickier at low temperatures and higher humidity, making it more likely to deposit on surfaces.

Glass transition temperature, T_g, is defined as the boundary temperature for a materials state between being at a glassy, non-sticky state or a rubbery, sticky state [10]. The relationship T-T_g is a non-linear measure of stickiness through viscosity, where T is defined as the air temperature. Brooks [11] developed an polynomial empirical model for amorphous lactose, defining T_g in °C depending on the surface water activity, a_w, presented in Equation 2.3.

$$T_g = -530.66(a_w)^3 + 652.06(a_w)^2 - 366.33(a_w) + 99.458 \quad (2.3)$$
$$[0 < a_w < 0.575]$$

To have the lowest possible stickiness will decrease the fouling. It can be achieved by decreasing the surface water activity, leading to a higher T_g and thereby a lower stickiness.

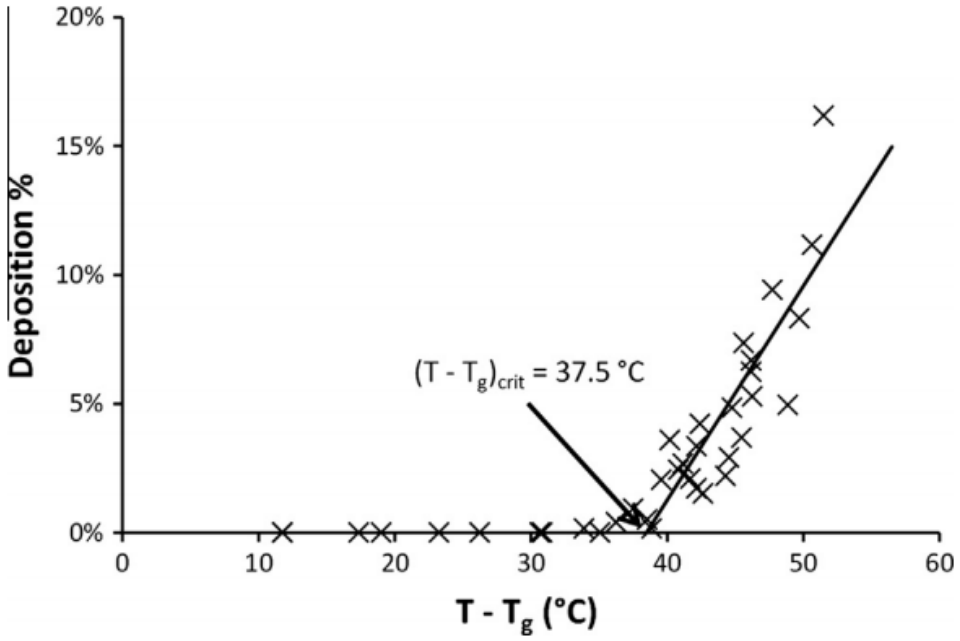

Figure 2.5: Critical value for the stickiness of milk powder

Figure 2.5 illustrates the critical region for stickiness, presented by Walmsley et al.(2013)

[10]. Fouling will not occur if the T-T_g relationship is kept below 37.5°C. After the critical point a rapidly increase occurs, causing troubles for the system.

There are challenges regarding efficiency and the critical fouling value. If air exits the dryer at 75 °C and leaves the heat recovery unit at a temperate of 65°C, fouling is avoided. However, from an energy efficiency point of view, only recovering 10°C of heat is inefficient. On the contrary, if 20 °C is extracted, the exit temperature ends up at 55 °C with an T-T_g value of 49°C [10]. As seen in Figure 2.5, this causes a deposition of around 8%. Therefore, the outlet temperature of the heat recovery unit will be a critical value in the design and should be analysed before any recommendations are made.

Different heat recovery units with different tubing will also have an effect on the fouling. Walmsley [12] studied the differences when using round, elliptical and squared tubes in a cross-flow heat exchanger. For circular and elliptical tubes, fouling occurred quite similarly around the front of the tube, and the thickness of the powder layer increases with stickiness. For a square tube, the fouling was found to be depended on the combination of impact angle and wall shear stress. A fully covered face of the pipe was seen, with an increasing thickness with an increasing stickiness.

Other design parameters that can decrease fouling include increasing the velocity, implanting inserts between or within tubes, non-standard tube geometries, low surface energy coatings and non-standard fin geometries [13].

2.6 Problem Statement, Limitations and Possible Solution

The problem statement of this thesis is to increase the energy efficiency of a spray-drying process. The limitations are summarised as follows;

- The final product quality cannot be affected by the changes

There is an absolute requirement of not affecting the specifications of the produced milk powder. Changing the inlet and outlet temperature can increase the thermal efficiency of the process but can cause changes to the actual product. This is not an option, causing the inlet and outlet temperatures to stay constant at 180-250°C and 75-115°C respectively.

- The solution has to suit as an add-on to existing spray-dryers

Heat requirement and temperature difference have the same challenges. There are ways to decrease the heat requirements of a spray-dryer, but it requires new or improved equipment. Instead, the solution shall focus on improving existing spray-dryers, rather than

designing a new spray-drying system. Therefore, the heat requirements and the temperatures from the process has to be kept as the limiting factors.

- Avoidance of bacteria growth

The final product cannot be affected by the changes, and the hygienic requirements have to be followed. Therefore, the recirculation of excess air is not a possibility. The excess air has traces of milk powder particles, which can cause bacteria growth in the new milk powder if recycled. The quality of the product is more important than energy efficiency, and recirculation can therefore not be utilized.

Using a high-temperature heat pump is a possible solution. It can increase the energy efficiency of the spray-dryer without doing any changes to the production, by being added on to an existing spray-dryer and take advantage of the excess air. It can utilize both a large amount of latent heat and a smaller amount of sensible heat of the excess heat and produce the high-temperature hot air the process requires, using lower amounts of energy than the heaters are using.

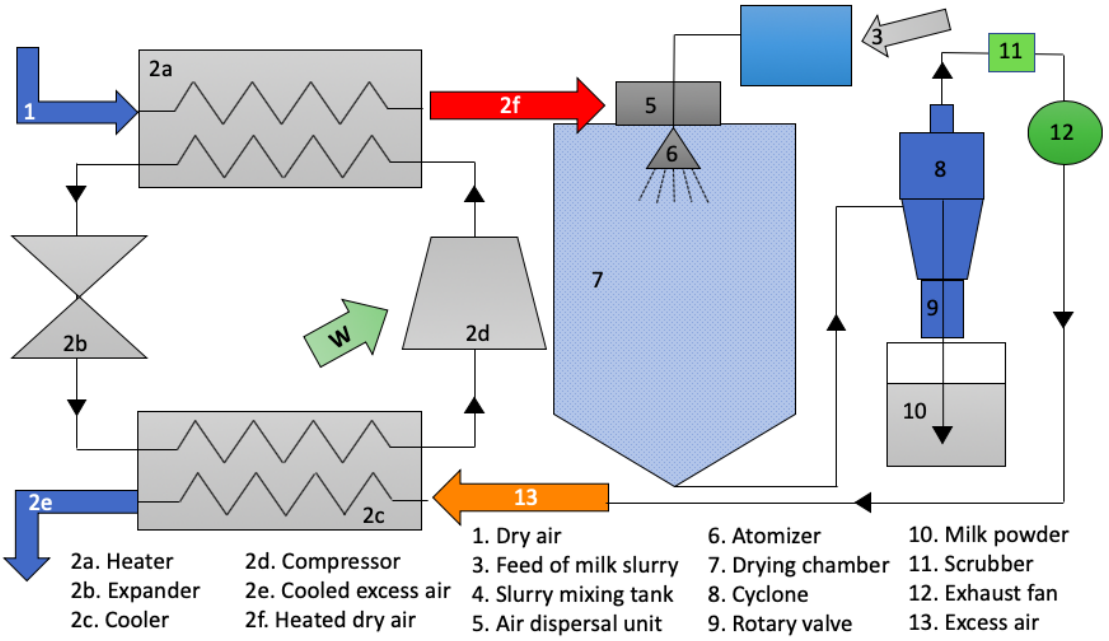

Figure 2.6: Heat pump solution for the spray-drying process

Figure 2.6 presents the possible heat pump cycle for a spray-drying unit. The heating unit is replaced with a heater from the heat pump, as seen with components 2a and 2f. The heat pump is used to produce the heat load required to heat dry air to a temperature between 180-250°C. The excess heat is utilized as the heat load required in the heat pump cycle.

Fouling cannot be ignored in the heat pump solution. The cooling unit, 2c, is affected by

fouling, causing the heat transfer rate to decrease and increase the pressure losses. It can lead to high maintenance requirements and a reduction in economic advantage. Still, by taking fouling into consideration, especially Equation 2.3 and Figure 2.5 during the design process, the effects can be minimized.

Also, due to fouling, it is not possible to have an extra heat exchanger to pre-heat the dry air before it enters the gas cooler, which in other applications would be considered.

3 High Temperature Industrial Heat Pumps

3.1 High Temperature Heat Pump Potential and Requirements

An industrial process describes different procedures, all with different challenges to overcome to become more sustainable. What many of them have in common is an energy-intensive heat demand. All factories require heat, whether it is space heating, hot water or higher temperatures for the processes. Figure 3.1 [14] specifies the different temperature requirements for different processes in the chemical, paper, food, machinery, wood, transport, and textile industry. The requirement of high-temperature heat is significant in most industries, showing an especially good market potential for the chemical, paper and food industry.

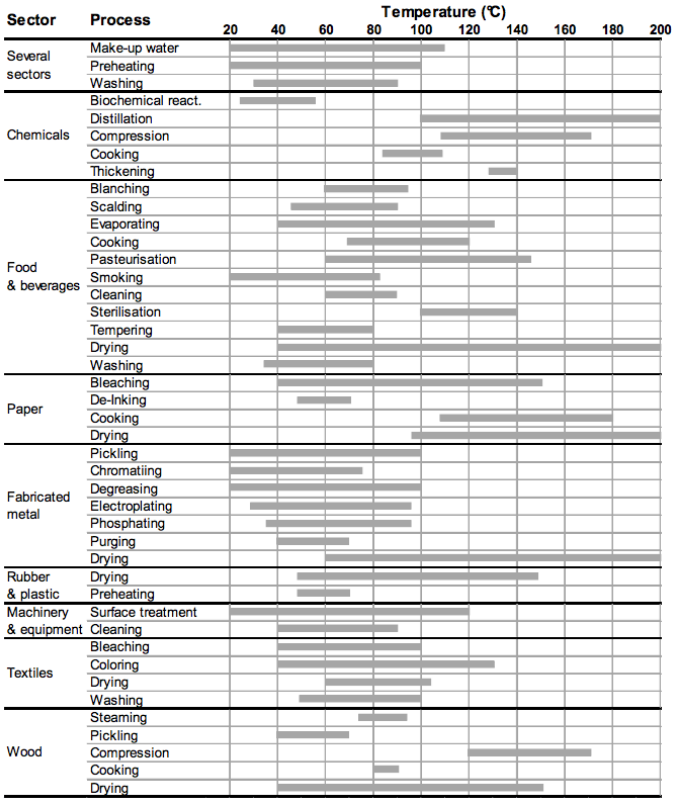

Figure 3.1: Summary of the heat demand in different industries

Producing high temperature heat is very energy consuming. Oil burners are often used, a procedure that should be phased out to reach the sustainability goals provided by the UN. With each process that uses high-temperature heat, quantities of waste heat emerge. Bamigbetan (2017) [15] estimates that 60% of the waste heat is at low temperature. Low temperature waste heat has low direct thermal and economic value and is therefore not taken advantage off.

A heat pump is a thermodynamic process designed to take advantage of the energy found in heat sources to produce higher temperatures by adding mechanical work. The process can be used to take advantage of the low-value waste heat from industrial processes and be used to produce high-temperature heat.

A basic heat pump cycle consists of four main components, an evaporator, a compressor, a condenser and an expander, presented in Figure 3.2. A working fluid is used to transfer energy through the components. The working fluid is heated and evaporated utilizing heat from a heat source in the evaporator and compressed to a higher temperature and pressure in the compressor. Then, it is condensed to reject heat to the heat sink in the condenser, before being expanded down to the initial conditions. The cycle is called a sub-critical heat pump cycle, as the working fluids stay in the subcritical region throughout the whole process. When determining the proper heat pump applications, heat demand and type of available waste heat are factors that have to be considered.

Figure 3.2: The Principle of a vapor compression heat pump cycle

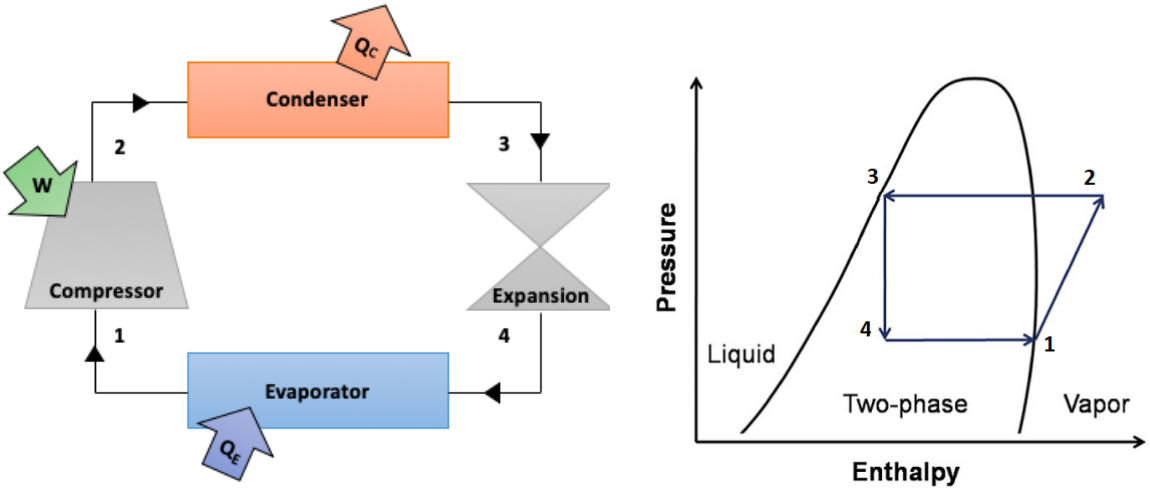

(a) The four main components of a closed, vapor compression cycle

(b) Enthalpy diagram of the vapor compression cycle

Coefficient of performance (COP) is used to determent the efficiency of the heat pump. It calculates the relationship between the heat produced and the required work to produce this heat, presented in Equation 3.1.

$$COP = \frac{\dot{Q}_{cond}}{\dot{W}} \tag{3.1}$$

Where $\dot{Q}_{cond}$ is the heating capacity of the condenser and $\dot{W}$ is the compression work, both in W. COP is used to indicate how efficiently a heat pump is running. From an industrial point of view, a heat pump is aiming to reduce energy costs. Therefore, an

economic advantage has to be proven for the industry to invest in a heat pump, which is shown by the process having a high COP.

In 1993 [16] a high temperature heat pump was defined to deliver temperatures above 80°C. In later years, the term is used for a variety of temperatures, some defining it up to temperatures around 250°C, whereas others separate the term into high temperatures and super high temperatures.

There are two main challenges in designing a heat pump for higher temperatures, finding a working fluid that condenses at high enough temperatures and developing equipment that can handle that working fluid at this high-temperature state.

Table 3.1: Natural working fluids and their potential for high-temperature use

Working fluid	**Name**	**Critical Pressure MPa**	**Critical Temp ºC**	**h_E, 0°C, kJ/kg**	**GWP**	**Toxic**	**Flammable**
Carbon dioxide	R744	7.39	31.1	231	0	No	No
Water	R718	22	374	2260	0	No	No
Ammonia	R717	11	78.5	1262	0	Yes	No
Butane	R600	3.72	152	381.9	4	No	Yes
Isobutane	R600a	3.72	134.7	355.6	3	No	Yes
Propane	R290	4.25	96.7	373.4	3	No	Yes
Propylene	R1270	4.61	91.8	378.3	2	No	Yes

Table 3.1 presents the characteristics of the most common natural working fluids. The critical temperature defines as the highest temperature where the working fluid can be liquefied by pressure alone and is what determines the highest possible condensation temperature. Butane has the highest critical temperature of 152°C, but would still not provide the temperature required for spray-drying. Synthetic working fluids is also a possibility, but a working fluid reaching temperatures of 250°C is yet to be developed. Where the industry used to develop the perfect working fluid synthetically for different types of heat pumps, the focus has changed towards designing components and systems that can utilize natural working fluids. Synthetic working fluids are therefore not considered further in this thesis.

Finding suitable components is the second challenge in developing high-temperature heat pumps. The compressor has to increase the temperature of the working fluid enough to condense at high temperatures, but most compressors have a limiting discharge temperature of 180°C [17]. With the increasing temperatures, an increase in pressure fol-

lows, also challenging the components. To develop compressors, heat exchangers, condensers, evaporators, and expansion devices that can handle higher temperatures and higher pressures while still operating at high efficiencies has proven to be challenging. Still, it is something the market has to solve before high-temperature heat pumps can be used in industrial facilities.

As a conclusion, one can state that a subcritical heat pump approach will be very difficult to implement for high-temperature usage, as none of the natural working fluids has a critical temperature higher than 180-250°C. However, there are three types of other heat pump cycles that are showing potential to be adaptable for high-temperature usage;

- Transcritical cycle
- Supercritical cycle
- Compression-absorption cycle

These are discussed and analysed in the following sections.

3.2 Transcritical Cycle

The transcritical heat pump cycle is illustrated in Figure 3.3a and is defined by having a working fluid that operates right outside the subcritical state, shown in Figure3.3b. Instead of using a condenser to deliver heat, heat rejection occurs in the supercritical region, where the working fluid never goes through a phase change. A gas cooler is used for the heat rejection, allowing a temperature glide compared to a subcritical cycle where condensation occurs at a constant temperature. After leaving the gas cooler, the working fluid moves through an expander and into the subcritical area, before being evaporated through the evaporator and compressed to the desired pressure.

Figure 3.3: The transcritical heat pump cycle

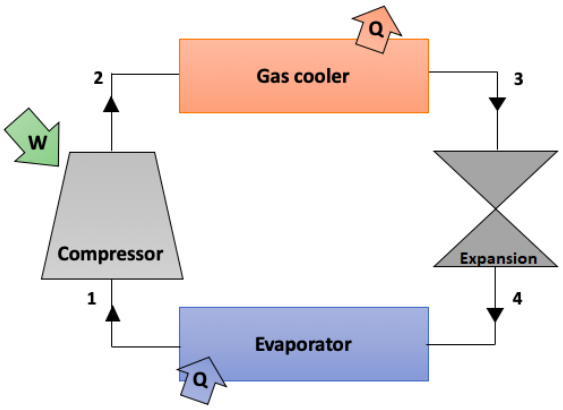

(a) The four main components in the transcritical cycle

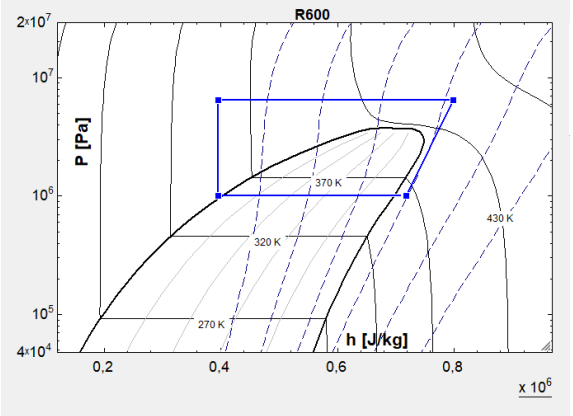

(b) P-h diagram for a transcritical butane cycle

Transcritical cycles are showing potential to be used as high-temperature heat pumps because of the heat rejection in the supercritical area. As condensation is not required, the maximum temperature is no longer at the critical point, and the process can reach even higher temperatures. It challenges the components, especially the compressor technology, which today is limited by the suction gas temperature being 180°C for natural lubricants. The corresponding suction gas pressure and pressure through the gas cooler will also challenge the equipment but is different for each working fluid [18].

CO_2 is one of the most common natural working fluid for transcritical heat pump cycles in commercial use. With a critical temperature of 31.1°C and a critical pressure of 7.39MPa it is suited to produce temperatures around 60°C used for hot water heating. Nekså studied the potential already in 1998 [17], where a COP of 4.3 was achieved and potential to reach temperatures as high as 90°C if the component technology improved was presented.

If the temperature were to be increased further, to reach the temperatures required for high temperature heat pumps, higher pressure ratios would be required. It causes an increase in the compression and expansion losses of the transcritical CO_2 cycle. Yang (2017) [19] tried to reduce these losses by utilizing a cascade model with CO_2 in a transcritical cycle and R152a in a subcritical cycle. The R152a subcritical cycle was used to pre-heat the working fluid, to increase the evaporating temperature and pressure of CO_2 in the transcritical cycle. Due to this, the pressure difference between the evaporator and gas cooler is decreased, leading to a higher COP. The cycle reached a maximum temperature of 102°C.

CO_2 is struggling to reach the temperatures between 180°C and 250°C that are required

for spray-drying. Sakar et al.(2007) [20] compared ammonia, carbon dioxide, propane and iso-butane in a transcritical cycle to determine which is more suitable for high-temperature applications. CO_2 was shown to have a poor COP and very high discharge pressure and was found to be unsuitable for high-temperature use. Ammonia, propane and iso-butane achieved very similar results, all suitable for high-temperature use, with ammonia having a slightly higher COP.

Having a high critical temperature is beneficial for a high-temperature transcritical heat pump cycle. Table 3.1 presents butane as the natural working fluid with the highest critical temperature, with a corresponding low critical pressure. The high critical temperature causes the working fluid to stay close by the critical point through the heat rejection, and low critical pressure decreases the required pressure rates compared to the case for CO_2.

Another benefit of using butane is the low viscosity. Having a low viscosity decreases the pressure loss in the heat pump components, especially noticeable in heat exchangers and pipelines. As a transcritical cycle generally has higher pressure rates than a subcritical cycle, being less viscous is a greater advantage for a transcritical working fluid than a subcritical one. Viscosities for butane, propane, ammonia, CO_2 and R134a are presented in Figure 3.4 [21].

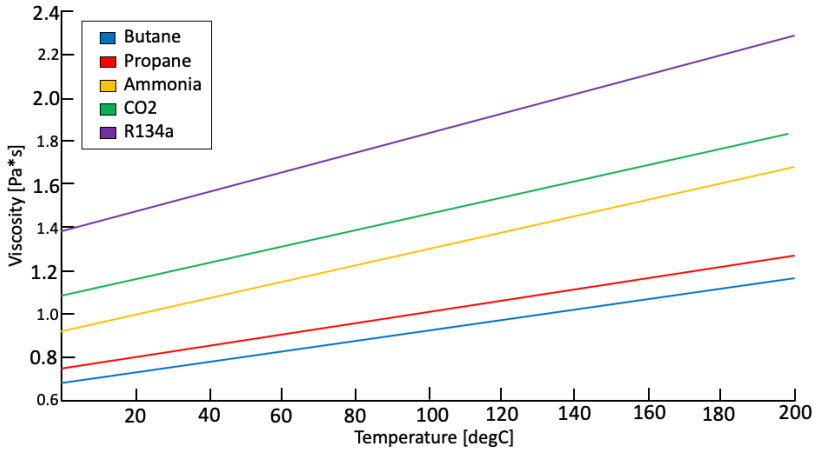

Figure 3.4: Viscosity change for different working fluids with an increasing temperature

Butane reached a temperature of 180°C with a COP of 4 in a transcritical heat pump simulation model by Olafsen (2018) [22]. The compressor was found to be the main challenge in producing high-temperature heat for the transcritical butane cycle, but an increase in COP was found by reducing the friction losses by decreasing the RPM. Bamigbetan (2018) [23] presents experimental data on a new compressor using butane as the working fluid in producing temperatures of 115°C from 50°C excess heat. A compressor efficiency of

74% was achieved, with a volumetric efficiency of 83%.

The disadvantage of using butane as the working fluid in high-temperature configurations is the autoignition temperature of 365°C. The autoignition temperature is defined as the lowest temperature where a working fluid can spontaneously ignite in a normal atmosphere without an external source of ignition. Therefore, the surface temperature of each component is limited to be 100° below the autoignition temperature for safety reasons. It makes the upper limit for high-temperature usage of butane to be 265°C. Butane can be utilized in a heat pump for spray-dryers, as the required temperature is between 180°Cand 250°C, but is limiting for other high-temperature applications. By changing the working fluid to iso-butane, the autoignition temperature increases to 460°C, without any drastic changes in the other values presented in Table 3.1. Therefore, iso-butane is recommended to replace butane as the working fluid for this analysis.

3.3 Supercritical Cycle

A fluid is defined as supercritical when the temperature and pressure are above the critical point, as illustrated in Figure 3.5. In the supercritical region, the fluid is neither gas or liquid but can adopt properties midway between the two, being able to diffuse through a solid like a gas and dissolve materials like a liquid. A supercritical fluid has no surface tension and can be tuned in to become more gas-like or liquid-like.

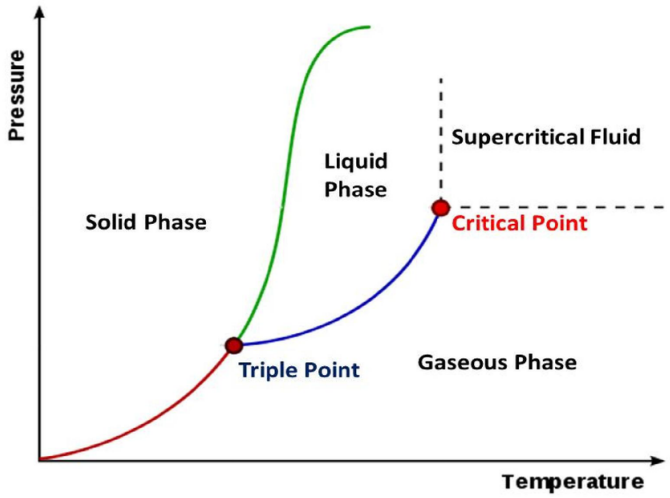

Figure 3.5: Phase change of a working fluid

The supercritical cycle takes advantage of the supercritical working fluid and the lack of limitations that follows. The cycle is based on the Brayton cycle, a gas cycle where no phase change occurs. Without phase change, the evaporator is not necessary, and it is

replaced by a gas heater. The gas heater works opposite of a gas cooler, taking advantage of the heat extracted from waste heat from industrial processes to heat the working fluid before compression. Both the gas cooler and gas heater has a temperature glide. The supercritical heat pump cycle is illustrated in Figure 3.6.

Figure 3.6: The supercritical heat pump cycle

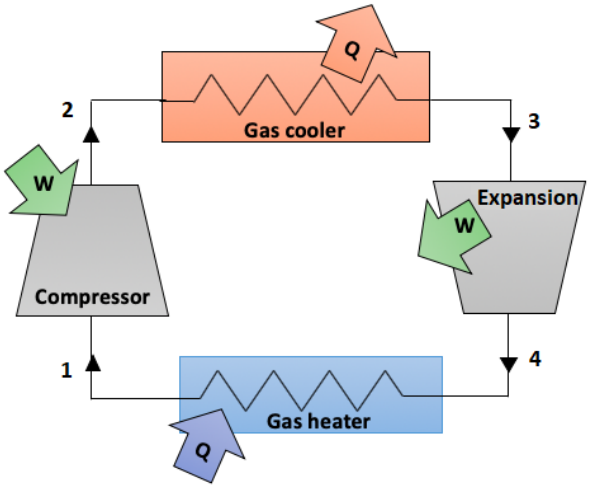

(a) The four main components in the supercritical cycle

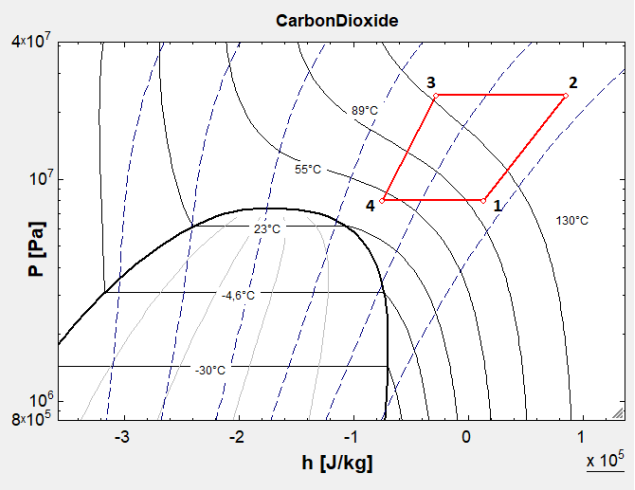

(b) Enthalpy diagram of the supercritcal cycle

An advantage with the supercritical cycle compared to the sub-critical and transcritical cycles is the availability of large-scale machinery. It has no limitations on high temperatures, but there are challenges in finding equipment that can handle the high temperatures and pressures. The expander and compressor are required to be 10-15% higher efficiency to be competitive with the transcritical cycles analysed [24].

For the supercritical application in this study, CO_2 is chosen as the working fluid. With qualities as being non-flammable, having low toxicity, low global warming potential, low ozone depletion potential, and being chemically inactive, CO_2 is a very promising refrigerant. It is suitable for supercritical use as it shows thermal stability up to 1500°C and has a high density at the operating conditions. The critical temperature of 31.1°C is low compared to other refrigerants, simplifying the requirement of always keeping the temperature above the critical temperature. The corresponding critical pressure of CO_2 is as high as 73.9bar. It does not affect the ability of CO_2 to work in a supercritical cycle but challenges the equipment with high operational pressures. Supercritical heat pump cycles are a new concept, and not many studies are found on the matter. Nekså [17] studied supercritical CO_2 cycles already in 1998, but the cycle presented is more similar to what today is described as a transcritical cycle.

Still, an increasing interest in supercritical CO_2 is seen, both due to the focus on using natural refrigerants and the aim to increase the efficiency in high temperature applications. In October 2016, the U.S Department of Energy (DOE) awarded $80 million into developing a pilot plant test facility for a supercritical carbon dioxide cycle. The aim is to design, build and operate a 10MWe test plant to improve future power plants, both regarding energy efficiency and size reduction. By having a test facility, both the industry and government get the opportunity to develop and mature the idea of using CO_2 in supercritical heat pump cycles.

Supercritical cycles are seen investigated in many industries. In 2004, V. Dostal et al. [25] published a report on using supercritical carbon dioxide cycle for the next generation nuclear reactors. The concept is based on using a recompression cycle to achieve the very high temperatures required and it is seen that CO_2 shows better potential than helium for the industry. Sabau et al. (2011) [26] uses supercritical CO_2 in a Rankine cycle for geothermal power plants and achieves a 10% increase in efficiency by moving from a transcritical cycle to a supercritical cycle. In a molten carbonate fuel cell, CO_2 supercritical cycles are investigated as the power generating option because the efficiency is higher than for the air Brayton cycle, reported by Bae et al. (2014) [27]. Bauer et al. (2016) [28] uses variations of the supercritical Brayton CO_2 cycle to generate electricity at a competitive price with the aim to reduce the cost of electricity. The technology is reportedly showing potential to be very beneficial for concentrated solar power incorporations. Zhang et al. (2018) [29] investigates the possibility of supercritical CO_2 cycles in solar power plants. The significant advantage with using CO_2 supercritical cycles in solar power plants is its ability to handle the variation in the changing heat source due to variations in weather and season and focuses the report on designing a suitable turbine.

The the concept of CO_2 application for spray-drying using a supercritical cycle should be analysed in comparison with iso-butane transcritical cycles, due to the absent of literature issues about the problem.

3.4 Compression-Absorption Cycle

The compression-absorption cycle, also called hybrid heat pump, is showing potential for high-temperature usage by being efficient up to a temperature of 150°C with a temperature lift of 60K [30]. It differs from other thermodynamic cycles by using a zeotropic working fluid, a two-component solution consisting of one volatile component called the refrigerant and one non-volatile component called the absorbent. Figure 3.7 illustrates the compression-absorption cycle.

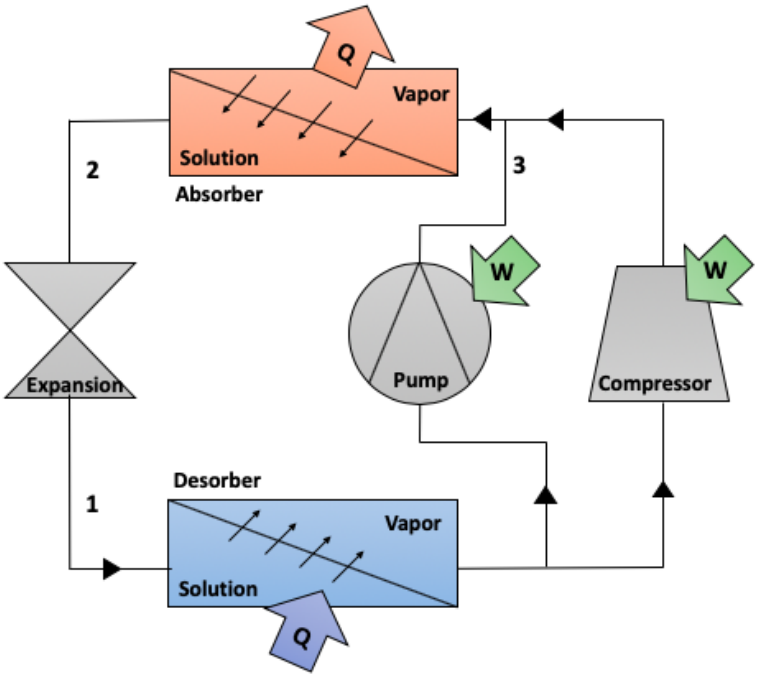

Figure 3.7: Operating principle of a compression-absorption heat pump cycle

A low pressured solution rich on the refrigerant is introduced to the desorber, where heat is added to vaporize the refrigerant only. This vapor is sent to be compressed to a higher pressure. The not vaporized, absorbent is sent to the solution pump for compression. The two flow-rates are then mixed and sent to through absorber to generate heat to be absorbed by the heat sink. The rich solution is expanded and returned to the desorber to complete the cycle.

The advantage of having a zeotropic working fluid is that the saturation temperature becomes depended on both the pressure and the mixture composition. The refrigerant evaporates/condensates quicker, changing the concentration and therefore also the saturation temperature of the mixture. The concentration of the absorbent increases through the desorber, which again causes a reduction in the vapor pressure of the mixture.

The compression-absorption cycle offers flexibility, being adjustable to changes in the temperature of both the heat source, heat sink and the temperature difference between the two. The heat source can have relatively low temperatures, and the cycle can achieve a high COP at high temperatures. Also, the decrease in the irreversibility of the cycle and entropy generation increases the energy efficiency [31].

Ammonia-water mixture is the most common natural working fluid mixture for compression-absorption heat pumps. Ammonia is showing good potential as a high temperature working fluid, as presented by Sakar (2007) [20]. Due to the good heat transfer abilities, ammonia heat pumps can be small and compact, which is beneficial for industrial appli-

cations where larger heat loads are required, but large spaces are not always available. It is also a cheap and accessible working fluid suitable for Norwegian conditions.

What limits ammonia as a high-temperature working fluid is the relatively low boiling point and high saturation pressure of 62.6bar at 100°C [21]. By mixing ammonia with an absorbent, the saturation pressure decreases drastically and the boiling point increases, making the mixture better suited for high-temperature applications. A 90:10 weigth-% mixture of ammonia and water decreases the saturation pressure down to 54.4bar and at a 50:50 weight-% mixture, the saturation pressure is 23.6bar. In the compression-absorption heat pump mixture, ammonia is the more volatile component and water is the absorbent.

For the compression-absorption heat pump to be suitable for high-temperature use, the temperature lift should be as large as possible. By increasing the recirculation ratio f, the relationship between the mass flow rate of the rich solution and the lean solution, an increase in temperature lift were found for excess heat temperatures of 60°C, 80°C, 100°C, and 120°C [31]. A change in the ammonia mass fraction, x_r was also reported to increase the temperature lift.

Figure 3.8: Change in COP and heat sink temperature with different mass fractions and recircualtion ratios

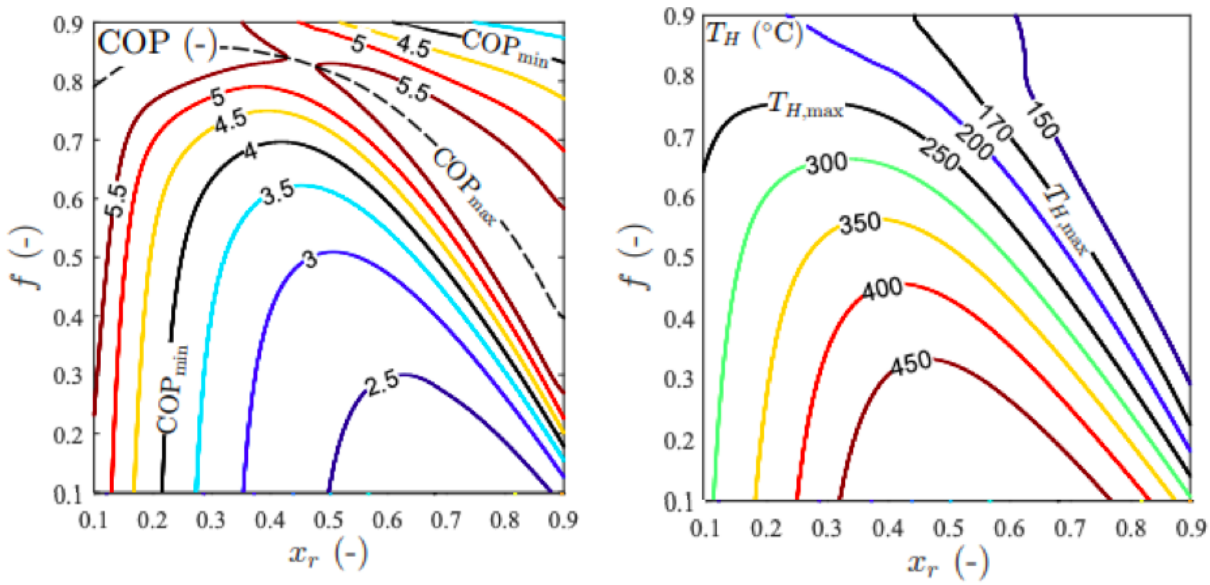

(a) Change in COP with changing mass fractions and recirculation ratio

(b) Change in heat sink temperature with changing mass fractions and recirculation ratio

Figure 3.8 presents how both how the COP and heat sink temperature changes with the different mass fraction of ammonia and by the recirculation ratio [32]. All mass

fractions have an optimal correlating circulation ratio, the dotted line in figure 3.8a, where the maximum COP is achieved. Figure 3.8b presents the heat sink temperature for the different combinations of mass fraction and recirculation ratio.

3.5 Components Used in the Heat Pump Cycles

3.5.1 Compressor

There are three main types of compressors used in an industrial scale; piston-, screw and turbo- compressors. The required size of a compressor is dependent on the heat load being produced in the gas cooler, as an increasing heating capacity increases the working fluid flow rate. Having a larger flow rate through the compressor increases the required size and cost of the compressor.

$$V_S = \frac{\dot{m}}{\rho_g \eta_v} \tag{3.2}$$

The swept volume is defined by Equation 3.2, where $\dot{m}$ is the mass flow rate, ρ_g is the density of the gas and η_v is the volumetric efficiency. The different compressors are suitable for different swept volumes, presented in Figure 3.9.

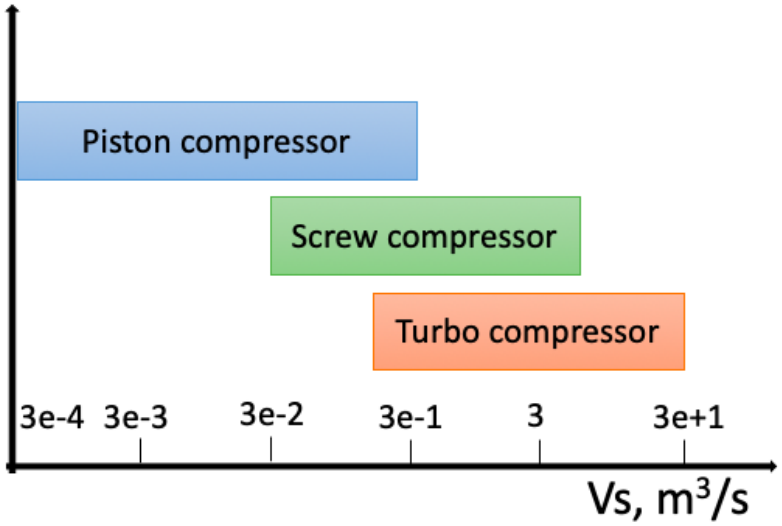

Figure 3.9: Swept volume range for the different compressor types

The amount of work required for the compression is depended on the pressure ratio, as defined in Equation 3.3. With an increasing pressure ratio, the required compression work increases and thereby decreases the overall efficiency of the heat pump.

$$PR = \frac{\text{Discharge pressure}}{\text{Suction pressure}} \tag{3.3}$$

Lubricant oil is used to reduce friction losses in the compressor and is what causes the limiting discharge temperatures of a compressor. If the temperature is too high, the lubricant oil overheats, causing it to cook and thereby damaging the compressor. The maximum discharge temperature is dependant on the thermal stability of both the working fluid and the lubricant oil. Natural lubricant oils generally have an upper limit of 180°C, while some synthetic oils are reaching a maximum temperature of 250°C.

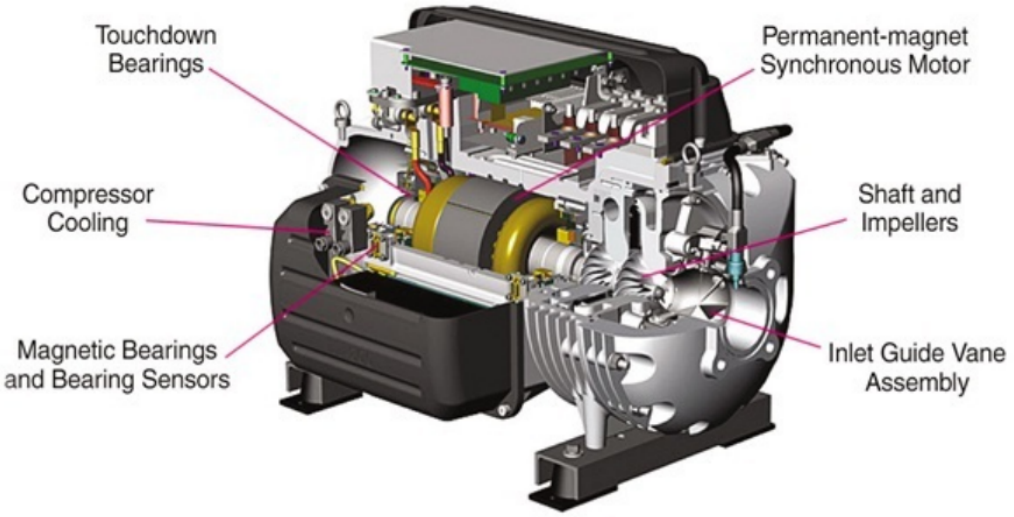

Figure 3.10: The schematics of a turbo compressor

The turbo compressor, presented in Figure 3.10, is showing great potential for high-temperature use, as it uses very little lubricant oil. It is a technology based on digitally controlling a magnetic bearing system designed with both permanent magnets and electromagnets, causing a frictionless compressor shaft to be the only moving component of the compressor. Due to this, very little lubricant is required compared to other compressor systems that have more components with friction. Therefore, the limiting temperature factor is removed, and the compressor can reach higher temperatures. Other benefits are that oil managing systems are avoided, including oil pumps, sumps, heaters, coolers and oil separators, and reduces the maintenance time and cost.

3.5.2 Gas Cooler and Gas Heater

In the transcritical and supercritical heat pump cycle, the condenser is replaced by a gas cooler, as no phase change occurs. Here, heat is rejected at a temperature glide, compared to a condenser that transfers heat at a constant temperature. A gas cooler aims to deliver as much heat as possible to the heat sink and to cool down the working fluid as much as possible before throttling to reducing the expansion losses. Maximum efficiency of the

cycle is achieved when all the possible heat in the working fluid is transferred, using as little work as possible.

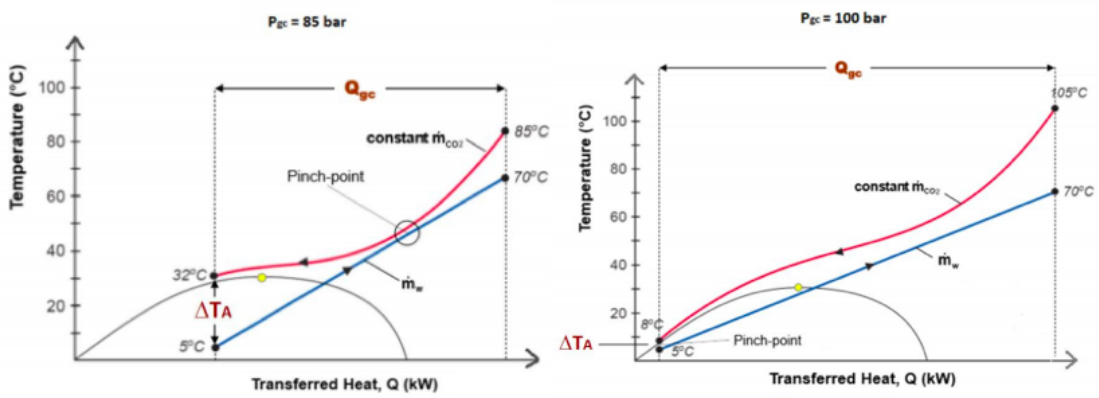

Figure 3.11: The change in pinch point when changing the discharge pressure

The pinch point is the lowest temperature between the working fluid and the heat sink. Maximum efficiency is achieved when the pinch point is located on either end of the gas cooler, and the heat transfer rate reduces if the point is located somewhere else. Each gas cooler has an ideal discharge pressure, depending on the temperature of the heat sink, the working fluid and the pressure rate, and the location of the pinch point can be changed by changing the discharge pressure [18]. Figure 3.11 illustrates how an increase in the gas cooler pressure moves the pinch point for the same mass flow rate of CO_2.

For the supercritical cycle, the evaporator is replaced by a gas heater, based on the same principle as the gas cooler, but differs in that the working fluid is heated instead of cooled, taking advantage of the heat in the excess air.

3.5.3 Absorber and Desorber

In the compression-absorption heat pump, an absorber replaces the condenser, and a desorber replaces the evaporator. The absorber is based on the same principle as a condenser; it cools down the zeotropic working fluid and thereby deliver heat to the required industrial process. The desorber is very similar to an evaporator, by extracting heat from the industrial processes and uses it to evaporate the zeotropic working fluid.

3.5.4 Internal Heat Exchanger

An internal heat exchanger (IHX) is aiming to heat the working fluid further before entering the compressor by cooling the working fluid that is leaving the gas cooler further.

The IHX can operate as long as the outlet temperature of the gas cooler is higher than the compressor suction temperature and can be added to all three heat pump cycles.

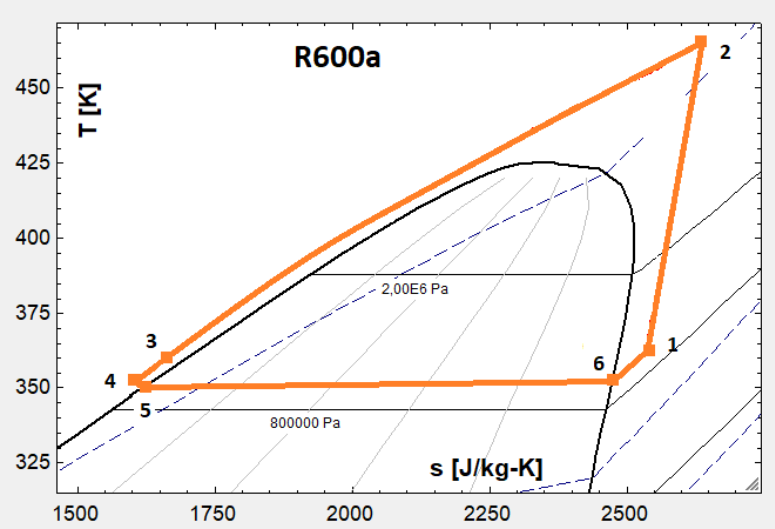

Figure 3.12: T-s diagram for a transcritical heat pump cycle with an IHX

Figure 3.12 presents the T-s diagram of transcritical heat pump cycle of iso-butane with an internal heat exchanger, where step 6-1 is heating the working fluid further and step 3-4 is cooling it down further.

$$\eta_{IHX} = \frac{h_1 - h_6}{h_3 - h_4} \tag{3.4}$$

The IHX is based on enthalpy balance, and an efficiency, η_{IHX} definiens how well heat is transferred, calculated using Equation 3.4. In cycles with phase change, the main advantage of using an IHX is to avoid droplets of liquid entering the compressor. It is especially important for the turbo compressor, as it is extra sensitive to liquid droplets. Decreasing the temperatures of the working fluid further before it enters the expansion valve reduces the throttling losses, increasing the efficiency of the cycle.

3.5.5 Heat exchanger

The plate heat exchanger (PHE) is chosen as the basic design for both the gas cooler, gas heater and the internal heat exchanger, mainly due to its ability to be utilized for a single-phase flow as well as in condensers and evaporators. Another benefit with the PHE is its ability to access the different plate surfaces for cleaning, which is necessary for milk powder applications where fouling is a challenge.

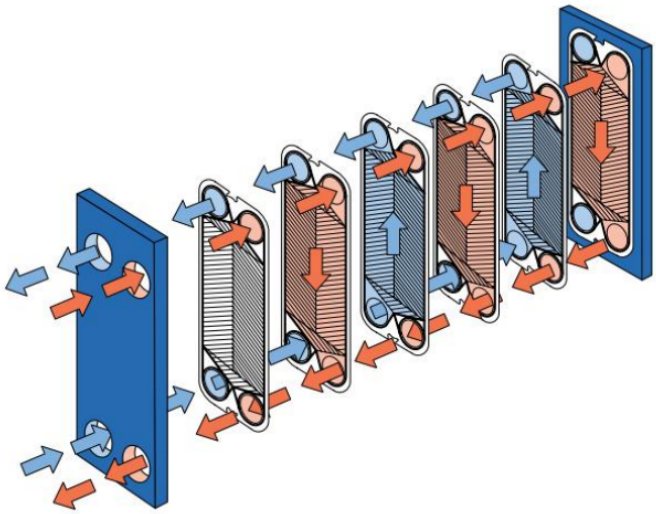

Figure 3.13: Illustration of the plate heat exchanger

The PHE is composed of a number of thin, corrugated metal plates compressed together with a frame, with gaskets placed between each plate to seal the space between them. The gaskets also make sure that the hot and cold fluids flow in different channels, as presented in Figure 3.13. Different suppliers use different materials for the gaskets, chosen regarding the required tolerances of temperature and pressure. The suppliers design their own patterns on the plates implemented to induce turbulence. Turbulence decreases fouling as well as increasing heat transfer efficiency [33]. Specifications for the PHE is presented in Table 3.2 [33].

Table 3.2: General information about the PHE

Heat transfer area range	$0.02m^2$ to $4.45m^2$
Temperature range	-35°C to +200°C
Design Pressure	Up to 40 bar
Flow rates	Up to 5,000 m^3/hour
Fouling Resistance	25%

There are four main types of plate heat exchangers; plate and frame heat exchanger, partly welded heat exchanger, fully welded heat exchanger and the blazed heat exchanger [33]. When using a heat exchanger in higher pressures and temperature ranges, the main challenges for the PHEs is the gaskets. Most gaskets cannot handle temperatures over 200 °C, as presented in Table 3.2. The brazing heat exchanger, on the other hand, the plates are brazed together instead of using gaskets, and the fully welded heat exchanger uses welding instead of gaskets. These two models are therefore the better alternatives

in a high-temperature heat pump application [34], as the temperatures can be increased beyond 200°C.

3.5.6 Expanders

Expanding devices are used to decrease the pressure after the heat rejection. By decreasing the pressure before reheating, less heat is required to heat the working fluid before compression. Two types of devices are used in this thesis, expansion valves and turbine expanders.

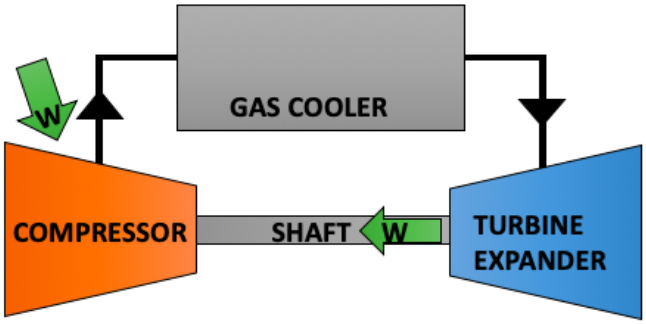

Figure 3.14: Illustration of a turbine expander

For the supercritical cycle, a turbine expander is utilized. A shaft connects the turbine expander to the compressor, illustrated in Figure 3.14. When the expansion occurs, energy is released, and the turbine expander aims convert this into useful work that can be utilized in the compressor. It can decrease the amount of required compression work and thereby increases the COP. The work available from the expansion process is given by Equation 3.5

$$W_t = \dot{m} \times (h_{in} - h_{out}) \tag{3.5}$$

There will be losses in the process, the same way a compressor is subjected to an isentropic efficiency, given in Equation 4.5.

$$\eta_{is,turbine} = \frac{h_{in} - h_{out}}{h_{in} - h_{out,is}} \tag{3.6}$$

The turbine expander is suitable because the supercritical cycle is a gas cycle. Cavitation tends to occur when the turbine expander is used in a cycle with phase change. Therefore, the transcritical cycle uses an expansion valve, as it is more suitable to handle two-phase flow. Expansion valves are often assumed isenthalpic. The disadvantage with an expansion valve is that the available energy in the expansion is lost.

3.6 Case Description

Table 3.3 presents the values for a specific spray-dryer, and it is these values the thesis will be based on. The problem statement is to heat outdoor air from a temperature of 15°C to the required air temperatures of 200°C. The heat source will be the excess air from the process at a temperature of 98°C and the air flow rate of $8.75 kg/s$.

Table 3.3: Design parameters for the spray dryer

Operation parameter	Value
Inlet air temperature	200°C
Outlet air temperature	98°C
Air rate	8.75kg/s
Air pressure	1 atm
Moisture content	108.5(% DB)

By using these values, three different heat pump configurations will analysed and compared. The three heat pumps models are;

- Transcritical heat pump cycle using iso-butane as the working fluid
- Supercritical heat pump cycle using carbon dioxide as the working fluid
- Compression-absorption heat pump cycle using a mixture of ammonia and water as the working fluid

Calculations will be conducted on the transcritical and supercritical heat pump cycle. EES is used to develop heat pump models for the calculations, and the study consist of a thermodynamic analysis of the two cycles, followed by a study to optimize the heat transfer through the gas cooler and gas heater. Each model requires different pressures, temperatures and mass flow rates. The cycles will have different challenges and different limitations which will be presented and analyzed.

A literature review will then be conducted in compression-absorption systems found for similar spray-dryer situations, and the results will be compared to what was found for the transcritical and supercritical cycle. The final aim is to provide a recommendation on the potential of each heat pump cycle.

4 Methodology

To be able to study the different heat pump cycles, the heating demand, heat load and limitations from the spray-drying facility has to be defined. When these values are calculated, the methodology chapter will present the set-up for the thermodynamic analysis and the set-up of the heat exchangers used.

4.1 Heating capacity from the Spray-Dryer

4.1.1 Heating Capacity for the Heat Pump

The heat pump solutions are required to heat air from a temperature of 15°C to a temperature of 200°C. The mass flow rate of air, $\dot{m}_{air}$, is constant at 8.75 kg/s and the air pressure is constant at 1 atm. Using Equation 4.1, the heating load required in the heat pump cycles, $\dot{Q}_{air}$, is 1.64MW.

$$\dot{Q}_{air} = \dot{m}_{air} \times (h_{in} - h_{out}) \tag{4.1}$$

Where h_{in} and h_{out} are the enthalpies in J/kg for the inlet and outlet air, for the temperature and pressure presented.

4.1.2 Heating Load from the Excess Air

The excess air from the spray-dryer provides the heat load to the heat pump solutions. From Table 3.3 presents an excess air temperature is 98°C, a pressure of 1atm and has a flow rate of 8.75kg/s. To determine the heat load provided, the outlet temperature after heat extraction has to be calculated, taking fouling into consideration.

Equation 2.3 calculates the glass transition temperature using the surface water activity, but for the given case, the surface water activity is unknown. However, the case description presents the moisture content on a dry basis to be 108.5.

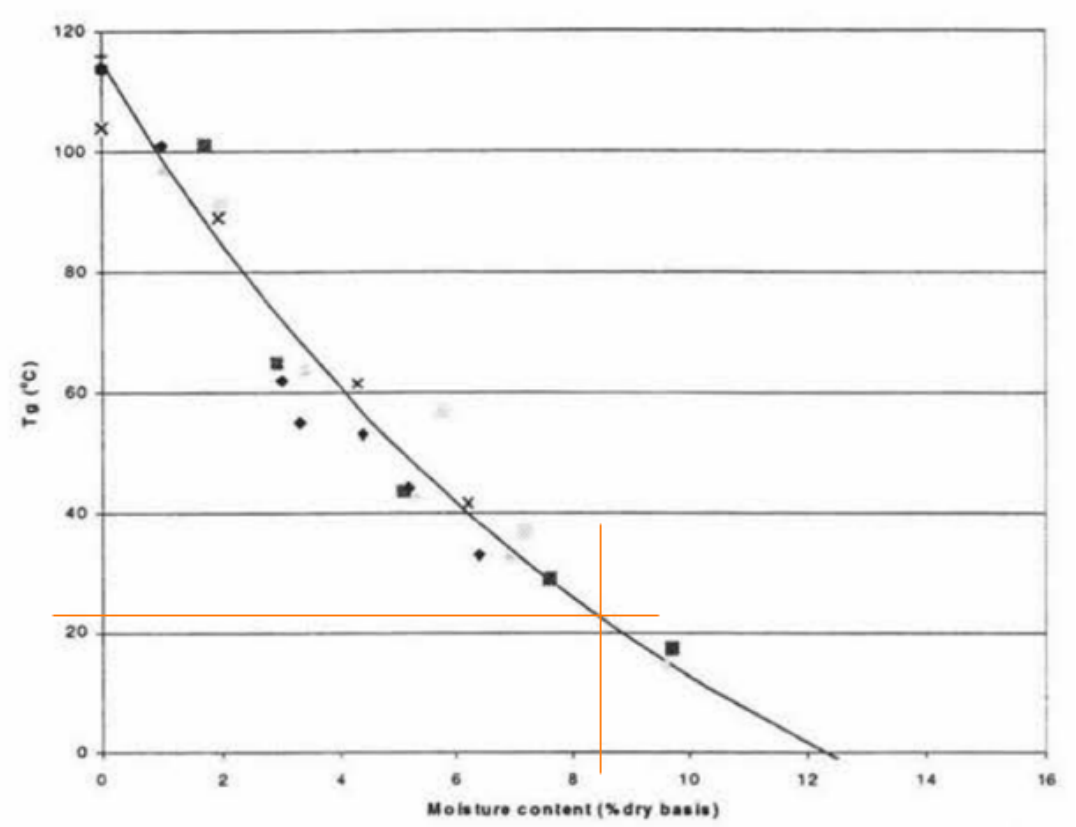

Figure 4.1: Glass transition temperature vs moisture content

Figure 4.1 [11] relates the moisture content to glass transition temperatures. For the specific scenario, the T_g is found to be 22 °C. Using T-T_g=38°C relationship, the minimum temperature to avoid fouling is 60°C.

By designing the heat extraction with an outlet temperature of 60°C, fouling should be avoided, and the pressure drop and the reduction in heat transfer rate described in Section 4.1.2 is excluded from the rest of the study.

Using Equation 4.1 with an inlet air temperature of 98°C, outlet air temperature of 60°C, a pressure of 1 atm and a mass flow rate of 8.75kg/s gives a heat load of 0.34MW from the excess air.

4.1.3 Limitations in Heating Capacity

A heat load of 0.34MW cannot alone be utilized in a heat pump solution to produce a heating capacity of 1.64MW. The full mass flow rate of air can simply not be heated to a temperature of 200°C with the heat provided. As the aim of the thesis is to study the possibilities of a high-temperature heat pump solution, the analysis is chosen to focus on increasing the temperature of air from a temperature of 15°C to 200°. It is achieved by

reducing the mass flow rate that is heated, and the result will present the mass flow rate of air that can be heated in the different heat pump solutions.

As the heat pump solution does not cover the full heating demand, an electric heater or oil burner will have to be utilized somewhere in the process. Still, if the heat pump solution can reduce the mass flow of air that requires heating by an electrical heater or oil burner, it is an improvement and a step in the right direction in making the process more sustainable.

4.2 Thermodynamic Analysis Set-Up

The thermodynamic analysis is conducted using EES to find the optimum heat pump design for the transcritical and supercritical heat pump cycle. The EES codes are placed in the appendix.

The pressure difference in the gas coolers is high for both cycles. Therefore, the temperature difference between the two flows is set to be 20K. Therefore, the compressor discharge temperature aims to reach a temperature of 220°C.

The compressor efficiency is set to constant at 70% for both cycles, and the volumetric efficiency is constant at 80 %.

4.2.1 Transcritical Cycle

The transcritical cycle heat pump cycle is constructed by four main stages, presented in the pressure-enthalpy diagram in Figure 4.2.

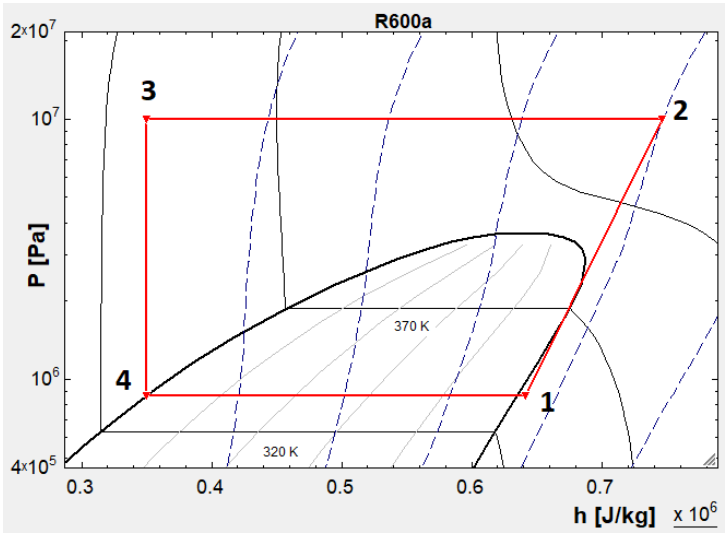

Figure 4.2: P-h diagram for the transcritical heat pump cycle using iso-butane as the working fluid

- **Evaporator, Stage 4 - 1**

The heat load of 0.34MW is utilized in the evaporator. The evaporation temperature cannot be higher than the temperature of the excess air temperature for heat transfer to occur. Therefore, 60°C is set as the lower temperature limit. It is possible to have a higher evaporation temperature, but it will decrease the heating load for the process to utilize. As the heating load is already low, it would be un-ideal to decrease it further. Therefore, the evaporation temperature is defined as constant for the solution, chosen to be 60°C.

Such a temperature gives an opportunity to sub-cool the working fluid significantly before expansion. Due to this, the full evaporation energy of iso-butane can be utilized, as illustrated between point 4 and 1 in Figure 4.2.

With these conditions, the ideal evaporation pressure is 8.7bar, and the mass flow rate of iso-butane, $\dot{m}_{R600a}$, is 1.2 kg/s. Both are kept constant through the analysis.

- **Compressor, Stage 1 - 2**

The compressor increases the temperature by compressing the working fluid and aims to reach a discharge temperature of 220°C. For an ideal heat pump cycle, the compression is assumed isentropic. For the transcritical cycle, compression losses is taken into consideration. An efficiency of 0.7 is assumed, η_{comp}, defining the compression discharge point by Equation 4.2.

$$\eta_{comp} = \frac{h_{2s} - h_1}{h_2 - h_1} \tag{4.2}$$

Where h_1 and h_2 are the enthalpies at compression inlet and outlet, respectively, and h_{2s}

is the isentropic enthalpy at the compressor discharge point. The compression work is calculated using Equation 4.3.

$$W_{comp} = \dot{m}_{R600a}(h_2 - h_1) \tag{4.3}$$

The swept volume of the working fluid is calculated at Stage 1, using Equation 3.2 and a volumetric efficiency of 60%.

The compression aims to reach a temperature of 220°C, but a discharge temperature between 200°C and 220°C is analysed in the thermodynamic analysis.

- **Gas cooler, Stage 2 - 3**

The discharge pressure from the compressor is the pressure in the gas cooler, as piping losses are excluded from the analysis.

$$\dot{Q}_{GC} = \dot{m}_{R600a} \times (h_2 - h_3) \tag{4.4}$$

Equation 4.4 is used to calculate the heat rejected in the gas cooler. The gas cooler utilized in the thermodynamic heat pump cycle is assumed isobaric, and will be analysed further in the heat exchanger optimization.

- **Expansion valve, Stage 3 - 4**

As the working fluid is going through a phase change after being cooled down, it is challenging to use a turbine expander. Instead, an expansion valve is utilized, having a constant enthalpy. Therefore, the enthalpy at the gas cooler exit, point 3 is defined by the enthalpy at point 4. Point 4 is already defined by a constant evaporation temperature of 60°C. The COP of the cycle is calculated using Equation 3.1

Table 4.1 summarizes the known and unknown values in the transcritical heat pump cycle. The unknown values will be calculated in the thermodynamic analysis.

Table 4.1: Known values from the transcritical iso-butane heat pump set-up

	m	**P**	**T**	**h**
Point 1	1.2 kg/s	8.7 bar	60°C	633kJ/kg
Point 2	1.2 kg/s	Varies	Varies	Varies
Point 3	1.2 kg/s	Varies	Varies	350kJ/kg
Point 4	1.2 kg/s	8.7bar	60°C	350kJ/kg

4.2.2 Supercritical Cycle

The supercritical cycle differs from the transcritical cycle by never entering the two-phase region. Instead, the whole process occurs in the supercritical region, with no phase change. The supercritical cycle is illustrated in Figure 4.3.

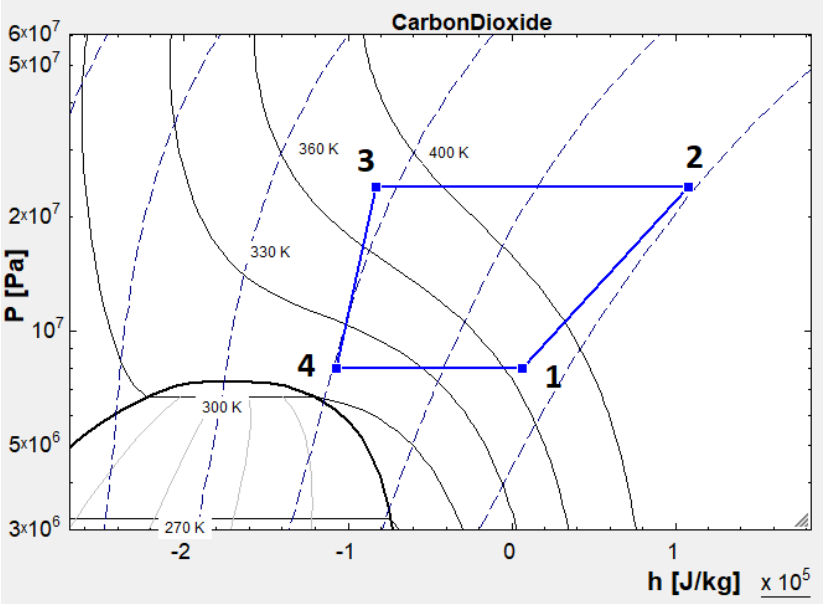

Figure 4.3: P-h diagram for the supercritical heat pump cycle using carbon dioxide as the working fluid

- **Gas heater, Stage 4 - 1**

A gas heater is used to utilize the 0.34MW of heat from the excess air. The gas heater has a lower pressure limit, as the pressure has to be above the critical pressure. The critical pressure of CO_2 is 7.39 MPa, so the lowest possible gas heating pressure is set to 7.5 MPa.

The maximum gas heater pressure is set to 10 MPa. In theory, it is possible for the supercritical cycle to work at even higher pressures, but by increasing the gas heating pressure, the gas cooler pressure increases as well. Regarding equipment, it is very challenging to operate under higher pressures, so the limitation is set to increase the likelihood of developing equipment that handles the conditions.

The gas heater inlet temperature is limited by the outlet temperature of the excess air, 60°C. Since the gas cooler allows a temperature glide, the gas cooler outlet temperature has a maximum temperature of 98°C.

The gas heater ΔT is set to 15K, as the pressure difference between the working fluid and the air flow is large. Therefore, the outlet temperature is 83°C.

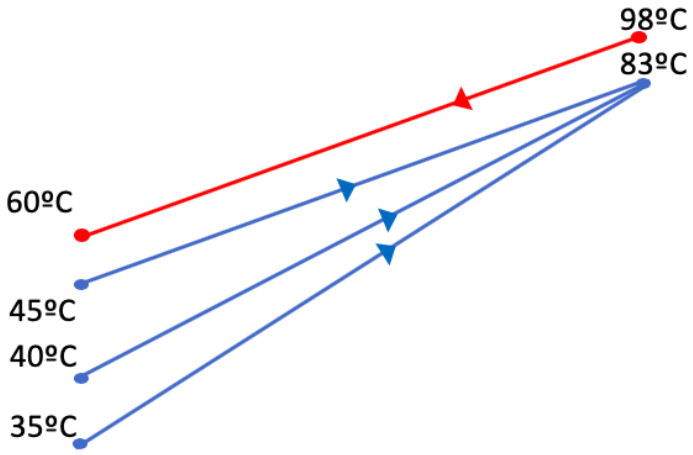

Figure 4.4: Possible inlet temperatures in the gas heater

The gas cooler inlet temperature can vary, as presented in Figure 4.4, as a reduction in inlet temperature does not reduce the heat load utilized. Still, for simplicity, the ΔT is kept constant at both the inlet and outlet of the gas heater, making the gas heater inlet temperature to be 45°C.

The gas heater is assumed isobaric in the transcritical analysis, and studied further in the heat exchanger optimization.

- **Compressor - Stage 1 - 2**

The compression is modelled the same way as for the transcritical cycle. The discharge temperature of the compression aims to reach a temperature of 220 °C and the isentropic efficiency is assumed to be 0.7.

- **Gas cooler - Stage 2 - 3**

The gas cooler is modelled the same way as for the transcritical cycle. It is assumed isobaric and analysed further in the heat exchange optimization section.

- **Turbine expander - Stage 3 - 4**

A turbine expander is utilized to decrease the pressure from stage 3 - 4, and produces usable work. The turbine expander has an efficiency of 0.6, and the gas cooler exit point is defined by Equation 4.5.

$$\eta_{is,turbine} = \frac{h_3 - h_4}{h_3 - h_{4s}} \tag{4.5}$$

For the supercritical cycle, the COP is depended on the heating capacity of the gas cooler, the work used by the compressor and the work produced by the turbine expander, and is

calculated using Equation 4.6.

$$COP = \frac{Q_{GC}}{W_{comp} - W_{TX}} \tag{4.6}$$

The mass flow rate is unknown for the cycle. It cannot be defined directly, but will be depended on the gas heater pressure. It will therefore be calculated and optimized in Section 5.1.5.

The values are summarised in Table 4.2. The unknown values will be calculated in the thermodynamic analysis.

Table 4.2: Known values from the supercritical CO_2 heat pump set-up

	m	**P**	**T**
Point 1	Varies	7.5MPa-10MPa	83°C
Point 2	Varies	Varies	220°C
Point 3	Varies	Varies	Varies
Point 4	Varies	7.5MPa-10MPa	45°C

4.3 Heat Exchanger Calculations

For the thermodynamic analysis, an isobaric heat transfer is assumed, and the heat load is based on $Q = \dot{m}(h_{in} - h_{out})$. The heat exchanger analysis aims to study how the heat transfer is behaving and how it can be optimized. It is done using plate heat exchanger with a counter-flow configuration. The study focuses on optimizing the geometry and is used to determine which heat pump solutions that should be recommended.

The calculations of the gas cooler and gas heater will be the same thermodynamically, but differs in which fluid is the hot fluid and which one is the cold fluid, summarized in Table 4.3.

Table 4.3: Hot side and cold side for the different heat exchange configurations

	Transcritical gas cooler	**Supercritical gas cooler**	**Supercritical gas heater**
Cold side	Air	Air	CO_2
Hot side	Iso-butane	CO_2	Air

The scenarios will have different mass flow rates and pressures, causing different geometries to be necessary for each scenario.

Both the gas cooler and gas heater is based on the design of a plate heat exchanger in a counter-flow configuration. EES is used to model the heat exchanger and for the calculations, with a model based on a sub-heat exchanger set-up, which iteratively calculates the heat transfer in each heat exchange unit. This is illustrated in Figure 4.5.

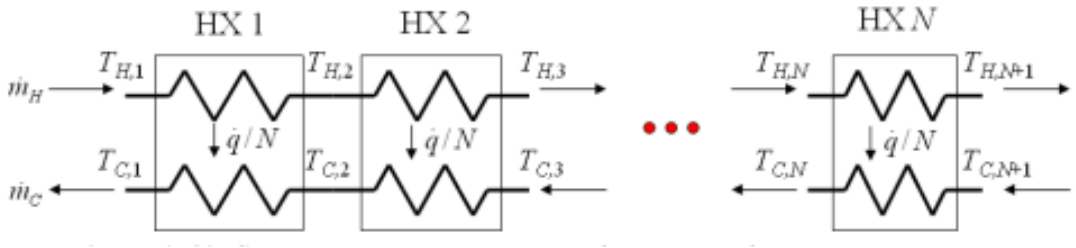

Figure 4.5: Model illustrating the concept of sub-heat exchangers for a counter-flow configuration

Values from the thermodynamic analysis are used in the heat exchanger calculations. The inlet temperature, outlet temperature and pressure of the air being heated up are defined in the case description. The thermodynamic analysis provides the inlet and outlet temperature, the pressure, the mass flow rate of the working fluid and the heating load from each thermodynamic cycle. The air flow rate in the gas heater will be 8.75kg/s, while the gas cooler heating load is used to calculate the mass flow rate of air that can be heated, using Equation 4.7.

$$\dot{m}_{air} = \frac{\text{Heating capacity of the heat pump solution}}{\text{Enthalpy difference in the gas cooler}} \tag{4.7}$$

The aim of the gas cooler is to heat the air between the given temperatures utilizing the heat load produced in the heat exchanger. The aim of the gas heater is to utilize the heat load from the excess heat to provide enough heat to the heat pump. By keeping these values constant, it is the geometry of the heat exchanger that will vary.

The geometries values of width, W, number of channel pairs, N_{ch}, channel width on the hot and cold side, t_h and t_c, and thickness of the plate,t_m, are the geometry values that the calculations are based on, and are assumed known. When the geometry is optimized, these values are varied to achieve the best possible solution.

The heat exchanger calculations are based on a changing length to be suitable for the heat transfer and geometry defined.

For each sub-heat exchanger, the ϵ-NTU method is applied. The hot and cold side capacitance rates for each sub-heat exchanger, calculated through equation 4.8 and 4.9.

$$\dot{C}_{H,i} = \dot{m}_H \times \frac{(i_{H,i} - i_{H,i+1})}{(T_{H,i} - T_{H,i+1})} \tag{4.8}$$

$$\dot{C}_{C,i} = \dot{m}_C \times \frac{(i_{C,i} - i_{C,i+1})}{(T_{C,i} - T_{C,i+1})} \tag{4.9}$$

Where i_{H_i} and $i_{H,i+1}$ is the hot-side inlet and outlet enthalpy in each sub-heat exchanger, J/kg, and i_{C_i} and $i_{C,i+1}$ is the cold-side inlet and outlet enthalpy in each sub-heat exchanger, J/K. $T_{H,i}$ and $T_{C,i}$ are the inlet temperatures into each sub-heat exchanger, in °K.

It can be calculated as the mass flow rate, pressure, inlet temperature and outlet temperature is known for the flows. The minimum capacity rates are then used together with the temperature difference between the air and the working fluid to calculate the effectiveness, ϵ in each sub-heat exchanger.

$$\epsilon_i = \frac{\dot{q}/N}{MIN(\dot{C}_{C,i}, \dot{C}_{H,i})(T_{H,i} - T_{C,i+1})} \tag{4.10}$$

Where q is the heat load in each sub-heat exchanger and N is the number of sub-heat exchangers. N is set to be 15 for all the calculations.

The effectiveness is defined as the ratio between the actual heat transfer rate to the maximum heat transfer rate, $\epsilon = \frac{\dot{Q}}{\dot{Q}_{max}}$. For the gas coolers and the gas heater, the effectiveness will be quite low, due to the large pressure difference between the hot and cold fluid and the large temperature differences.

$$UA_i = NTU_i MIN(\dot{C}_{C,i}, \dot{C}_{H,i}) \tag{4.11}$$

The conductance of each sub-heat exchanger, UA_i, is calculated using Equation 4.11. It is depended on the NTU_i value, which is found in EES, depending on the effectiveness and the capacities in each sub-heat exchanger.

$$\Delta x_i = \frac{UA_i}{2N_{ch}W}\left(\frac{1}{h_{C,i}} + \frac{th_m}{k_{m,i}} + \frac{1}{h_{H,i}}\right) \tag{4.12}$$

The conductance of each sub-heat exchanger is translated into a physical size of the heat exchanger, based on equation 4.12. $h_{c,i}$ and $h_{h,i}$ are the local heat transfer coefficient of the cold and hot side, respectively, found by calling the function DuctFlow_local in EES. $k_{m,i}$ is the conductivity of the metal at the local average temperature. Aluminum is the

chosen metal for the heat exhanger in the simulations. With the values for Δx, the length of the full heat exchanger is calculated by Equation 4.13.

$$x_{i+1} = x_i + \Delta x \tag{4.13}$$

$h_{h,i}$ is dependent of the temperature difference in the sub-heat exchanger, the pressure of the hot fluid, mass flow rate of the hot fluid, channel width on the hot side and width of the heat exchanger. The same goes for the $h_{c,i}$, only with the cold properties. Therefore, when using Equation 4.13, all the geometry values is affecting the required length of the heat exchanger.

$$err = \frac{|\, x_{N+1} \,| - L}{L} \tag{4.14}$$

The final step of the model is to calculate the difference in the guessed value of the length and the x that was found, using Equation 4.14.

By changing the different geometry variables, the model is aiming to design an efficient heat exchanger. With all the geometry changes a different length is required and a different heating load used. As the value of the working fluid outlet temperature is not defined but known in the analysis, this is done to determine whether or not the given solution is suitable in the thermodynamic cycle that is defined.

The full EES code is presented in Appendix, and based on a model found in the EES guide book Heat Transfer [35].

5 Results and Discussion

The result and discussion section are divided into 3 parts. Part 5.1 is a thermodynamic analysis aiming to design a heat pump solution suitable for the given case, producing a compressor discharge temperature of 220°C. A transcritical cycle using iso-butane as the working fluid and a supercritical cycle using CO2 are studied. Part 5.2 analyses the possibility of utilizing the heat found in the excess air and to heat the air, with the specifications given by the two heat pump cycles. Part 5.3 compares the results of part 5.1 and 5.2 with the literature found on a compression-absorption heat pump cycle.

5.1 Thermodynamic Analysis

The heat pump cycles are designed to utilize the heat load from the excess air to heat dry air from 15°C to 200°C. The temperature difference in the gas cooler is set to be 20K, due to the pressure difference between the working fluid and the air. Therefore, the compressor discharge temperature aims to reach a minimum temperature of 220°C. The heat load from the excess heat was found to be 0.34MW in Section 4.1.2. The analysis is focusing on COP and the heating capacity of gas cooler.

5.1.1 Transcritical Heat Pump Cycle using Iso-Butane as the Working Fluid

The values from Table 4.1 are used in the thermodynamic analysis of the transcritical cycle. By evaluating the compressor discharge temperature and gas cooler pressure, the analysis aims to optimize the heat pump cycle, through increasing the COP and heating capacity. The compressor efficiency is 0.7, and the expansion is isenthalpic through the full analysis.

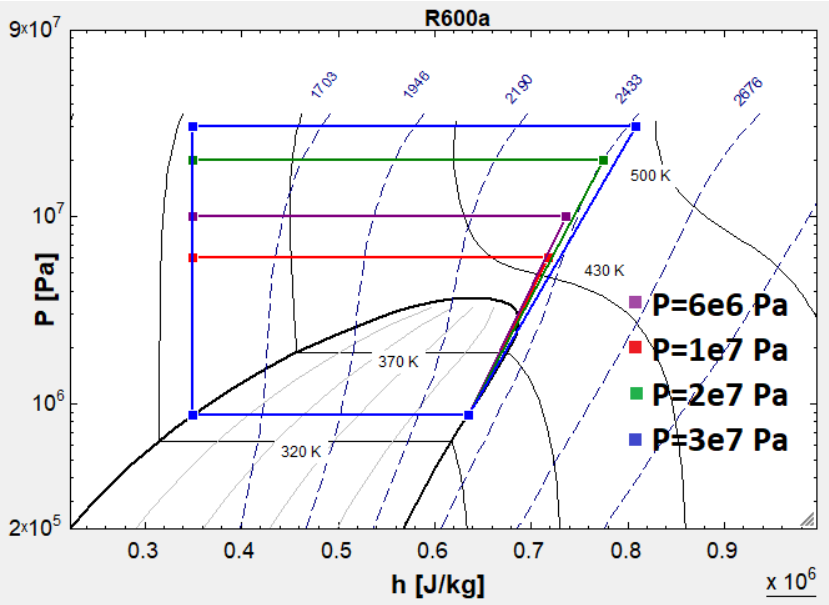

Figure 5.1: P-h diagram for the transcritical iso-butane cycle for different gas cooler pressures

For the scenario described in Section 4.2.1 and with the the values given in Table 4.1, there is no possible solution. Due to the overhanging liquid-vapour dome of iso-butane and the efficiency of the compressor, liquid droplets will appear in the compression. This is illustrated in Figure 5.1 and is a solution that cannot be used.

There are two possible solutions to the problem that will be discussed further;

- The use of an internal heat exchanger
- To overheat the working fluid in the evaporator

The solutions are presented in Figure 5.2.

Figure 5.2: Improved transcritical cycles using iso-butane as the working fluid

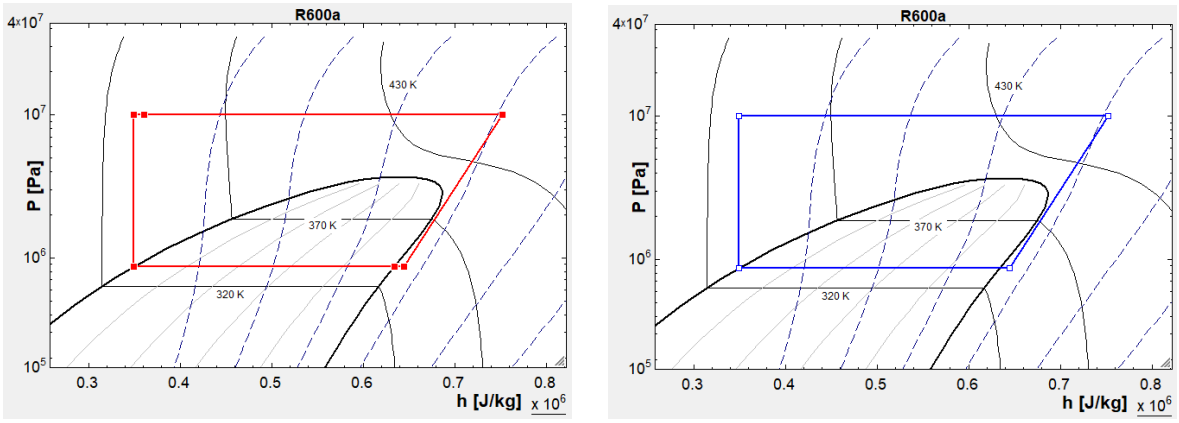

(a) Iso-butane transcritical cycle with an internal heat exchanger

(b) Iso-butane transcritical cycle with a overheated working fluid

Both solutions increase the compressor suction gas temperature, assuring that the working fluid does not enter the two-phase region during compression. The minimum temperature increase is 3 °C, causing the suction gas temperature to be at least 63°C.

The use of an internal heat exchanger (IHX) is illustrated in Figure 5.2a, based on the principle explained in Section 3.5.4. It requires the system to add another component and causes a lower heating load produced in the gas cooler, as some of the heat is utilized in the IHX. The advantage is that the mass flow rate does not change. In the overheated solution, the mass flow rate is decreased for the process to utilize the same heating load of 0.34MW. The solution does not require any new components, but the overheating has to be taken into consideration when designing the evaporator. The solution is presented in Figure 5.2b.

The analysis aims to determine the effect of increasing the suction gas temperature, how it affects the gas cooler pressure, the heating capacity, the COP and the swept volume. The two solutions are analyzed separately and compared to give a recommendation.

5.1.2 Transcritical Iso-Butane Heat Pump Cycle with an Internal Heat Exchanger

The first analysis studies the effect of utilizing an internal heat exchanger. The study is conducted assuming an IHX efficiency of 0.95, and the solutions are plotted for the IHX temperature increase of ΔT=3K, ΔT=5K, ΔT=10K and ΔT=15K. Figure 5.3 presents the change in compressor discharge temperature with an increased gas cooler pressure, for the different ΔT configurations. The critical pressure of iso-butane is 3.72 bar, so the

calculations were started at 4bar. The lower and upper temperature limits are 200°C and 220°C, respectively.

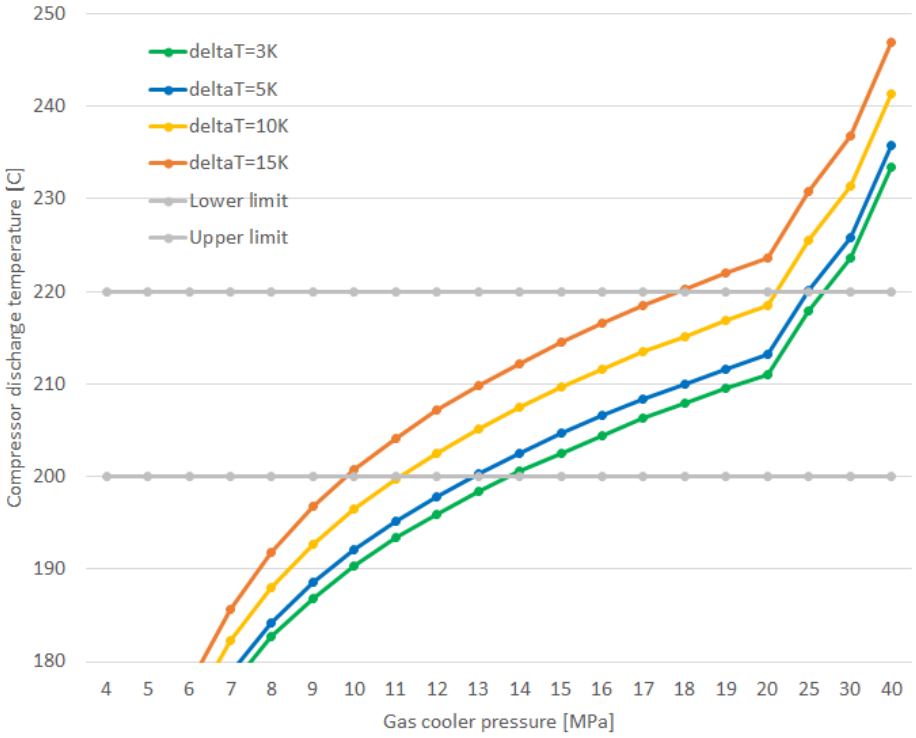

Figure 5.3: Discharge temperature vs gas cooler pressure for a transcritical cycle with an IHX, plotted for the different suction gas temperatures

By increasing the suction gas temperature, the gas cooler pressure can be lower and still reach the desired temperatures. ΔT=15K reaches 220°C at the lowest gas cooler pressure of 18MPa, whereas ΔT of 3K requires a pressure of 26MPa to reach the same temperature. It is caused as the increasing suction gas temperature increases the suction gas enthalpy. When the compressor efficiency is kept constant, a higher suction gas enthalpy gives a higher discharge enthalpy. Between the gas cooling pressures of 6 MPa and 30 MPa, the temperature curves change rapidly. Due to this, a small change in discharge enthalpy has a large effect on the gas cooler temperature and the required gas cooler pressure. The different upper and lower limits are summarized in Table 5.1.

Table 5.1: Summary of the required gas cooler pressures for the different ΔT values in the transcritical heat pump cycle with an IHX

	ΔT=3K	**ΔT=5K**	**ΔT=10K**	**ΔT=15K**
P_{GC} reaching 200°C	14MPa	13MPa	12MPa	10MPa
P_{GC} reaching 220°C	27MPa	25MPa	23MPa	18MPa

Figure 5.4 presents the heating capacity for the different suction gas temperatures at different gas cooler pressures. For each ΔT, the limitation of a discharge temperature between 200°C and 220°C is set, causing the solutions to be in different gas cooler pressures between 10 MPa and 25 MPa.

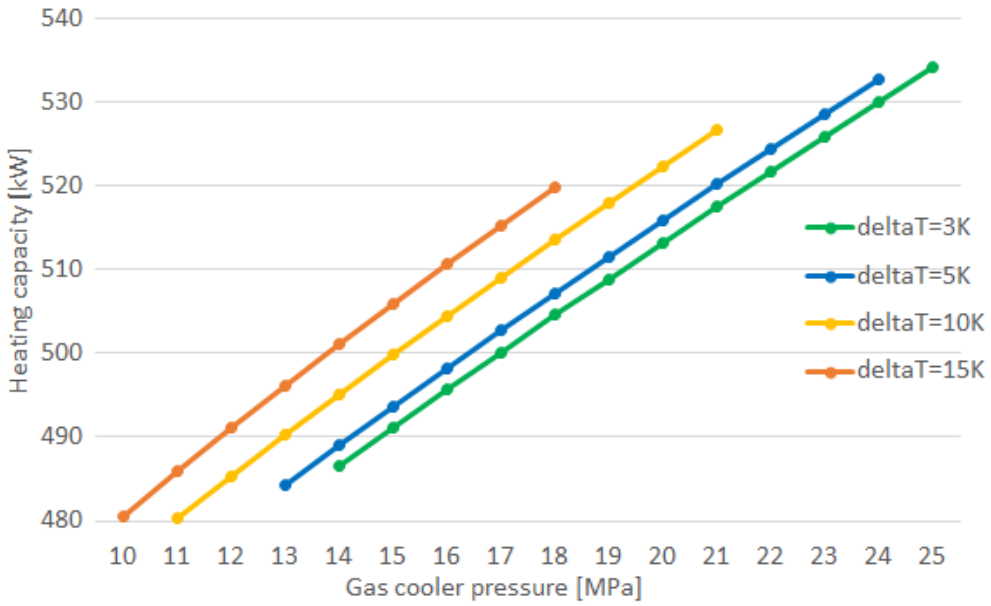

Figure 5.4: Heating capacity vs gas cooler pressure for a transcritical cycle with an IHX, plotted for the different suction gas temperatures

For each ΔT, the heating capacity increases with the gas cooler pressure, caused by an increase in the discharge temperature. The model is defined with a constant evaporation temperature of 60°C and an isenthalpic expansion, causing the gas cooler exit enthalpy to stay constant. Therefore, by increasing the discharge temperature, a higher enthalpy-difference is achieved in the gas cooler and thereby a larger heating capacity.

It is seen that the ΔT=3K can produce the highest heating capacity, even though all the results are plotted with a discharge temperature between 200°C and 220°C. It is caused as the IHX requires some of the heat that could have been utilized in the gas cooler. To increase the suction gas temperature with 15K requires a higher heating capacity than to increase it with 3K, causing the heating capacity in the gas cooler with a of 15K to be lower for the same discharge temperature.

The COP compares the heating capacity to the compression work, presented in Figure 5.5. The change in COP is plotted with an increasing gas cooler pressure, for the different ΔT values. The discharge temperature is limited between 200°C and 220°C, giving gas cooler pressures between 10 MPa and 25 MPa.

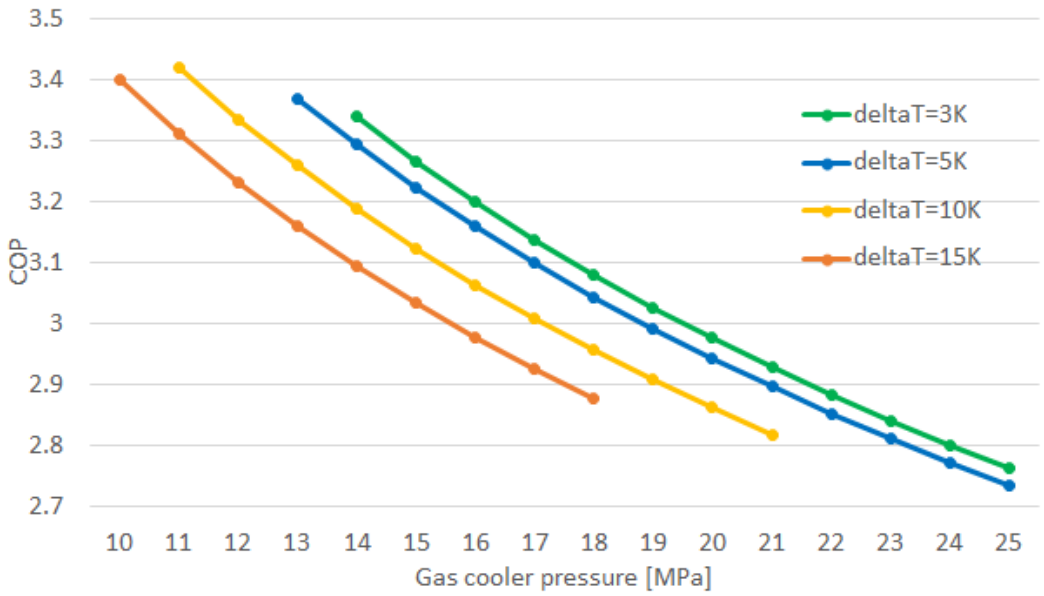

Figure 5.5: COP vs gas cooler pressure for a transcritical cycle with an IHX, plotted for the different suction gas temperatures

The result shows that the COP decreases with an increasing gas cooler pressure, for all the ΔT scenarios. It is caused by an increasing pressure ratio, which increases the compression work. On the other hand, the heating capacity from Figure 5.4 presented an increase with the increasing gas cooling pressure. Therefore, the compression work is found to be the more dominant factor in determining the COP.

If the COP is compared at a constant gas cooler pressure, giving a constant compressor PR, the lower ΔT has the higher COP. By studying the gas cooler pressure of 16MPa, it is seen that =3K has a COP of 3.2 while ΔT=15K has a COP of 2.96. At 16MPa, ΔT=15K has the highest discharge temperature, but the lower heating capacity causes it to have the lowest COP.

5.1.3 Transcritical Iso-Butane Heat Pump Cycle with an Overheated Working Fluid

To overheat the working fluid in the evaporator requires the mass flow rate to decrease, due to the constant excess heat load and the constant temperature of evaporation. The different mass flow rates are calculated and presented in Table 5.2, belonging to the different suction gas temperatures.

Table 5.2: Change in mass flow rate with a overheated working fluid in the transcritical iso-butane heat pump cycle

Increase in temperature [°C]	ΔT=0	ΔT=3	ΔT=5	ΔT=10	ΔT=15
New mass flow rate [kg/s]	1.195	1.169	1.152	1.112	1.074

The change in compressor discharge temperature with an increased gas cooling pressure should be analysed the same way as it was done for the IHX solution. However, the results are the same as when using an IHX. The reason is that the mass flow rate is changed to have the same increased suction gas temperatures as the IHX solution. The discharge temperature is depended on the gas cooler pressure, compressor efficiency, suction gas temperature and the evaporation pressure. All of these variables are the same for both cases, and the discharge temperature is not dependant on the mass flow rate. Therefore, the results are the same as presented in Figure 5.3 and Table 5.1.

The heating capacity for each ΔT are presented in Figure 5.6 with an increasing gas cooler pressure. The plot is limited to scenarios where the discharge temperature is between 200°C and 220°C. The heating capacity increases with an increasing gas cooler pressure, as a higher gas cooler pressure gives a higher discharge temperature.

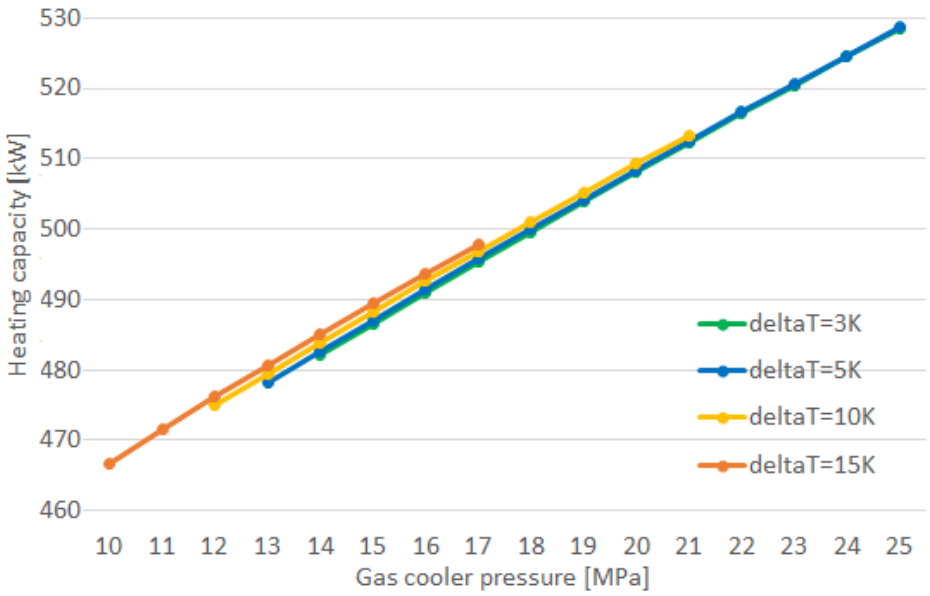

Figure 5.6: Heating capacity vs gas cooler pressure for a transcritical cycle with an overheated working fluid, plotted for the different suction gas temperatures

The lower values of ΔT has a higher heating capacity, even though all scenarios are reaching the same discharge temperatures. It is due to the higher mass flow rate at the

lower ΔT. The working fluid is used to transfer heat through the heat pump cycle, and by increasing the mass flow rate, more heat is transferred through the system.

When studying each gas cooling pressure separately, it is seen that the higher ΔT has a higher heating load, but the difference is a lot smaller than for the IHX. At a gas pressure of 16 MPa, the difference between the scenarios is less than 5kW, whereas the difference between ΔT=3K and ΔT=15K was found to be around 15kW for the IHX. The differences are caused by both the different mass flow rate and discharge temperature. ΔT=3K has a higher mass flow rate while ΔT=15K has a higher discharge temperature, which is giving a similar heating capacity at the same discharge pressure.

Figure 5.7 presents the change in COP for the different ΔT with an increasing gas cooler pressure. The plot is limited to scenarios where the discharge temperature is between 200°C and 220°C.

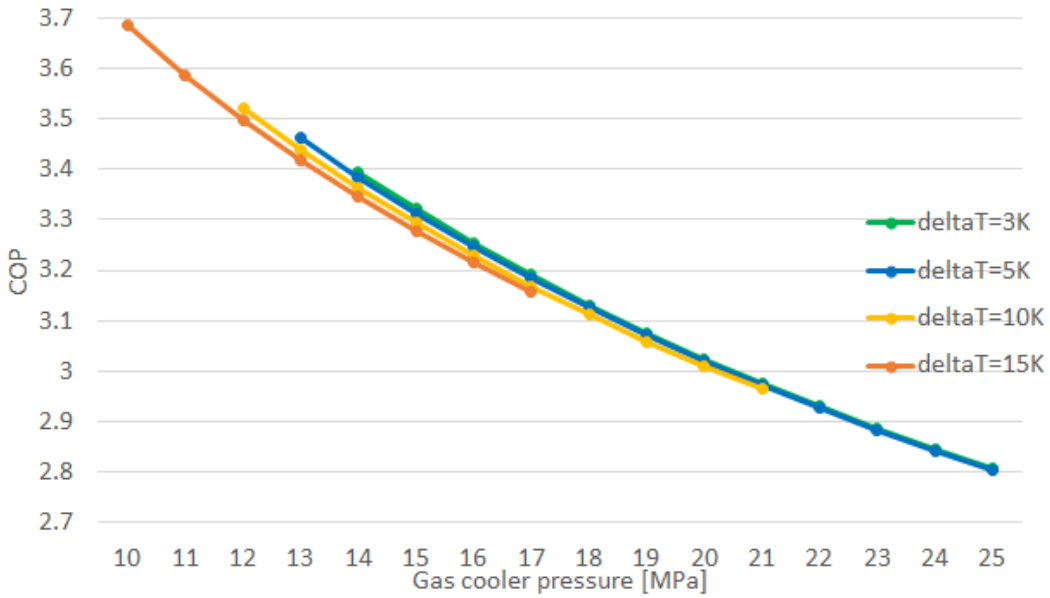

Figure 5.7: COP vs gas cooler pressure for a transcritical cycle with an overheated working fluid, plotted for the different suction gas temperatures

The COP is decreasing with the increasing gas cooling pressure, as the pressure ratio increases. The lower ΔT values have the lowest COP, as the pressure ratio is larger, increasing the compressor work. Also, the required compression work increases with the increasing mass flow rate. Together, the required compression work increases more than the increased heating capacity of the lower ΔT scenarios, decreasing the COP.

5.1.4 Transcritical Comparison and Recommendation

The swept volume should be taken into consideration when comparing the two solutions. It is calculated using Equation 3.2 and presented in Figure 5.8. The density is depended on the suction gas temperature and the evaporation pressure but independent of the pressure in the gas cooler. Therefore, it is plotted for an increasing ΔT.

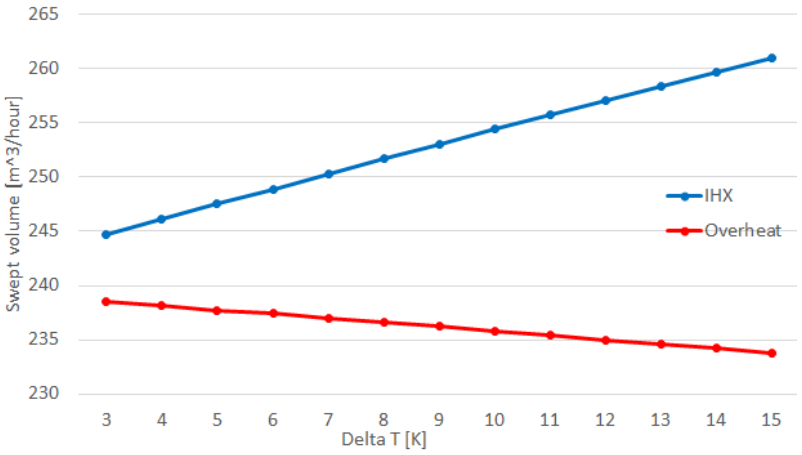

Figure 5.8: Swept volume vs suction gas temperatures, comparing the IHX and the overheated transcritical iso-butane cycles

When the ΔT increases, the specific volume of the gas increases as well. The specific volume is the reciprocal of density, so an increase in the specific volume increases the swept volume. The swept volume is bigger for the IHX solution as the mass flow rate is larger and the swept volume increase with an increasing suction gas temperature. For the overheated solution, the mass flow rate decreases while the specific volume increases, causing the swept volume to change very little.

Table 5.3 compares the heating capacity and the COP when using an IHX and an overheated working fluid. The heating capacity is slightly higher for the IHX than the overheated solution, while the COP is higher for the overheated solution for every simulation. Both the difference in heating load and COP increases between the two scenarios with an increasing ΔT.

Table 5.3: Comparison of the COP and heating load when using an IHX and an overheated working fluid

		ΔT=3K		**ΔT=5K**		**ΔT=10K**		**ΔT=15K**	
Discharge temp.		200°C	220°C	200°C	220°C	200°C	220°C	200°C	220°C
$\mathbf{P}_{GC}$		14MPa	27MPa	13MPa	25MPa	12MPa	23MPa	10MPa	18MPa
IHX	Q [kW]	487	534	484	533	480	526	480	520
	COP	3.34	2.76	3.36	2.73	3.42	2.82	3.4	2.89
OH	Q [kW]	482	528	478	529	475	513	467	498
	COP	3.39	2.81	3.46	2.80	3.52	2.96	3.69	3.16

It is seen that the heating capacity is very similar for all scenarios. Therefore, it does not affect the solution much, and COP is chosen as the decisive factor for the recommendation.With this in mind, the scenario of overheating the working fluid is favourable over the IHX solution, as the COP is higher for every ΔT. The lower swept volume is beneficial for the overheated solution and from an economic point of view, the heat pump cycle will be cheaper by having fewer components and easier to maintain.

Bamigbetan (2018) [23] is presenting a study on designing a compressor for high temperature butane compressors. The study agrees that the suction gas has to be heated before entering the compressor but has chosen to use an internal heat exchanger. The study is different from this one by being a sub-critical cycle and requires sub-cooling before expansion. In such a scenario, an internal heat exchanger is the better option. For this case, sub-cooling is not necessary, and the internal heat exchanger only decreases the heating load and thereby also the COP. Therefore, the use of an overheated working fluid is the recommended solution. The studies can be compared as butane and iso-butane have a very similar liquid-vapour dome.

The efficiency of the IHX is very high, which might not be possible in the transcritical cycle. Sakar 2007 [20] presents a very similar transcritical iso-butane study. However, the IHX efficiency used was 0.6. If the same efficiency were used for this study, the COP and heating capacity would be even lower. Therefore, the overheated solution is recommended.

To recommend an ideal ΔT to provide a gas cooler pressure is more challenging. The challenge in HTHP is for the equipment, as no equipment on the market can handle the high temperatures and the corresponding high pressures. The highest ΔT has the highest COP and the lowest gas cooler pressure, making it beneficial.

The transcritical iso-butane study presented by Sakar et al. (2007) [20] studies the opti-

mum discharge pressure. The study was using an IHX but concluded that both the effect of the IHX the isentropic efficiency of the compressor was neglectable compared to the optimum evaporating temperature and gas cooler exit temperature. For an evaporation temperature of 20°C, a ΔT of 10K and a discharge temperature of 205 °C, the optimum gas cooler pressure was 12 MPa with a COP of 2.65. The result is similar to the result of this study, presented in Table 5.3 and can be used to validate the results. It agrees that a ΔT=10K is a suitable value to reach 200°C, but does not study the possibility to increase it further or to reach higher pressure rates.

The thesis aims to reach 220°C, and ΔT=15K has the highest COP with lowest gas cooler pressure. The disadvantage of using ΔT=15K is the required increase in the evaporator area. Therefore, a ΔT=10K can be a better option, as it does not increase the pressure rates too much, has a higher heating load and a higher mass flow rate, with only a slight decrease in the COP. The gas cooler pressure and ΔT will be studied further in Section 5.2.1 to find a recommendation.

5.1.5 Supercritical Heat Pump Cycle using Carbon Dioxide as the Working Fluid

The thermodynamic analysis of the CO_2 supercritical cycle is similar to the transcritical one with a compressor discharge temperature of 220°C and the excess heat load of 0.34 MW. It differs from the transcritical cycle by using a gas heater instead of an evaporator, allowing temperature glide. In the gas heater, the ΔT is defined to be 15K, due to the pressure difference between the working fluid and the excess air. Therefore, the compression suction gas temperature is 83°C. The gas cooler pressure is limited to a pressure between 7.5MPa and 10MPa, as described in Section 4.2.2. The supercritical cycle using CO_2 as the working fluid is illustrated in Figure 5.9.

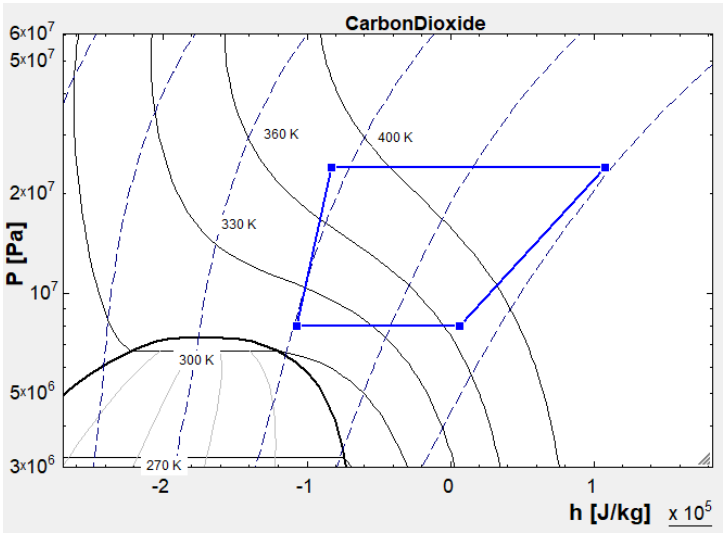

Figure 5.9: P-h diagram for the supercritical heat pump cycle with carbon dioxide as the working fluid

The limiting gas heater inlet temperature of 45 °C is used to calculate the mass flow rate for each scenario, presented in Figure 5.10. The gas heater has a constant heat load of 0.34 MW and an exit temperature of 83 °C, while the inlet temperature changes. All scenarios are plotted for when the cycle reaches 220 °C.

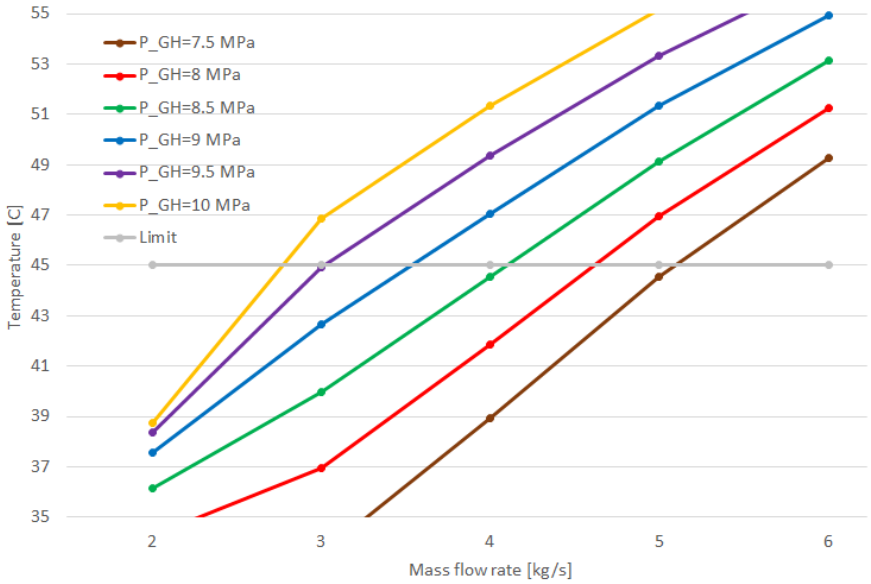

Figure 5.10: Gas heater inlet temperature vs mass flow rate for the supercritical cycle, plotted for the different gas heater pressures

The limiting temperature of 45°C gives the maximum CO_2 flow rate in the gas heater for each gas cooler. For an increasing gas heater pressure, the maximum flow rate decreases.

It is caused by a larger enthalpy difference between the temperature lines of 45 °C and 83°C when the pressure increases, as illustrated in Figure 5.11.

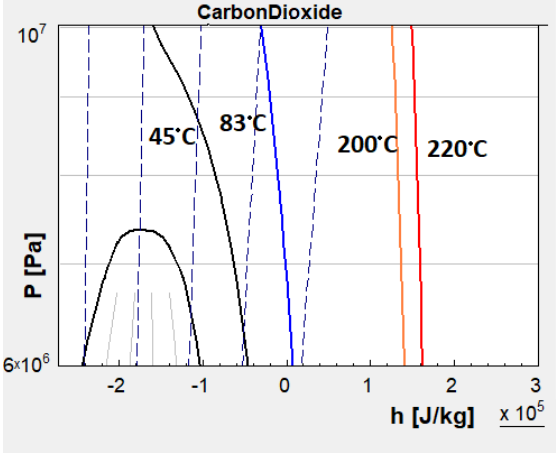

Figure 5.11: P-h diagram of CO_2 for the temperatures used in the supercritical thermodynamic analysis

When the enthalpy difference increases, the mass flow rate has to decrease for the gas heater to utilize the same heat load. The lowest gas heating pressure of 7.5 MPa can have a mass flow rate of 5.1 kg/s whereas the gas heating pressure of 10 MPa is restricted to a mass flow rate of 2.7 kg/s. The maximum flow rates are summarized in Table 5.4.

Table 5.4: The maximum mass flow rates for the different gas heater pressures when the solution reaches a temperature of 220 °C

P_{GH}	7.5 MPa	8.0 MPa	8.5 MPa	9.0 MPa	9.5 MPa	10 MPa
$\dot{m}_{max}$	5.1 kg/s	4.6 kg/s	4.1 kg/s	3.6 kg/s	3.0 kg/s	2.7 kg/s
$\dot{V}_S, kg/hour$	159.4	131.9	108.2	87.7	67.6	54.6

The swept volumes can be calculated for the different mass flow rates and is seen to decrease with the decreasing mass flow rates. The volumetric efficiency is assumed to be 80%.

Figure 5.12 presents the required gas cooler pressure to reach 200 °C and 220 °C for the heating pressures between 7.5 MPa and 10 MPa. The mass flow rate does not affect the gas cooler pressure, as discussed in the transcritical analysis.

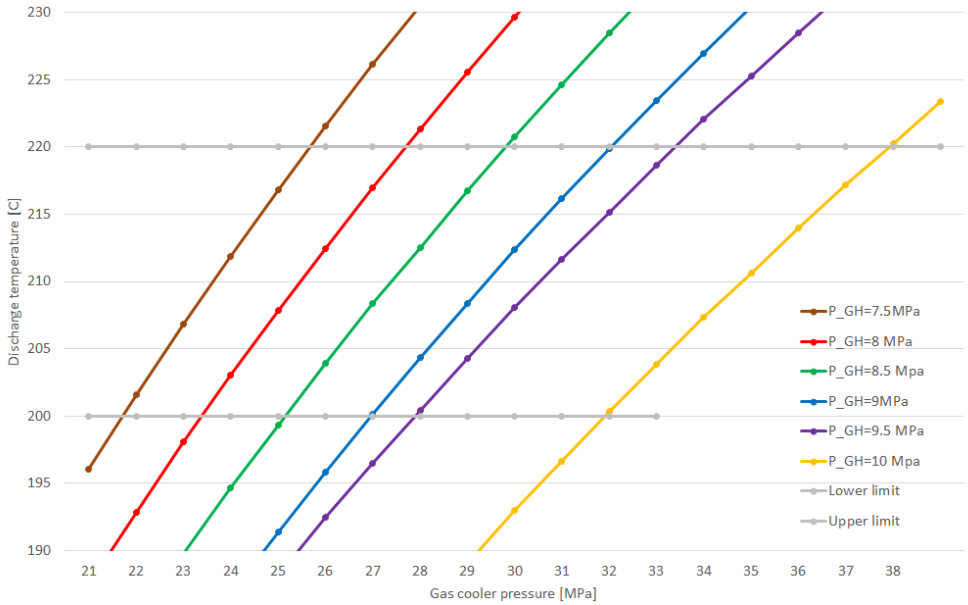

Figure 5.12: Discharge temperature vs gas cooler pressure reaching between 200 °C and 220 °C for the different gas heater pressures

With an increasing gas heater pressure, the required gas cooler pressure increases. By increasing the gas heater pressure, the temperature line of 83°C shifts slightly to the left, as seen in Figure 5.11, causing the enthalpy to decreases. The lines of 200°C and 220°C are also shifting slightly to the left but at a more constant slope. Therefore, the higher gas heater pressure is requiring a higher pressure ratio to achieve the temperatures. It is seen by the steeper slopes of the higher gas heater pressure in Figure 5.12 and the calculated as PR, summarized in Table 5.5.

Table 5.5: Required gas cooler pressure for different gas heater pressures

Gas heater pressure	**200 °C**		**220°C**	
	Gas cooler pressure	PR	Gas cooler pressure	PR
7.5 MPa	22 MPa	2.93	26 MPa	3.47
8.0 MPa	24 MPa	3.00	28 MPa	3.50
8.5 MPa	26 MPa	3.06	30 MPa	3.53
9.0 MPa	27 MPa	3.00	32 MPa	3.56
9.5 MPa	29 MPa	3.05	35 MPa	3.68
10 MPa	31 MPa	3.1	37 MPa	3.7

The heating capacity will be strongly affected by the mass flow rate. The gas heater pressure of 7.5MPa will have the highest heating loads as it has the highest mass flow rate, and the heating capacity will decrease with a decreasing mass flow rate. With the

large changes in mass flow rate, it is challenging to study how the gas cooler and gas heater pressures change the heating capacity. Therefore, in Figure 5.13, the mass flow rate is kept constant at 4 kg/s to study how the gas cooler and gas heater pressure affects the heating capacity of the heat pump. It is plotted for the gas cooling pressures of 23 MPa, 25 MPa, 27 MPa and 29 MPa and limited to the scenarios where the working fluid is heated up to a temperature between 200°C and 220°C.

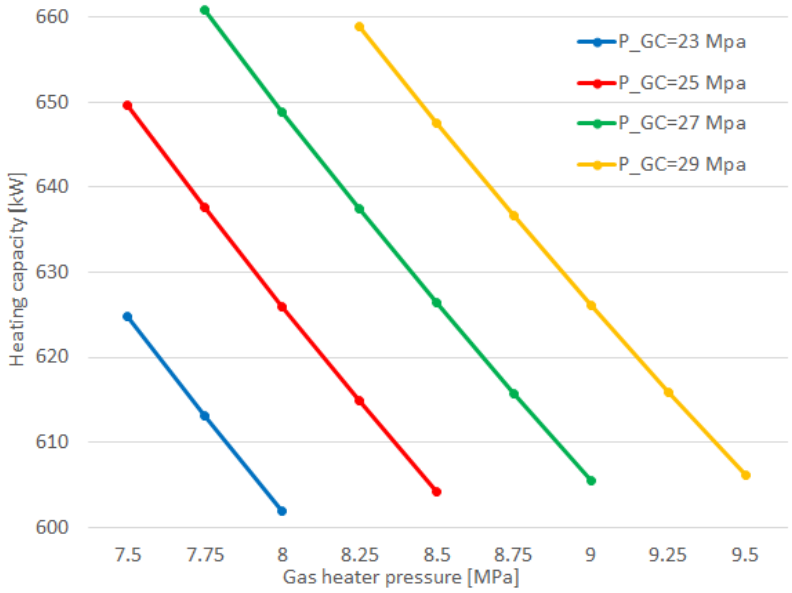

Figure 5.13: Heating capacity vs gas heater pressure, plotted for different gas cooler pressures when the mass flow rate is constant at 4 kg/s

For a constant gas cooler pressure, the heating capacity decreases with an increasing gas heater pressure. It is caused as a constant gas cooler pressure reaches a lower discharge temperature with a higher gas heater pressure, similar to what was found in Figure 5.12. The solution cannot reach 220°C without a certain pressure ratio, and the lower temperature decreases the heating load when the mass flow rate is kept constant. For a constant gas heater pressure, the heating load increases as the gas cooler pressure increases, as it leads to a higher discharge temperature.

By following the heating capacity lines horizontally, it is seen that the points plotted for each graph has very similar values. Studying the numbers behind the plots, it can be seen that for all the scenarios, a discharge temperature gives almost the same heating capacity with the same mass flow rate. Therefore, no conclusion can be made by comparing the heat load in Figure 5.13.

The set-up to evaluate the change in COP is the same as for the heating load, where Figure 5.14 calculates the changing COP with an increased gas heating pressure. It is

plotted for the gas cooling pressures of 23 MPa, 25 MPa, 27 MPa and 29 MPa, limited to the scenarios where the working fluid is heated up to a temperature between 200°C and 220°C. The mass flow rate is kept constant at 4 kg/s.

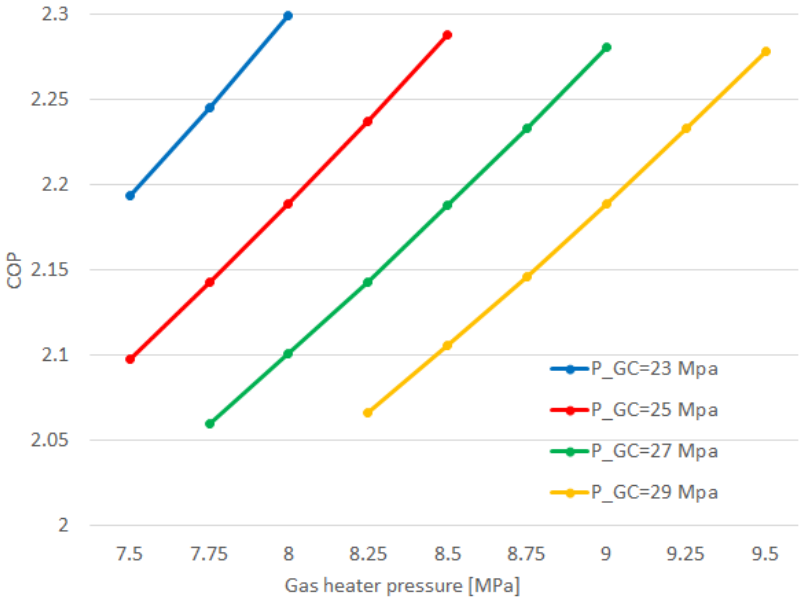

Figure 5.14: COP vs gas heater pressure, plotted for different gas cooler pressures when the mass flow rate is constant at 4 kg/s

For each gas cooler pressure, the figure presents an increasing COP with an increasing gas heating pressure. The increase in COP is caused by a decrease in PR, leading to less compression work. A turbine expander produces more work at a higher PR, but as it produces a lot less work than the compressor uses, the compressor is the deciding factor. For a given gas heating pressure, an increase in COP is seen with a decreasing gas cooler pressure, as the pressure ratio here also decreases.

Both the value of the COP and the heating capacity is depended on the mass flow rate, while the slope of the lines only depends on the gas cooler and gas heater pressures. The enthalpy differences in the compressor, gas cooler and turbine expander are depended on the required temperatures and pressures, while the COP and heating capacity also considers the mass flow rate. Therefore, only a plot for 4kg/s is necessary, but it can be concluded that the COP increases with a reduction in the mass flow and the heating load increases with an increasing mass flow rate.

Table 5.4 presents the maximum mass flow rate and Table 5.5 presents the gas cooler and gas heater pressure to reach 220 °C. With these numbers, the COP and heating capacity are calculated for the scenarios, presented in Table 5.6. It can be concluded that the higher gas cooler pressure gives the highest COP, due to the slope of the temperature

and enthalpy lines of CO_2. On the other hand, the heating load is higher for the lower gas heater pressure, as the mass flow rate can be larger.

Table 5.6: The COP and heating load for the gas heater pressures when reaching a discharge temeprature of 220 °C

Gas heater pressure	7.5 MPa	8 MPa	8.5 MPa	9 MPa	9.5 MPa	10 MPa
Gas cooler pressure	26 MPa	28 MPa	30 MPa	32 MPa	35 MPa	37 MPa
COP	1.87	1.96	2.05	2.19	2.34	2.50
Q [kW]	733	696	664	625	594	566

When choosing the recommended solution, it has to be decided whether COP or heating capacity is the more crucial factor. From the perspective of this thesis, the heating load is the recommended crucial factor, as the aim is to heat as much air using the excess heat of a spray dryer. By having a higher heating load, more air can be heated to 220 °C. On the other hand, from an industrial perspective, COP is more important. For an industry to choose to invest in equipment, it has to have economic benefits. The economic perspective is essential everywhere, so COP has to be taken into consideration. In the transcritical solution, the heating load was very similar for all the solutions. Here, on the other hand, the difference in heating capacity is large and cannot just be ignored. A compromise has to be made between the two.

Another point to consider is the pressure rates and the mass flow rates that are required. To decrease the pressure rates, the high heating capacity solution is recommended, and to decrease the mass flow rates, the high COP solution is beneficial.

The standard gas cooler used in a transcritical CO2 heat pump cycle is limited by a maximum pressure of 14MPa and a temperature of 250°C, according to Jensen et al.2015[32]. Having a temperature limit of 250°C is within the temperature of the case description. On the other hand, the results in Table 5.6 have all higher gas cooler pressures than 14MPa. As it is the pressure that differs the transcritical and supercritical cycle, causing one to always be above the critical point, the same gas cooler cannot be used for both cycles. Therefore, a new gas cooler has to be developed. Still, to reach a discharge pressure of 37MPa is very much higher than what is found on the market, and a lower pressure solution could be recommended.

There are benefits with choosing both the lower and higher gas cooler pressure. These pressures are studied further in the heat exchanger optimization to make a recommendation on the better option.

5.2 Heat Exchanger Geometry Optimization

The geometry optimization is conducted for a transcritical gas cooler, supercritical gas cooler and supercritical gas heater. The evaporator is not studied, as a similar one that was used by Sarkar [20] or Bamigbetan [23] can be used.

5.2.1 Transcritical Gas Cooler using Overheated Iso-Butane

The recommended solution in Section 5.1.1 was the overheated working fluid, as it gave a higher COP. Therefore, only this solution is analyzed further.

The gas cooler is using air as the basis for the calculations, where the temperature increases from 15 °C to 200°C. A new mass flow rate of dry air is calculated through energy balance with the heat load reaching 220 °C from the transcritical heat pump cycle, presented in Table 5.7. The mass flow rate is seen to be between 2.8 and 2.6, which is around 30% of the air required in the spray-drying process.

Table 5.7: Specifications from the transcritical heat pump cycle used to calculate the mass flow rate of air in the gas cooler

	ΔT=3K	**ΔT=5K**	**ΔT=10K**	**ΔT=15K**
Q_{HP} [kW]	528	529	513	498
$\dot{m}_{R600a}$ [kg/s]	1.169	1.152	1.112	1.074
P_{GC} [MPa]	27	25	23	18
$\dot{m}_{air}$ [kg/s]	2.773	2.747	2.667	2.632
P_{GC} [MPa]	27	25	23	18

When the mass flow rate is calculated, the next step is to optimize the geometry of the gas cooler. Figure 5.15 analyses the change in the required length when the width increases. The width of the hot- and cold-side channel is kept constant at 2mm, the thickness of the plates is 0.5mm, and the simulation has 100 channel pairs.

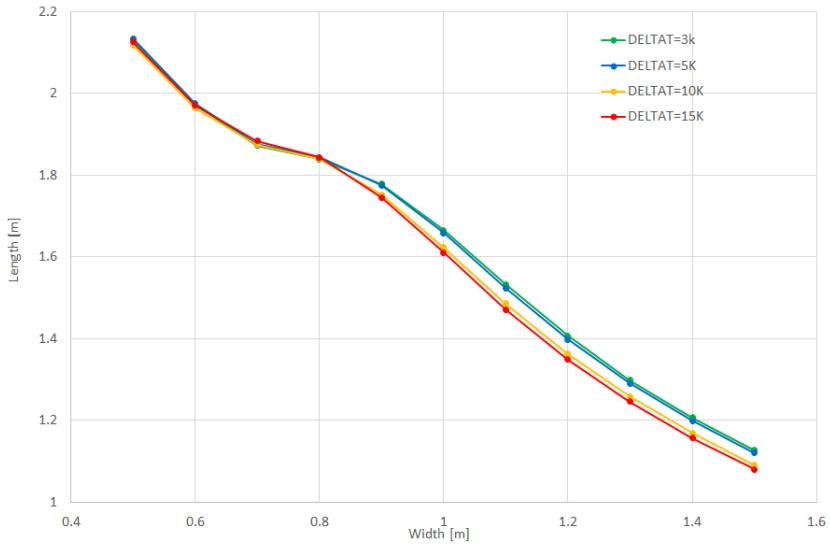

Figure 5.15: Lenght vs width in a iso-butane gas cooler

It is seen that the required length of the gas cooler decreases when the width increases. The slope becomes steeper with widths larger than 0.8m. The change is very similar for all the ΔT, but it is seen that ΔT=3K and ΔT=5K has a slightly higher length requirement at the higher widths.

A gas cooler aims to transfer as much heat as possible on the lowest possible area. The gas cooler is designed on the concept of Q=UAΔT, where A is defined by $2 \times L \times W$. The heat load and ΔT is defined and kept constant. Therefore, by decreasing the area, the heat transfer coefficient increases. From the plot, the different areas is calculated and presented in Table 5.8.

Table 5.8: Areas with an increasing gas cooler lenght for a transcritical overheated cycle

W [m]	0.6	0.8	1.0	1.2	1.4
A [m^2]	2.4	3.0	3.2	3.4	3.4

By comparing the different areas, it is seen that the lowest area occurs at a width of 0.6m and a length of 2m. This solution has the highest heat transfer coefficient. However, the pressure drop in the gas cooler increases with an increasing length. The pressure of drop iso-butane stays below 10 Pa in each sub-heat exchanger and therefore assumed isobaric. The pressure drop for the heated air, on the other hand, has higher values. Figure 5.16 presents the decrease in pressure drop in the cold circuit with an increasing gas cooler width.

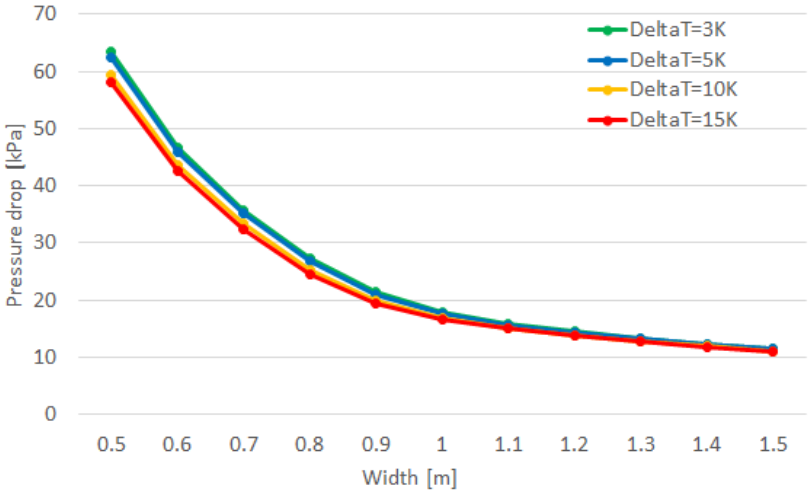

Figure 5.16: Pressure drop vs width of the transcritical, overheated gas cooler, presented for the different suction gas temperatures

The pressure drop, dP/dx, increases with an increasing gas cooler length, as the airflow travels longer. By increasing the width, the required gas cooler length decreases, and the same does the pressure drop. The lowest gas cooler area occurs when using a width of 0.6m, which gives the highest pressure loss. By increasing the width to 0.8m, the pressure drop can be halved by only increasing the area with 25%.

The question is how much pressure drop the heat exchanger should allow. By increasing the allowable pressure drop, the required gas cooler size decreases, making the gas cooler smaller and cheaper. However, by accepting a higher pressure loss, the air has to be pumped back to the required pressure before entering the spray-dryer. Also, a higher pressure loss increases the cost to pump the air through the gas cooler. According to Alfa Laval [36], a guide of allowable pressure losses lays between 20 and 100kPa. As seen in Figure 5.16, the heat exchanger within this pressure loss for all scenarios. Still, at a width of 0.6m, the pressure drop is 50% of the initial pressure. The value is significant, and the width is increased to 0.8m to decrease the pressure losses. It leads to a gas cooler length of 1.8m for all ΔT.

The next step is to optimize the width of the hot-side and cold-side channel, the thickness of the plates and the number of channel pairs. According to Alfa Laval [36], the thickness of the plates tends to vary between 0.3 and 0.6 mm. The change in thickens causes a slight change in the area, changing the heat transfer coefficient. Still, for the given gas cooler scenario, this change is too small to be of interest, and the thickness is therefore kept constant at 0.5mm.

The change in pressure drop is analyzed to determine the ideal width of the cold-side

channels. Figure 5.17 presents the decrease in pressure drop by increasing the number of channel pairs for the channel widths of 2mm, 3mm and 4mm. The width of the hot-side channel does not affect pressure drop in the cold-side channel and is therefore kept constant at 2mm.

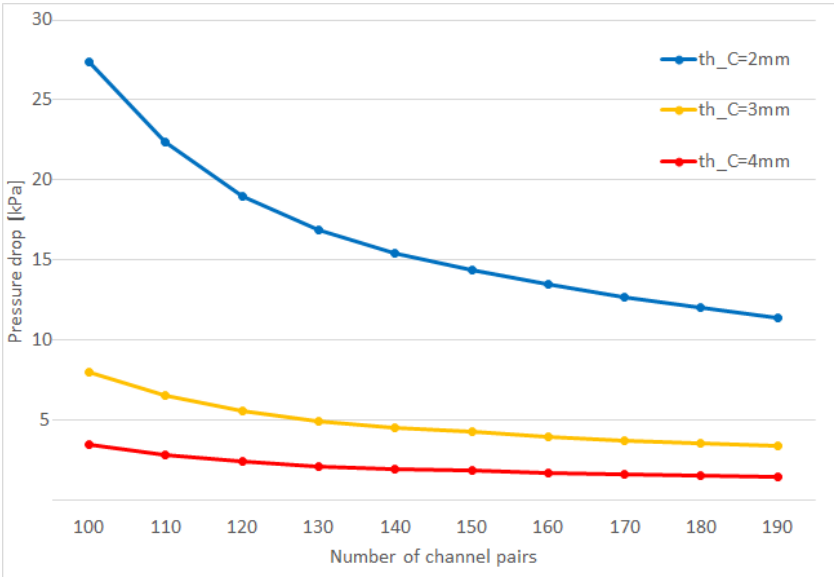

Figure 5.17: Pressure drop vs number of channels with a changing cold-side channel widths

By increasing the width of the cold-side channel, the pressure drop decreases drastically. Due to continuity, by increasing the channel area, the velocity decreases, causing a reduction in pressure drop. The most significant change is seen to be between the width of 2mm and 3mm. Therefore, it is recommended to have a wider cold-side channel.

The calculations are conducted using ΔT=3K, as it is the largest mass flow rate and highest pressure. By increasing the ΔT, the mass flow rate and pressure decrease, but a very similar change occur. The values of the pressure drop decrease, but the slopes are the same. All solutions will benefit by increasing the width of the cold-side flow.

To find the hot-side channel width to suit the increasing cold-side width, Figure 5.18 plots the change in length with an increasing number of channels. The cold-side width is plotted for 3mm and 4mm, and the hot-side between 2mm and 4mm. From Figure 5.15, it was found that the length in the gas cooler should be around 1.8m. For this to be possible, the number of channels will have to be increased from 100 to a value between 160 and 180.

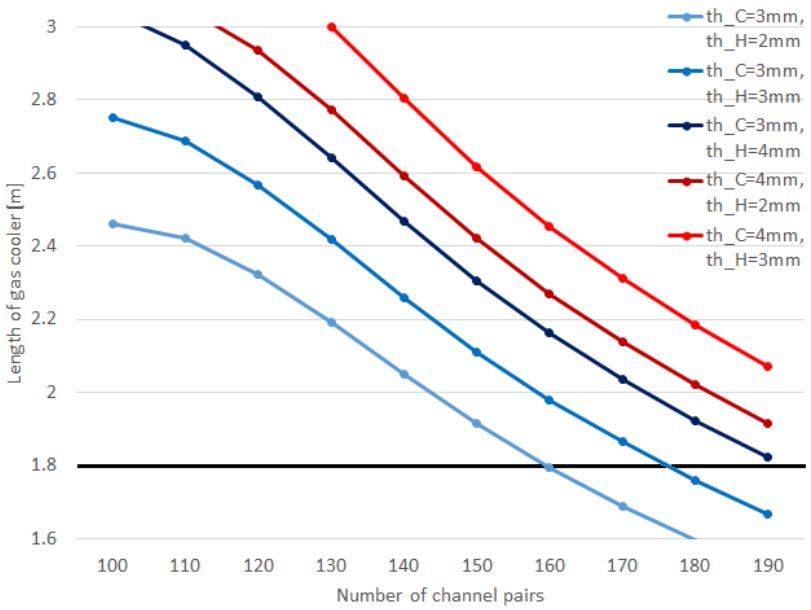

Figure 5.18: Length of gas cooler vs number of channels for changing hot and cold channel widths

By having a cold-side width of 4mm, the gas cooler has to increase the length beyond 1.8m, and the chosen cold-side width is 3mm. Here, if the hot-side width is 3 mm, the number of channel pairs is 178, whereas a width of 2mm only requires 160 channel pairs. It is beneficial to have the lowest possible number of channels, as it decreases the heat transfer area and the cost of the gas cooler [36]. Therefore, the recommended width is 2mm and 3mm for the hot-side and cold-side, respectively.

However, if the number of channel pairs were to be increased even further, the required length of the gas cooler would be decreased further. It increases the heat transfer coefficient and decreases the pressure drop. If the aim is to have the highest possible heat transfer coefficient, the recommended choice is to increase the number of channel pairs further, and if the cost also should be taken into consideration, the number of channel pairs has to be limited.

Figure 5.18 was plotted for ΔT=3K, as it has the highest values. Figure 5.19 presents the length requirements for the different ΔT with an increasing number of channel pairs. The hot- and cold-side channel width is kept as 2mm and 3mm, respectively.

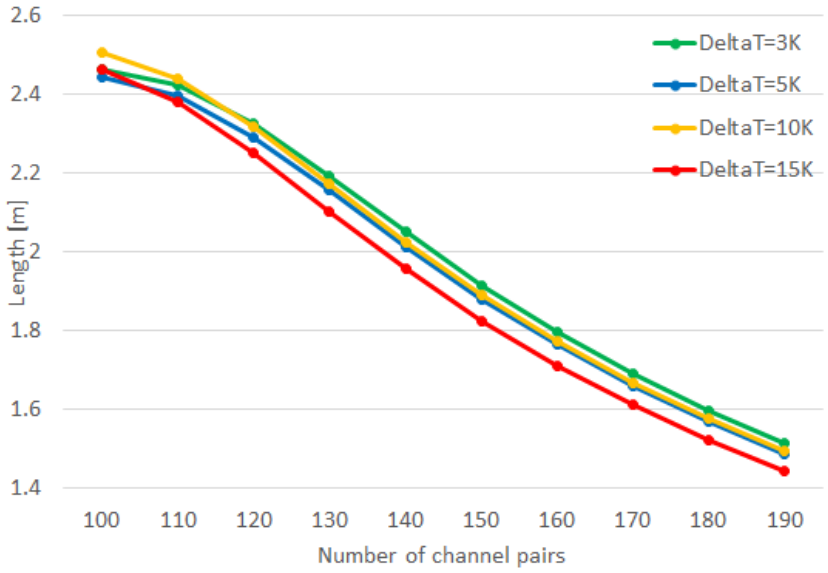

Figure 5.19: Length of gas cooler vs number of channel pairs for the different ΔT values

It is seen that for ΔT=5K, the required number of channel pairs is still 160. At a ΔT=10K the number decreases to 155 and ΔT=15K requires 150 channel pairs. It is caused by the decreasing mass flow rate if the increasing suction gas temperatures. With the changing number of channel pairs, the geometry changes slightly. The values are summarized in Table 5.9.

Table 5.9: Ideal geometry for the transcritical gas cooler using iso-butane as the working fluid

	ΔT=3K	ΔT=5K	ΔT=10K	ΔT=15K
Number of channel pairs	160	160	155	150
Width	0.8			
Length	1.8m			
Thickness of plates	5 mm			
Width cold-side channel	3 mm			
Width hot-side channel	2 mm			

.

With the optimized gas cooler geometry, the pinch point analysis is presented in Figure 5.20.

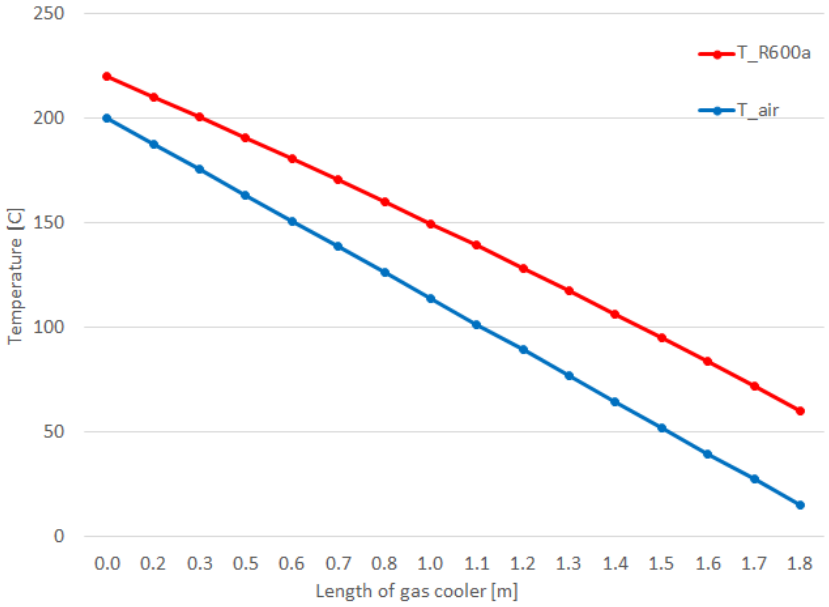

Figure 5.20: Pinch point for optimal gas cooler design

As the problem description defines the air temperature to have a constant inlet and outlet temperature and the gas cooler have a constant inlet and outlet temperature, the pinch analysis will be very similar for all the scenarios. The pressures varies a little for each scenario, but does not affect the pinch much here. The result gives an effectiveness of 38% at the pinch point and decreases down to an effectiveness of 22% at with the largest temperature difference.

The effectiveness can be increased by pre-heating the air. As the ΔT of the gas cooler is defined as 20K due to the pressure losses, the effectiveness is constant at x=0. The gas cooler effectiveness at x=1.8m could be increased slightly by pre-heating the air to a temperature of 40°C, decreasing the temperature difference.

When studying the literature for similar cases, ΔT=20K was used by Atkins et al.(2011) [37]. Jensen et al.(2015) [38] and Zuhlsdorf et al.(2017)[7] both uses a ΔT of 10K, but has a lower temperature difference than this one. Walmsley et al.(2017) [39] uses a ΔT=15K in a similar scenario. Therefore, it can be said that the gas cooler can aim for a ΔT of 15K, but 20K is reasonable.

5.2.2 Supercritical Gas Cooler Using Carbon Dioxide as the Working Fluid

The supercritical gas cooler is optimized using the values found in Section 5.1.5. The gas cooler pressures reaching a compressor discharge temperature of 220°C is analyzed. Each gas cooler pressure has a different heating capacity, that is utilized to heat the air.

Therefore, each gas cooler can heat different air flow rates. The values are presented in Table 5.10.

Table 5.10: Design parameters for supercritical gas cooler, found in the thermodynamic analysis, used to calculate the optimum air flow rate in the gas cooler

Gas heating pressure [MPa]	7.5	8.0	8.5	9.0	9.5	10
Gas cooling pressure [MPa]	26	28	30	32	35	37
$\dot{m}_{CO_2}$ [kg/s]	5.1	4.6	4.1	3.6	3	2.7
$\dot{Q}_{HP}$ [kW]	733	696	644	625	594	566
$T_{GC,exit}$ [C]	132	127	124	117	106	97
$\dot{m}_{air}$ [kg/s]	3.911	3.713	3.436	3.335	3.169	3.020

The supercritical gas cooler of 26MPa can heat 45% of the air required in the process, whereas the gas cooler of 37MPa only heats 35%. Both values are higher than what was found for the transcritical cycle.

To optimize the gas cooler geometry, Figure 5.21 presents the change in gas cooler length when the width increases. The solution has a plate thickness of 0.5mm, hot- and cold-side channel widths of 2mm and 100 channel pairs, the same starting points as for the transcritical gas cooler. The figure shows that by increasing the gas cooler width, the required length varies.

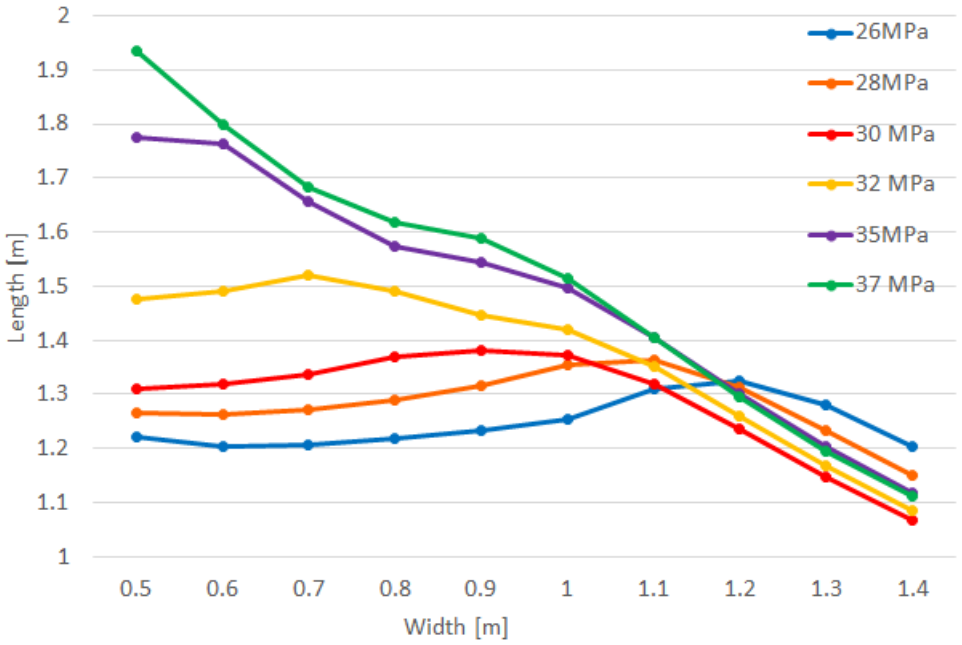

Figure 5.21: Length vs width for a supercritical gas cooler, for different gas cooler pressures

The length required for the gas cooler decreases the width of an increasing gas cooler width for the gas cooler pressures of 35MPa and 37MPa. It is similar to what was seen in the transcritical case, as the heating loads and mass flow rates are similar.

However, for the lower gas cooler pressures, an increasing width causes the length to increase as well. It is caused by a U-value that is decreasing more rapidly than the area increases with the increasing width, as the gas cooler entrance length is too short. When the entrance length is too short, the gas leaves the gas cooler before the heat transfer coefficient stabilizes. It is very un-ideal for a gas cooling design and is therefore changed.

There are two ways to decrease the entrance length of a gas cooler, to increase the number of channel pairs and to increase the width of the channel. Figure 5.22 presents the change in gas cooler length with an increased gas cooler width when the number of channels is increased to 200 and the hot- and cold-side channel width is increased to 3mm and 4mm, respectively. The channel widths are increased as the mass flow rates are larger.

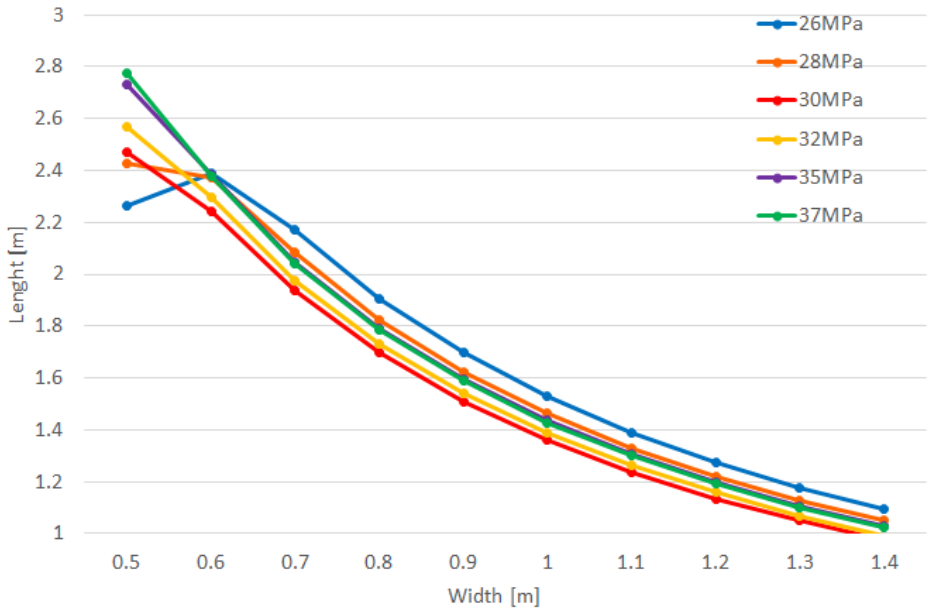

Figure 5.22: Length vs width of a supercritical gas cooler for different gas cooler pressures, with a higher number of channel pairs and wider channel widths

With the changes in the number of channel pairs and width of hot and cold side channels, the required length of the gas cooler decreases with an increasing width. For the gas cooler pressure of 26MPa and 28 MPa, the entrance length is still too short for a width of 0.5m and are therefore limited by a minimum width of 0.6m. The reason why the lower gas cooler pressures have a longer entrance length is the larger mass flow rate that increases the Reynolds number and the velocity in the channel.

With the new channel widths and the increased number of channels, Figure 5.23 presents the pressure drop for the scenarios. The pressure drop is seen to decrease with an increasing gas cooler width, as the gas cooler length decreases.

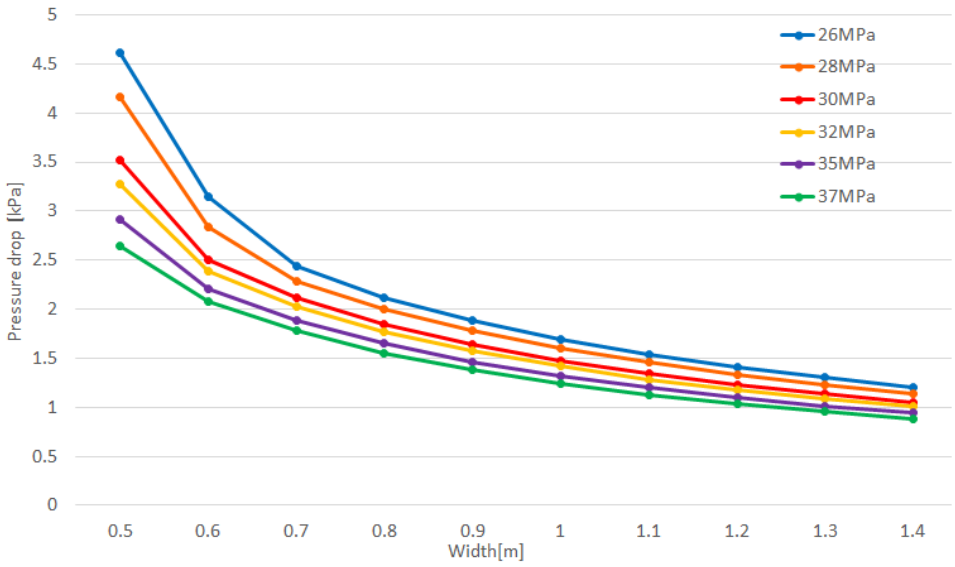

Figure 5.23: Change in pressure drop vs width of a supercritical gas cooler with a higher number of channel pairs and wider channel widths

To increase the channel widths and the number of channel pairs was the adjustments made to decrease the pressure drop for the transcritical cycle. Here, these adjustments are already made, which is why the pressure drop is much lower. It causes the length of the gas cooler to be much longer.

The chosen gas cooler width is 0.6m, as all the scenarios are outside the critical entrance length region, it causes the lowest gas cooler area, and the pressure loss is very low. It gives a gas cooler length between 2.2m and 2.4m for the different gas cooler pressures. For the rest of the optimizing, the focus will be opposite than for the transcritical cycle. The choice of 200 channel pairs and width of 3mm and 4mm are large values. The study focuses on if some of the values can be decreased to decrease the gas cooler length.

When the width is constant, each solution will be limited by a critical value of number of channel pairs to assure that the entrance length is long enough. The limiting number of channel pairs will be constant for each solution, and a decrease in gas cooler length can be achieved by changing the channel-widths. The numbers of channel pairs are summarized in Table 5.11.

Table 5.11: The minimum number of channel pairs in the gas cooler for the different gas cooler pressures

	26MPa	**28MPa**	**30MPa**	**32MPa**	**35MPa**	**37MPa**
Number of channel pairs	200	180	150	120	90	80

The required number of channel pairs is seen to be high for a gas cooler pressure of 26MPa and decreases with an increasing gas cooler pressure. It is due to the larger mass flow rate of CO_2, causing the flow to have a higher Reynolds number.

The analysis focuses on 26MPa and 37MPa, as the upper and lower limits. The rest of the gas cooler pressures will have solutions in between the two.

The pressure drop of interest is found in the cold-side channel. Figure 5.24 presents the decreasing gas cooler pressure drop with an increasing cold-side channel width. The figure is plotted when both gas cooler pressure uses the optimum number of channel pairs found in Table 5.11.

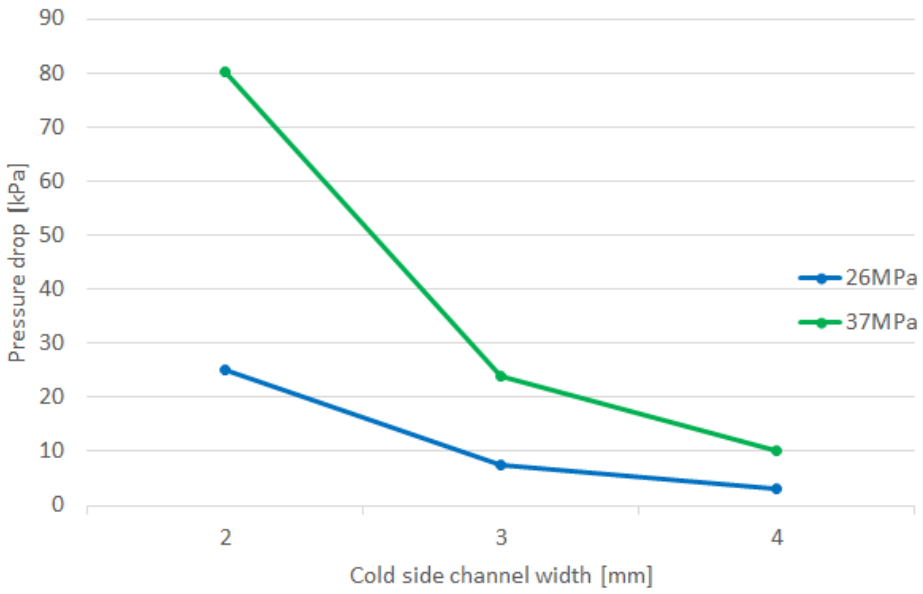

Figure 5.24: Change in pressure drop vs cold-side channel width for the supercritical gas cooler with a gas cooler pressure of 26MPa and 37MPa

Looking at Figure 5.24, the pressure loss for 37MPa is very high. Therefore, a cold-side width of 4mm could be recommended. However, the gas cooler is modelled with 80 channel pairs, which is a low value. By increasing it, the pressure drop will decrease, and the cold-side channel width can be lower, either at 2mm or 3mm.

For the gas cooler pressure of 26MPa, the pressure drop is lower as 200 channel pairs are utilized. The pressure drop can be decreased further by increasing the number, but as the number is already high, it is desirable to rather increase the cold-side channel width. Therefore, a cold-side width of 3mm or 4mm is recommended.

Figure 5.25 presents the change in gas cooler length with an increasing hot-side channel width. It is plotted for the gas cooler pressure of 26MPa, cold-side channel widths of 3mm

and 4mm for 200 channel pairs, and for the gas cooler pressure of 37MPa, the cold-side widths of 2mm and 3mm and 80 channel pairs.

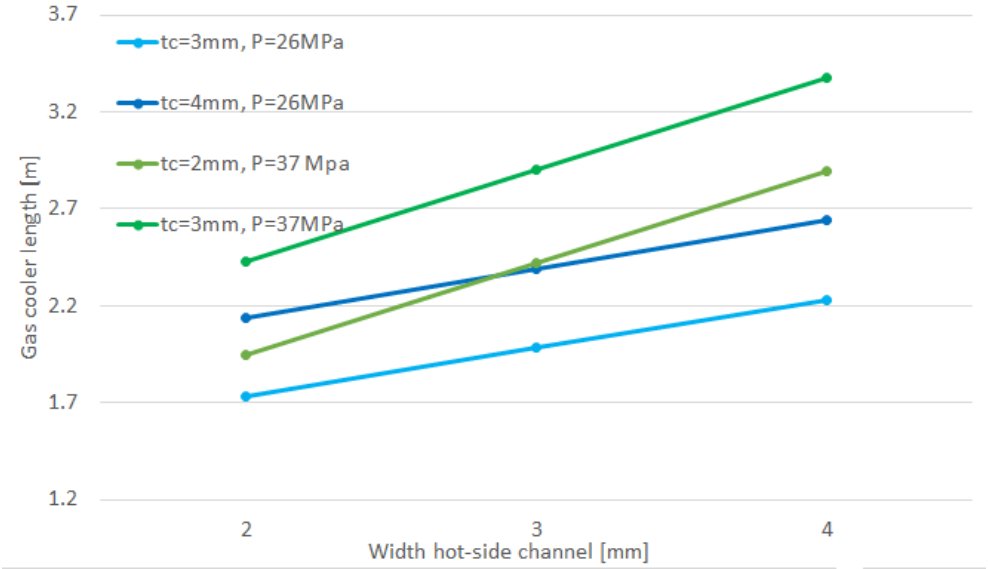

Figure 5.25: Change in pressure drop vs cold-side channel width

By decreasing the width of the hot-side channel, the length requirement of the gas cooler becomes lower. Also, by decreasing the cold-side channel width the length requirement decreases. Both gives the gas cooler a lower area and is therefore the recommended solution. For the gas cooler pressure of 26MPa, a cold-side channel width of 3mm and a hot-side with of 2mm is recommended. It gives a gas cooler length of 1.7m.

For the gas cooler pressure of 37MPa, the hot-side channel width is recommended to be 2mm. For the cold-side channel width, Figure 5.26 studies the widths of 2mm and 3mm further.

Figure 5.26: Optimizing the number of channel pairs for the gas cooler of 37MPa

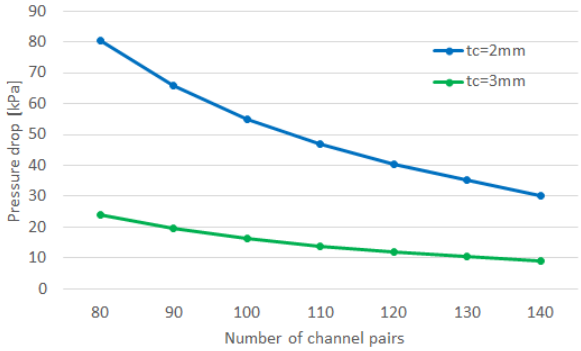

(a) Change in pressure drop vs number of channel pairs for different cold-side channel widths in a 37MPa gas cooler

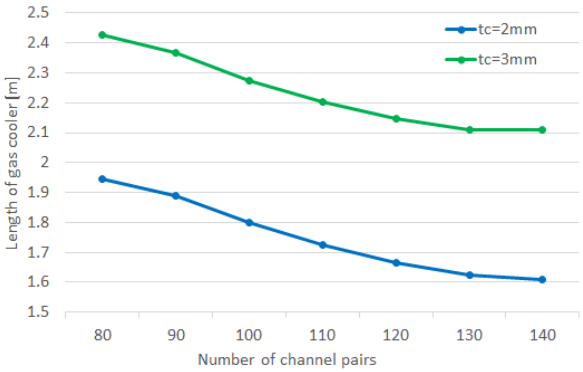

(b) Change in length requirement vs number of channel pairs for different widths in a 37MPa gas cooler

It is seen that the pressure drop is still large for the width of 2mm, even when the number of channel pairs increases. Therefore, the recommended width is 3mm. The number of channel pairs is chosen to be 130, giving a gas cooler length of 2.1m.

The recommended gas cooler geometry size is summarized in Table 5.6

Table 5.12: Recommended geometry parameters for a supercritical gas cooler using CO_2 as the working fluid

	P=26MPa	**P=37MPa**
Width	0.6m	
Hot-side channel width	2mm	
Cold-side channel width	3mm	
Plante thickness	0.5mm	
Number of channel pairs	200	130
Length	1.7m	2.1m

The values are used to analyse the gas cooler pinch points, presented in Figure 5.27. The pinch is plotted for a gas cooler pressures of 26MPa and 37MPa.

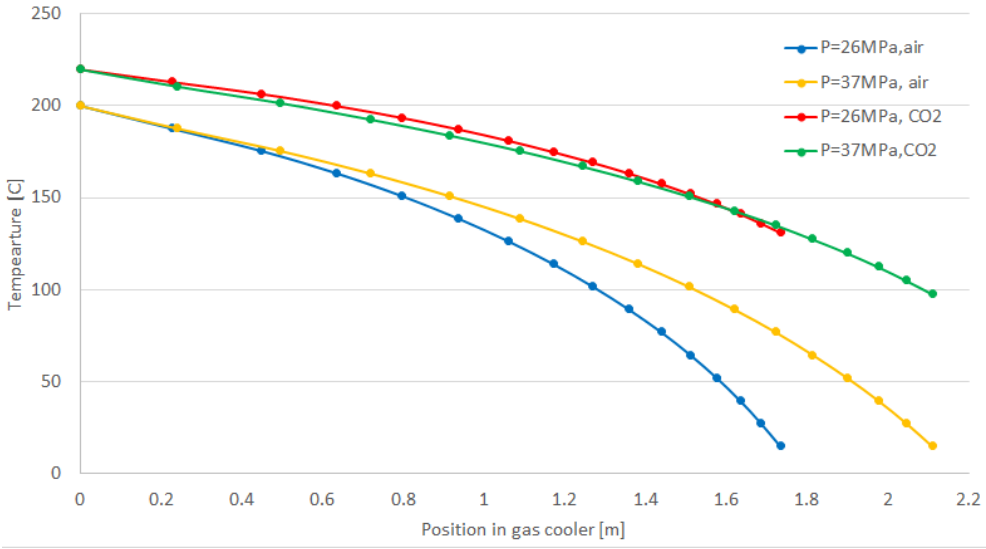

Figure 5.27: Pinch point analysis for with the recommended geometries for the gas cooler of 37MPa

The pinch point is located at the air outlet and CO_2 inlet point, at x=0m. After the pinch point, the temperature difference between the flow increases, decreasing the local effectiveness. As the change in air temperature is constant, it is the gas cooler exit temperature that affects the effectiveness. The gas cooler has a higher effectiveness by decreasing the temperature difference between the two solutions, solved by increasing the gas cooler exit temperature. For the heat pump solution, this is achieved by increasing the gas cooler pressure, as presented in Table 5.10. Therefore, the recommended gas cooler is the ones with the highest pressure.

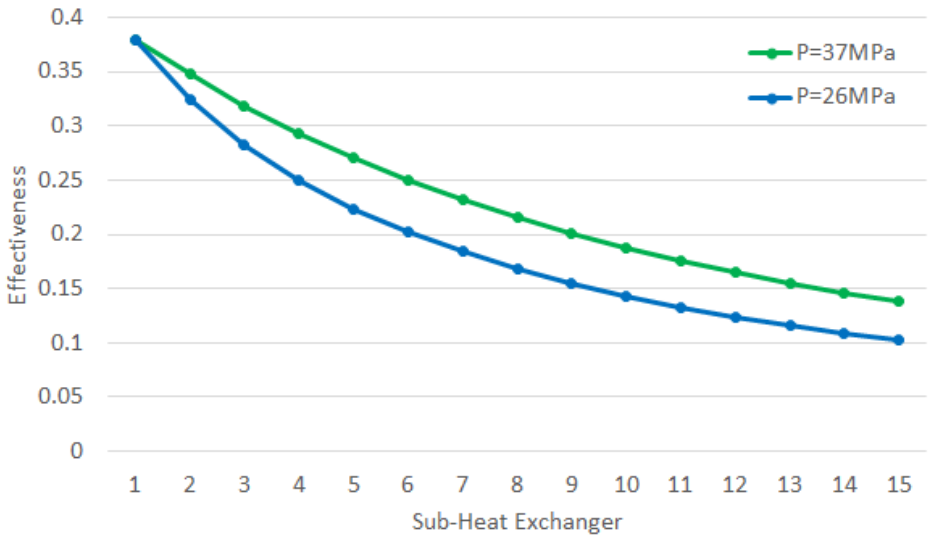

Figure 5.28: Effectiveness in each sub-heat exchanger for the gas cooler pressure of 26MPa and 37MPa

Figure 5.28 presents the effectiveness in each sub-heat exchanger, where P=37MPa has higher values due to the lower temperature difference through the gas cooler.

The effectiveness of the gas cooler is still low, as the temperature difference for both cases is very large. It is caused by having to heat the air from a temperature of 15°C. By pre-heating the air, the temperature difference between the gas cooler outlet and the air decreases, and the local effectiveness in the sub-heat exchanger increases.

Gas cooler pressure can also be changed to increase the efficiency. For this thesis, the change in gas cooler pressure would change the whole thermodynamic analysis and is therefore excluded.

5.2.3 Supercritical Gas Heater Using Carbon Dioxide as the Working Fluid

For the supercritical gas cooler, the mass flow rate of air is 8.75 kg/s and the ideal mass flow rates of CO_2 was found in Section 5.1.5. They are not changed, as the excess heating capacity was the starting point in the heat pump design. The values are summarized in Table 5.13 and used as the starting point for the optimization process of the supercritical gas heater.

Table 5.13: Pressure in gas heater providing maximum mass flow rate when the cycle reaches 220 °C

P_{GH}	7.5 MPa	8.0 MPa	8.5 MPa	9.0 MPa	9.5 MPa	10 MPa
$\dot{m}_{max}$	5.1 kg/s	4.6 kg/s	4.1 kg/s	3.6 kg/s	3.0 kg/s	2.7 kg/s

The gas heater is defined to have an inlet temperature of 45 °C and an exit temperature of 83°C. The pressure drop in the cold channel, where the CO_2 flows, is considered isobaric. In the hot channels, where the air flows, the pressure drop is larger. However, after the air has passed through the gas heater, the rest of the heat cannot be utilized due to fouling. Therefore, it does not matter if the pressure drop is high. Instead, the gas heater should focus on being as efficient as possible. Therefore, the optimization focuses on having the lowest possible area. Figure 5.29 presents the required length with an increasing gas heater width.

A long entrance length challenges the gas heater. It can be solved by increasing the width and the number of channel pairs. For the given scenario, only increasing the number of channel pairs will require too many channels. Therefore, the width is increased as well, setting the lower limit to 1m. With those values, all the gas heater is outside the entrance

length region when having 200 channel pairs, a plate thickness of 5mm and a hot-, and cold-side channel width of 3mm.

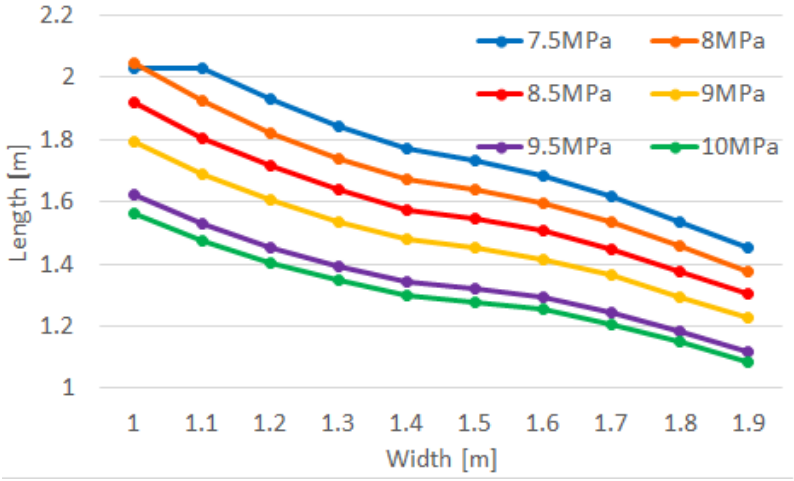

Figure 5.29: Length vs width in a supercritical gas heater

As seen in Figure 5.29, the increasing width reduces the required gas heater length. For the gas heater pressure of 7.5MPa, the change is very little between the widths of 1m and 1.1m, indicating that the solution barely exits the entrance length region. Therefore, the width chosen is 1.1m. It assures that all solutions are outside the entrance area while still keeping the area as low as possible.

The limiting number of channel pairs is found the same way as for section 5.2.2. As the pressure drop does not affect the scenario, the minimum number of channel pair is the ideal design solution. It leads to corresponding gas heater lengths, and both values are presented in Table 5.14.

Table 5.14: The minimum number of channel pairs in the gas heater for the different gas heater pressures and the corresponding gas heater lengths

	7.5MPa	**8MPa**	**8.5MPa**	**9MPa**	**9.5MPa**	**10MPa**
Number of channels required	200	180	150	130	100	90
Length of gas heater	2.03	2.06	2.15	2.24	2.38	2.52

The required number of channel pairs decreases with an increasing gas heater pressure. It is due to the lower mass flow rate in the higher gas cooler pressure, leading to a lower Reynolds number.

The gas cooler lengths are calculated for a hot and cold-side channel width of 3mm and are seen to be very large in Table 5.14. By decreasing these widths, the gas cooler length

is optimized. Figure 5.30 illustrates this for the gas heater pressure of 7.5MPa and 10MPa. As the upper and lower limit, the rest of the gas heater pressures has solutions in between.

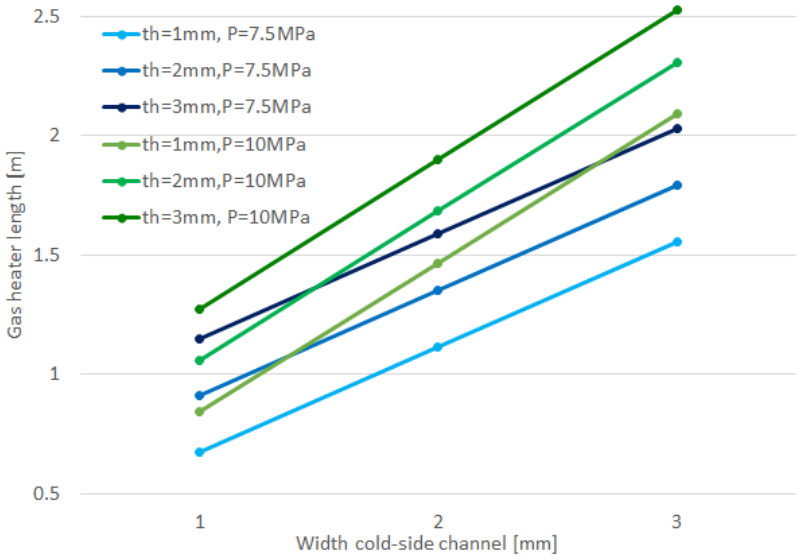

Figure 5.30: Change in gas heater length with an increasing cold-side width, presented for different hod-side widths

The figure shows that by decreasing the channel widths, the gas heater length decreases as well, for both the hot and cold side channels. The optimization process of the gas heater is focusing on having the lowest possible area. Therefore, the channel widths of 1mm can be recommended.

However, the pressure drop of the air is very high if the hot-side width is 1mm. The air is not utilized further and can leave the gas heater at a lower pressure, but by decreasing the pressure too much, a pump will have to be utilized to move the air through the gas heater. A larger pump will increase the investment cost, and it requires more work. Instead, it is recommended to rather invest in a larger gas heater. Therefore, a hot-side width of 3mm is recommended. The low width of the hot-side channel does not affect the hot-side pressure drop much and can stay at 1mm.

With these values, the optimum gas heater length is calculated. The result is presented in Table 5.15.

Table 5.15: Optimized geometry for the supercritical gas heater

	7.5MPa	8MPa	8.5MPa	9MPa	9.5MPa	10MPa
Width cold side	1mm					
Width hot side	3mm					
Plate thickness	0.5mm					
Number of channels required	200	180	150	130	100	90
Length of gas heater	1.14m	1.14m	1.16m	1.19m	1.22m	1.27m

The length increases slightly with an increasing gas heater pressure, caused by the lower number of channel pairs.

Figure 5.31 presents the pinch point analysis of the optimized gas heater at a pressure of 7.5MPa and 10MPa. The pinch points are located on each side of the gas cooler.

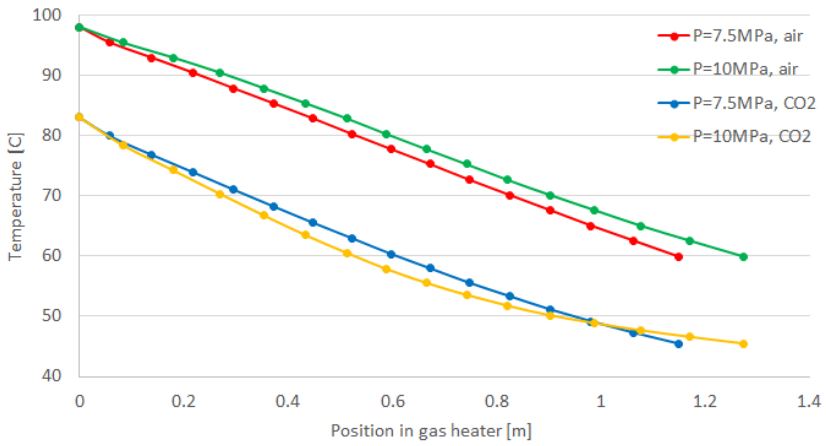

Figure 5.31: Pinch point analysis of the supercritical gas heater at a pressure of 7.5MPa and 10MPa

It is seen that for the gas cooler pressure of 7.5MPa, the temperature difference between the two flows is close to 15K through the whole gas heater, optimizing the efficiency. For the gas heater pressure of 10MPa temperature difference increases through the gas heater, decreasing the average efficiency. It is caused by the thermodynamic abilities for the CO_2 at the different pressures. With this in mind, it is recommended for the gas heater to have the lowest possible pressure.

Still, the efficiency of the gas heater optimized for the supercritical cycle is very low. It is a known problem, and to develop heat exchangers to utilize the heat recovery from excess air from spray-dryer is a separate field of study. Significant energy potential is found in the air flow, but challenges including the low excess air temperature, the low

heat transfer coefficient of air, the pressure difference and the particles of milk powder left in the air causing fouling on the gas cooler decreases the efficiency [37].

Many studies have been conducted on developing better heat exchangers to utilize the excess air from spray-dryers, including [9], [10], [12], and [37]. The most common optimization is to utilize a coupled-loop heat exchanger solution. The concept is based on using an additional fluid loop to transport the heat from the heat source to the heat sink stream[9]. By using an average face velocity of 4m/s, a 71% internal rate of return was achieved by Walmsley et al.(2015). Still, no suitable heat exchanger is found on the market for this thesis.

5.3 Compression-Absorption Heat Pump Cycle

As described in Section 3.4, the compression-absorption cycle is a sub-critical heat pump cycle utilizing a zeotropic working fluid, increasing the boiling point to allow condensation at higher temperatures. Therefore, it is suitable to produce the 200°C required for the spray-drying case in this thesis.

Jensen et al.(2015) [38] uses a compression-absorption heat pump cycle to increase the energy efficiency of a spray-drying facility. The spray-dryer requires an inlet air temperature of 200°C and releases excess air with a temperature of 80°C. The dry air has an ambient temperature of 20°C, a mass flow rate of 28kg/s and requires a heat load of 6.1MW. The case is very similar to the one in this thesis but has a 3.7 times larger heating capacity requirement, where the heat pump cycle only covers parts of the heating demand. By using an ammonia mass fraction of 0.82 and a circulation ratio of 0.43, the COP is found to be around 3. The study differs from this one by pre-heating the dry air to a temperature of 80°C, before the heat pump cycle is used to add between 10% and 30 % of the required heat load of 6.1MW before a gas burner finishes the heating.

Walmsley et al.(2017) [39] also uses a compression-absorption heat pump solution to improve the energy efficiency of a spray-dryer with an excess air temperature of 75°C and a mass flow rate of 1.25kg/s. The mixture consisted of 80 mol % of ammonia and 20 mol% water, and the cycle reached a COP of 3 with a desorber temperature of 25 °C and an absorber temperature of 80°C. The air is required to be 200°C at the spray-dryer inlet point. Hence, the cycle only heats the air to a temperature around 80°C, and cannot fully be defined as a high-temperature heat pump as the final temperature lift is achieved using a heater.

Zühlsdorf et al.(2017) [7] are also using a hybrid-heat pump cycle to increase the energy-

efficiency of a spray-dryer but differs from the two others by using propane, butane and propane zeotropic working fluid. The solution uses a similar compression-absorption heat pump cycle, has an excess air temperature of 70°C cooled down to 45°C, releasing a heat load of 1.55MW. It is used to heat the dry air from a temperature of 70°C to a temperature of 120°C. The COP varies between 2.4 and 3.1, where a 50/50 mixture of propane and isopentane gives the highest COP.

The results can be summarized that the compression-absorption cycles have been tried to be used to increase the energy-efficiency of spray-dryers and can give similar heating loads and COPs as the transcritical and supercritical cycles. However, the compression-absorption heat pump cycles are not heating the air from 15°C to 200°C but instead chooses a lower temperature lift with a higher mass flow rate. Future studies could be conducted on more variations of lower temperature lifts for the transcritical and supercritical cycles as well, to see if this would improve the cycles.

6 Conclusion

For the given spray-drying facility, the heat load is limited to 0.34MW due to the risk of fouling on the heat exchanger. A transcritical and supercritical heat pump cycle is designed to utilize this heat, to increase the temperature of dry air from a temperature of 15°C to a temperature of 200°C.

The transcritical heat pump cycle is showing the best potential to solve this problem by using an overheated iso-butane working fluid. The solution is limited by a constant evaporation temperature of 60°C and is calculated for the different suction gas temperature to reach 220°C. The highest COP is found if the suction gas is overheated with 15K, giving a COP of 3.16. The solution requires the lowest gas cooler pressure and has a heating capacity of 500kW. The corresponding gas cooler is optimized with a length of 1.8m, a width of 0.8m, hot and cold-side width of 2mm and 3mm respectively, a plate thickness of 0.5mm and 150 channel pairs. The solution can heat 30% of the air required in for the spray-drying process.

The supercritical CO_2 heat pump cycle has a more varying result. By using a gas cooler pressure of 7.5MPa, a heating capacity of 733MW is achieved at a COP of 1.87. The solution can heat 45% of the air required in the spray-drying process and decreases the pressure required in the gas cooler, increasing the likelihood of developing equipment that can handle the conditions. The gas heater pressure of 10MPa only produces a heating capacity of 566kW, but the COP is increased to 2.5. The solution can heat 35% of the air and requires a lower mass flow rate of working fluid. In regards to the heat transfer in the gas cooler and gas heater, the supercritical gas heater works more effectively at the low-pressure range, while the gas cooler favours being used in the higher-pressure region. Therefore, a solution in between the two is chosen as a compromise, using a gas heater pressure of 8.5MPa and a gas cooler pressure of 30MPa, which gives a heating capacity o 664kW and a COP of 2.05.

The compression-absorption heat pump cycles found in the literature are achieving a COP of 3 but differs from the heat pump cycles presented in this study by using the heat pump to heat more air, by either pre-heating the air or only heat the air to a lower temperature. The supercritical gas cooler would benefit more by pre-heating the air, as the gas cooler exit temperature is larger, giving a lower local effectiveness.

The heat pump cycles are thermodynamically able to produce the required temperatures of spray-drying. Regarding COP, the thermodynamic cycle is the best option found in this thesis, the supercritical cycle gives the highest heating capacity, and the compression-absorption cycle lays in between. The main challenge is to develop equipment that can

handle the conditions in an efficient way. When this is accomplished, the spray-drying process can become more energy efficient.

7 Further Work

The thesis presents the possibilities of a transcritical and supercritical heat pump cycle to achieve temperatures of 220°C. Future studies could study the possibility of utilizing different working fluids in the supercritical and transcritical cycle, comparing the possibilities to reach even higher COPs or higher heating capacities.

The heat transfer is very inefficient by heating the air from 15°C to 200°C using the high pressure working fluids of the high temperature heat pumps. Therefore, future work should study the possibility of changing the problem statement to allow a lower temperature lift. It the aim is to increase the energy efficiency of a spray-drying facility, this can be done using a low-temperature heat pump solution to heat the air to a temperature of around 60°C with the excess air. A high temperature heat pump could also be used, focusing on rather increasing the mass flow rate to be heated between a temperature of for example 120°C to 200°C. It should achieve better heat transfer in the gas cooler.

Further studies also include the development of high-temperature equipment for isobutane and CO_2 cycles, as high-temperature heat pumps cannot be produced before the equipment are developed to handle the conditions. Compressors were not studied much in this thesis, as there are no suitable compressors on the market that reaches temperatures higher than 120°C. Some gas coolers were found that could reach close to the required pressures in the transcritical cycle, but further developing is necessary for the cycle to be a reality.

The possibility of producing better scrubber systems for the spray-dryers should be studied. By decreasing the milk powder particles left in the excess air, fouling is decreased, and more heat can be extracted from the excess air.

References

[1] A. S. Mujumdar, *Handbook of Industrial Drying*. CRC Press, Taylor Francis Group, 2015.

[2] S. Moejes and A. Van Boxtel, "Energy saving potential of emerging technologies in milk powder production," *Trends in Food Science & Technology*, vol. 60, pp. 31–42, 2017.

[3] P. Schuck, "Spray drying of dairy products: state of the art," *Le Lait*, vol. 82, no. 4, pp. 375–382, 2002.

[4] F. Cheng, X. Zhou, and Y. Liu, "Methods for improvement of the thermal efficiency during spray drying," in *E3S Web of Conferences*, vol. 53, p. 01031, EDP Sciences, 2018.

[5] P. Schuck, R. Jeantet, B. Bhandari, X. D. Chen, Í. T. Perrone, A. F. de Carvalho, M. Fenelon, and P. Kelly, "Recent advances in spray drying relevant to the dairy industry: A comprehensive critical review," *Drying Technology*, vol. 34, no. 15, pp. 1773–1790, 2016.

[6] B. Golman and W. Julklang, "Analysis of heat recovery from a spray dryer by recirculation of exhaust air," *Energy Conversion and Management*, vol. 88, pp. 641–649, 2014.

[7] B. Zühlsdorf, F. Bühler, R. Mancini, S. Cignitti, and B. Elmegaard, "High temperature heat pump integration using zeotropic working fluids for spray drying facilities," in *12th IEA Heat Pump Conference*, 2017.

[8] D. Pineda Quijano, M. van der Pal, C. Infante Ferreira, R. de Boer, and J. Vollenbroek, "Heat recovery in milk powder drying by using a liquid sorption process," 2017.

[9] T. G. Walmsley, M. R. Walmsley, M. J. Atkins, J. R. Neale, and A. H. Tarighaleslami, "Thermo-economic optimisation of industrial milk spray dryer exhaust to inlet air heat recovery," *Energy*, vol. 90, pp. 95–104, 2015.

[10] T. G. Walmsley, M. R. Walmsley, M. J. Atkins, and J. R. Neale, "Fouling and pressure drop analysis of milk powder deposition on the front of parallel fins," *Advanced Powder Technology*, vol. 24, no. 4, pp. 780–785, 2013.

[11] G. F. Brooks, *The sticking and crystallisation of amorphous lactose: a thesis presented in partial fulfilment of the requirements for the degree of Master of Technology in Chemical Technology at Massey University*. PhD thesis, Massey University, 2000.

[12] T. G. Walmsley, M. R. Walmsley, M. J. Atkins, and J. R. Neale, "Analysis of skim milk powder deposition on stainless steel tubes in cross-flow," *Applied Thermal Engineering*, vol. 75, pp. 941–949, 2015.

[13] Z. Erbay, N. Koca, F. Kaymak-Ertekin, and M. Ucuncu, "Optimization of spray drying process in cheese powder production," *Food and Bioproducts Processing*, vol. 93, pp. 156–165, 2015.

[14] S. Wolf, J. Lambauer, M. Blesl, U. Fahl, and A. Voß, "Industrial heat pumps in germany: Potentials, technological development and market barriers," in *Proceedings of the ECEEE*, pp. 543–550, 2012.

[15] O. Bamigbetan, T. M. Eikevik, P. Nekså, and M. Bantle, "Review of vapour compression heat pumps for high temperature heating using natural working fluids," *International Journal of Refrigeration*, vol. 80, pp. 197–211, 2017.

[16] J. Stene, *Varmepumper - Industrielle anvendelser*. Trondheim: NTH - SINTEF Kuldeteknikk, 1993.

[17] P. Nekså, H. Rekstad, G. R. Zakeri, and P. A. Schiefloe, "Co2-heat pump water heater: characteristics, system design and experimental results," *International Journal of refrigeration*, vol. 21, no. 3, pp. 172–179, 1998.

[18] J. Sarkar, S. Bhattacharyya, and M. R. Gopal, "Optimization of a transcritical co2 heat pump cycle for simultaneous cooling and heating applications," *International Journal of Refrigeration*, vol. 27, no. 8, pp. 830–838, 2004.

[19] W.-w. Yang, X.-q. Cao, Y.-l. He, and F.-y. Yan, "Theoretical study of a high-temperature heat pump system composed of a co2 transcritical heat pump cycle and a r152a subcritical heat pump cycle," *Applied Thermal Engineering*, vol. 120, pp. 228–238, 2017.

[20] J. Sarkar, S. Bhattacharyya, and M. R. Gopal, "Natural refrigerant-based subcritical and transcritical cycles for high temperature heating," *International Journal of Refrigeration*, vol. 30, no. 1, pp. 3–10, 2007.

[21] A. Borgås, "Development of the hybrid absorption heat pump process at high temperature operation," Master's thesis, Institutt for energi-og prosessteknikk, 2014.

[22] M. Olafsen, "Optimization and process improvements of a high temperature heat pump using butane as working fluid," Master's thesis, NTNU, 2018.

[23] O. Bamigbetan, T. M. Eikevik, P. Nekså, M. Bantle, and C. Schlemminger, "Exper-

imental investigation of a prototype r-600 compressor for high temperature heat pump," *Energy*, 2018.

[24] J. Wang, C. Brown, and D. Cleland, "Heat pump heat recovery options for food industry dryers," *International Journal of Refrigeration*, vol. 86, pp. 48–55, 2018.

[25] V. Dostál, M. Driscoll, and P. Hejzlar, "A supercritical carbon dioxide cycle for next generation nuclear reactors. 2004," *Massachusetts Institute of Technology*.

[26] A. S. Sabau, H. Yin, A. Qualls, and J. McFarlane, "Investigations of supercritical co2 rankine cycles for geothermal power plants," tech. rep., Oak Ridge National Laboratory (ORNL), 2011.

[27] S. J. Bae, Y. Ahn, J. Lee, and J. I. Lee, "Various supercritical carbon dioxide cycle layouts study for molten carbonate fuel cell application," *Journal of Power Sources*, vol. 270, pp. 608–618, 2014.

[28] M. Bauer, R. Vijaykumar, M. Lausten, and J. Stekli, "Pathways to cost competitive concentrated solar power incorporating supercritical carbon dioxide power cycles," in *Proceedings of the 5th International Symposium–Supercritical CO2 Power Cycles, San Antonio, TX, USA*, pp. 28–31, 2016.

[29] D. Zhang, Y. Wang, and Y. Xie, "Investigation into off-design performance of a s-co2 turbine based on concentrated solar power," *Energies*, vol. 11, no. 11, p. 3014, 2018.

[30] T. Ommen, J. K. Jensen, W. B. Markussen, L. Reinholdt, and B. Elmegaard, "Technical and economic working domains of industrial heat pumps: Part 1–single stage vapour compression heat pumps," *International Journal of Refrigeration*, vol. 55, pp. 168–182, 2015.

[31] Z. Ma, H. Bao, and A. P. Roskilly, "Numerical study of a hybrid absorption-compression high temperature heat pump for industrial waste heat recovery," *Frontiers in Energy*, vol. 11, no. 4, pp. 503–509, 2017.

[32] J. K. Jensen, W. B. Markussen, L. Reinholdt, and B. Elmegaard, "On the development of high temperature ammonia–water hybrid absorption–compression heat pumps," *International Journal of Refrigeration*, vol. 58, pp. 79–89, 2015.

[33] U. K. W. A. C. L. ETSU, "Guide to compact heat exchangers," *Energy efficiency best practice programme*, 2000.

[34] Q. Li, G. Flamant, X. Yuan, P. Neveu, and L. Luo, "Compact heat exchangers: A review and future applications for a new generation of high temperature solar re-

ceivers," *Renewable and Sustainable Energy Reviews*, vol. 15, no. 9, pp. 4855–4875, 2011.

[35] S. G.Nellis, *Heat transfer*. Cambridge University Press, 2008.

[36] A. Laval, "The theory behind heat transfer, plate heat exchangers," 2004.

[37] M. J. Atkins, M. R. Walmsley, and J. R. Neale, "Integrating heat recovery from milk powder spray dryer exhausts in the dairy industry," *Applied Thermal Engineering*, vol. 31, no. 13, pp. 2101–2106, 2011.

[38] J. K. Jensen, W. B. Markussen, L. Reinholdt, and B. Elmegaard, "Exergoeconomic optimization of an ammonia–water hybrid absorption–compression heat pump for heat supply in a spray-drying facility," *International Journal of Energy and Environmental Engineering*, vol. 6, no. 2, pp. 195–211, 2015.

[39] T. G. Walmsley, J. J. Klemeš, M. R. Walmsley, M. J. Atkins, and P. S. Varbanov, "Innovative hybrid heat pump for dryer process integration," 2017.

Appendix

The EES codes are placed on the following page. For the supercritical cycle, only the one cycle was analysed. For the transcritical cycle, three different cycles were used, the first for Section 5.1.1, the second one for Section 5.1.2 and the third one for Section 5.1.3. The code is the same for the first and third configuration, only differing by the third code calculating the volumetric efficiencies. However, to keep better control over the different calculations with different variables, the codes were separated. For the Gas cooler and gas heater, the same code was used, based on a basic code found in the EES help book [35]. The configurations were a little different regarding gas cooler and gas heater, presented as the "if gas cooler" and "if gas heater" part of the calculations. When the gas cooler was calculated, the "if gas heater"-part was commented out, and the opposite when the gas heater was used.

```
$UnitSystem SI Mass Radian J K Pa
"-----------------------------
Supercritical heat pump cycle
Using carbon dioxide as the working fluid
-----------------------------"

eta_c=0.7[-] "Constant isentropic compressor efficiency"
eta_ex=0.6 [-] "Constant isentropic expander efficiency"
T_sg=356.15[K] "Suction gas temperature"
P_low=7.5e6[Pa] "Gas heater pressure"
P_high=2.6e7[Pa] "Gas cooler pressure"
R$='R744' "The working fluid used, CO2"
m_dot_R=5.1[kg/s] "Mass flow rate of CO2"
Q_ev=340044[W] "Heat load from the excess air, to be utilized in the evaporator"

"State 1- Gas heater outlet, compressor inlet. "
T[1]=T_sg "Defining the suction gas temperature"
P[1]=P_low "Defining the suction gas pressure"
s[1]=entropy(R$,T=T[1],P=P[1]) "Entropy at the compressor inlet"
h[1]=enthalpy(R$,T=T[1],P=P[1]) "Enthalpy at the compressor inlet"
v[1]=volume(R$,T=T[1],P=P[1]) "Specific volume at the compressor inlet"

"State 4 – Turbine expander outlet - Gas heater inlet. The gas heater is assumed isobaric and utilizes the heat load from the excess air"
P[4]=P_low    "Gas heater pressure"
Q_ev=m_dot_R*(h[1]-h[4]) "Energy balance, used to find the gas heater inlet enthalpy"
T[4]=temperature(R$,P=P[4],h=h[4]) "Temperature at gas heater inlet"
s[4]=entropy(R$,P=P[4],h=h[4]) "Entropy at the gas heater inlet"

"State 2 - compressor exit- gas cooler inlet"
P[2]=P_high  "Discharge pressure"
s_s[2]=s[1]    "The entropy of a loss free cycle "
h_s[2]=enthalpy(R$,P=P[2],s=s_s[2]) "Enthalpy of a loss free cycle"
W_dot_s_c\m_dot_R=h_s[2]-h[1] "Ideal compression work"
W_dot_c\m_dot_R=W_dot_s_c\m_dot_R/eta_c "Real compression work"
h[2]=W_dot_c\m_dot_R+h[1] "Compressor discharge enthalpy"
s[2]=entropy(R$,h=h[1],P=P[1]) "Compressor discharge entropy"
T[2]=temperature(R$,P=P[2],h=h[2]) "Compressor discharge temperature"

"State 3- Gas cooler exit - inlet turbine expander"
P[3]=P_high "Gas cooler pressure"
s_s[3]=s[4] "Entropy in loss free cycle"
h_s[3]=enthalpy(R$,P=P[3],s=s_s[3]) "Enthalpy if the process was loss free"
eta_ex=delta/(h[4]-h_s[3]) "Ideal expansion without losses"
h[3]=h[4]-delta   "Enthalpy when the turbine expander efficiency is considered"
s[3]=entropy(R$,P=P[3],h=h[3]) "Real entropy at the gas cooler exit"
T[3]=temperature(R$,P=P[3],h=h[3]) "Gas cooler exit temperature"

{
"state 3 – Gas cooler exit- inlet turbine expander - if loss free"
s[3]=s[4] "Entropy at gas cooler exit"
P[3]=P_high "Gas cooler pressure"
h[3]=enthalpy(R$,P=P[3],s=s[3]) "Enthaply at gas cooler exit"
T[3]=temperature(R$,P=P[3],s=s[3])} "Temperature at gas cooler exit"

"state 5 state1 – Used to close the cycle for the P-h diagram"
h[5]=h[1] "Enthalpy for closed cycle"
P[5]=P[1] "Pressure for closed cycle"
s[5]=s[1] "Entropy for closed cycle"
T[5]=T[1] "Temperature for closed cycle"

"Thermodyniamic relations"
W_dot_c=m_dot_R*(h[2]-h[1]) "Compressor Work"
W_dot_ex=m_dot_R*(h[3]-h[4]) "Expansion Work"
Q_cond=m_dot_R*(h[2]-h[3]) "Heating capacity of the gas cooler"
COP=(Q_cond)/(W_dot_c-W_dot_ex) "COP of the cycle"
```

```
$UnitSystem SI MASS RAD PA K J
$Tabstops 0.2 0.4 0.6 3.5 in
{"----------------------------
Simple Transciritcal heat pump cycle
 With no IHX or overheated working fluid.
----------------------------"
eta_c=0.7[-] "Constant isentropic compressor efficiency"
T_two=493.15[K] "Compressor discharge temperature "
P_low=8.7e5[Pa] "Evaporation pressure"
P_high=10e6[Pa] "Gas cooler pressure"
R$='R600a' "Iso-butane as the working fluid"
m_dot_R=1.074[kg/s] "Mass flow rate of the iso-butane"
Q_ev=340044[W] "Heat load from the excess air, to be utilized in the evaporator"


"state 4 -  Expansion valve exit - Evaporator inlet point"
x[4]=0.0001[-] "Liquid content at the evaporator inlet "
P[4]=P_low "Constant pressure in the evaporator "
T[4]=temperature(R$,P=P[4],x=x[4]) "Temperature at the inlet of the evaporator "
s[4]=entropy(R$,P=P[4],x=x[4]) " Entropy at the evaporator inlet"
h[4]=enthalpy(R$,P=P[4],x=x[4]) " Enthalpy at the evaporator inlet "

"State1 - Evaporator outlet point, compressor inlet"
x[1]=1[-] "Liquid fraction at the compressor inlet point"
P[1]=P_low " Compressor suction pressure "
T[1]=temperature(R$,P=P[1],x=x[1]) " Suction gas temperature compressor"
s[1]=entropy(R$,P=P[1],x=x[1]) " Entropy at the compressor inlet "
h[1]=enthalpy(R$,P=P[1],x=x[1]) " Enthalpy at the compressor inlet "

"State 2 - compressor exit- Gas cooler inlet"
P[2]=P_high " Compressor discharger pressure "
s_s[2]=s[1] "The entropy of a loss free cycle "
h_s[2]=enthalpy(R$,P=P[2],s=s_s[2]) "Enthalpy of a loss free cycle"
W_dot_s_c\m_dot_R=h_s[2]-h[1] "Ideal compression work"
W_dot_c\m_dot_R=W_dot_s_c\m_dot_R/eta_c "Real compression work"
h[2]=W_dot_c\m_dot_R+h[1] "Compressor discharge enthalpy"
s[2]=entropy(R$,h=h[1],P=P[1]) "Compressor discharge entropy"
T[2]=temperature(R$,P=P[2],h=h[2]) "Compressor discharge temperature"

"State3 -Gas cooler exit, expansion valve inlet "
h[3]=h[4] "Constant enthalpy through the expansion"
P[3]=P_high "Gas cooler pressure"
T[3]=temperature(R$,P=P[3],h=h[3]) "Gas cooler exit temperature "
s[3]=entropy(R$,P=P[3],h=h[3]) "Gas cooler exit enthalpy "

"state5-closing the cycle"
P[5]=P[1] " Pressure to close the cycle"
h[5]=h[1] " Enthalpy to close the cycle"
T[5]=T[1] " Temperature to close the cycle"
s[5]=s[1] "Entropy to close the cycle "


"Thermodyniamic relations"
W_dot_c=m_dot_R*(h[2]-h[1]) "Compressor Work"
Q=m_dot_R*(h[2]-h[3]) "Heating capacity of the gas cooler"
COP=(Q)/(W_dot_c) "COP of the cycle"}

"----------------------------
Transciritcal cycle with an internal heat exchanger
----------------------------"

eta_c=0.7[-] "compressor efficiency"
T_two=493.15[K] "Compressor discharge temperature"
P_low=8.7e5[Pa] "Evaporation pressure"
P_high=16e6[Pa] " Gas cooler pressure"
m_dot_R=1.2[kg/s] "Mass flow rate of R600a"
R$='R600a' "R600a as the working fluid"
Q_ev=340044[W] " Heat load utilized in the evaporator"
```

```
eta_ihx=0.95 " Internal heat exchanger efficiency"
eta_v=0.8 "Volumetric efficiency"
delta_T=3[K] "The increase in temperature using an IHX. The value changes for the different simulations"


 "state 5 Evaporator inlet point, expansion valve outlet "
x[5]=0.0001[-] "Liquid fraction at the evaporator inlet point"
P[5]=P_low "Evaporator pressure "
T[5]=temperature(R$,P=P[5],x=x[5]) "Temperature of evaporation "
s[5]=entropy(R$,P=P[5],x=x[5]) "Entropy at the evaporator inlet point "
h[5]=enthalpy(R$,P=P[5],x=x[5]) " Enthalpy at the evaporator inlet point"


"State6 - Evaporator outlet"
x[6]=1[-] " Liquid fraction at the evaporator exit point"
P[6]=P_low" Pressure in evaporator"
T[6]=temperature(R$,P=P[6],x=x[6]) "Tempearture at the evaporator outlet point "
s[6]=entropy(R$,P=P[6],x=x[6]) " Entropy at the evaporator outlet point"
h[6]=enthalpy(R$,P=P[6],x=x[6]) " Enthalpy at the evaporator outlet point"

"State 1- Compressor inlet"
T[1]=T[6]+delta_T "Suction gas temperature"
P[1]=P_low " Compression suction pressure "
s[1]=entropy(R$,T=T[1],P=P[1]) "Entropy at the compressor nlet"
h[1]=enthalpy(R$,T=T[1],P=P[1]) "Enthalpy at the compressor inlet"
 rho_s=density(R$,P=P[1],T=T[1]) "Density at the compression inlet"

"State 2 - compressor exit"
P[2]=P_high  "Discharge pressure"
s_s[2]=s[1]    "The entropy of a loss free cycle "
h_s[2]=enthalpy(R$,P=P[2],s=s_s[2]) "Enthalpy of a loss free cycle"
W_dot_s_c\m_dot_R=h_s[2]-h[1] "Ideal compression work"
W_dot_c\m_dot_R=W_dot_s_c\m_dot_R/eta_c "Real compression work"
h[2]=W_dot_c\m_dot_R+h[1] "Compressor discharge enthalpy"
s[2]=entropy(R$,h=h[1],P=P[1]) "Compressor discharge entropy"
T[2]=temperature(R$,P=P[2],h=h[2]) "Compressor discharge temperature"

"State4- IHX exit, expansion valve inlet"
h[4]=h[5] "Constant enthalpy through the expansion valve"
P[4]=P_high "Pessure in the IHX"
T[4]=temperature(R$,P=P[4],h=h[4]) "Tempearture at the IHX exit"
s[4]=entropy(R$,P=P[4],h=h[4])  " Entropy at the IHX exit"

"State 3- gas cooler exit, IHX inlet"
eta_ihx=(h[1]-h[6])/(h[3]-h[4]) "Enthalpy balance in the internal heat exchanger"
P[3]=P_high "Gas cooler pressure"
T[3]=temperature(R$,h=h[3],P=P[3]) "Temperature at the gas cooler exit"
s[3]=entropy(R$,h=h[3],P=P[3]) "Entropy at the gas cooler exit"

"state7-closing the cycle"
P[7]=P[1] " Pressure to close the cycle"
h[7]=h[1] " Enthalpy to close the cycle"
T[7]=T[1] " Temperature to close the cycle"
s[7]=s[1] "Entropy to close the cycle "


"Thermodynamic relations"
W_dot_c=m_dot_R*(h[2]-h[1])
Q=m_dot_R*(h[2]-h[3]) "Heating capacity from the gas heater"
COP=(Q)/(W_dot_c) "COP of the cycle"

V_s=m_dot_R/(rho_s*eta_v)*3600 "Swept volume at compresor inlet"

"----------------------------
Transciritcal cycle with overheat

----------------------------"
{eta_c=0.7[-] "compressor efficiency"
```

```
T_two=493.15[K] "Compressor discharge temperature"
P_low=8.7e5[Pa] "Evaporation pressure"
P_high=16e6[Pa] " Gas cooler pressure"
m_dot_R=1.169[kg/s] "Mass flow rate of R600a- changes with the changing deltaT"
R$='R600a' "R600a as the working fluid"
Q_ev=340044[W] " Heat load utilized in the evaporator"
eta_v=0.8 "Volumetric efficiency"

 "state 4 exit expansion valve- inlet evaporator"
x[4]=0.0001[-]"liquid content at the evaporation inlet"
P[4]=P_low "evaporation pressure"
T[4]=temperature(R$,P=P[4],x=x[4]) "Tempearure at the evaporation inlet point"
s[4]=entropy(R$,P=P[4],x=x[4]) "Entropy at the evaporator inlet point"
h[4]=enthalpy(R$,P=P[4],x=x[4]) "Enthalpy at the evaporator inlet point"

"State1 outlet evaporaor- compressor inlet "
Q_ev=m_dot_R*(h[1]-h[4]) "Heat load utilized in the evaporaor"
P[1]=P_low "Evaporation pressure"
T[1]=temperature(R$,P=P[1],h=h[1]) "Suction gas temperature"
s[1]=entropy(R$,P=P[1],h=h[1]) "Entropy at the compressor inlet"
rho_s=density(R$,P=P[1],h=h[1])  "Density at the compressor inlet"

"State 2 - compressor exit"
P[2]=P_high  "Discharge pressure"
s_s[2]=s[1]  "The entropy of a loss free cycle "
h_s[2]=enthalpy(R$,P=P[2],s=s_s[2]) "Enthalpy of a loss free cycle"
W_dot_s_c\m_dot_R=h_s[2]-h[1] "Ideal compression work"
W_dot_c\m_dot_R=W_dot_s_c\m_dot_R/eta_c "Real compression work"
h[2]=W_dot_c\m_dot_R+h[1] "Compressor discharge enthalpy"
s[2]=entropy(R$,h=h[1],P=P[1]) "Compressor discharge entropy"
T[2]=temperature(R$,P=P[2],h=h[2]) "Compressor discharge temperature"

"State3-gas cooler exit, expansion valve inlet "
h[3]=h[4] "Enthalpy at the gas cooler exit"
P[3]=P_high "Gas cooler pressure"
T[3]=temperature(R$,P=P[3],h=h[3]) "Temperatuire at the gas cooler exit"
s[3]=entropy(R$,P=P[3],h=h[3]) "Entropy at the gas cooler exit"

"state5-closing the cycle"
P[5]=P[1] " Pressure to close the cycle"
h[5]=h[1] " Enthalpy to close the cycle"
T[5]=T[1] " Temperature to close the cycle"
s[5]=s[1] "Entropy to close the cycle "


"Thermodynamic relations"
W_dot_c=m_dot_R*(h[2]-h[1]) "Compression work"
Q=m_dot_R*(h[2]-h[3]) "Heating capacity of the gas cooler"
COP=(Q)/(W_dot_c) "COP of the cycle"
V_s=m_dot_R/(rho_s*eta_v)*3600 "Swept volume" }
```

```
$UnitSystem SI MASS RAD PA K J
$Tabstops 0.2 0.4 0.6 3.5 in
"----------------------------------------
Gas cooler/Gas Heater
The gas heater and gas cooler is based on the same heat exchanger equations, but the hot-side and cold side will be different for the two.
----------------------------"


"----------------------------------------
IF GAS COOLER

Supercritical gas cooler / Transcritical gas cooler
hot- Carbon Dioxide, R744 / Iso-Butane, R600a
cold – Air
The difference between the gas cooler used in the transcritical and supercritical cycle is the optimum geometry, pressure rates and working fluid. The maths is the same, causing the same code to be used for both.
----------------------------"
"Inputs"
W=0.6[m] "Gas cooler width"
L=2.25[m] "Guessed length of gas cooler"
N_ch=130 [-] "Number of channel pairs"
th_H=2[mm]*convert(mm,m) "Width of hot-side channel"
th_C=3[mm]*convert(mm,m) "Width of cold-side channel "
th_m=0.6[mm]*convert(mm,m) "Plate thickness "
p_H=37e6[Pa] "CO2/Iso-Butane pressure"
p_C=1[atm]*convert(atm,Pa) "Air pressure"
m_dot_H=2.7[kg/s] "CO2/Iso-Butane mass flow rate"
m_dot_C=3.02[kg/s] "Air mass flow rate"
H$='R744' "CO2=R744 /Iso-Butane=R600a as the working fluid, "
C$='Air_ha' "Air as the cold-side fluid"
T_H_in=493.15 [K] "Inlet temperature of CO2/Iso-Butane "
T_C_in=288.15[K] "Inlet temperature of air"
T_C_out=473.15 [K] "Outlet temperature of air "

i_C_in=enthalpy(C$,T=T_C_in,P=p_C) "enthalpy of cold inlet fluid"
i_C_out=enthalpy(C$,T=T_C_out,P=p_C) "enthalpy of hot outlet fluid"
q_dot=m_dot_C*(i_C_out-i_C_in) "total heat transfer rate"

i_H_in=enthalpy(H$,T=T_H_in,P=p_H) "enthalpy of cold inlet fluid"
i_H_out=i_H_in-q_dot/m_dot_H "enthalpy of cold outlet fluid"
T_H_out=temperature(H$,h=i_H_out,P=p_H) "temperature of cold outlet fluid"

N=15 [-] "number of sub-heat exchangers"
Duplicate i=1,N
q_dot[i]=i*q_dot/N "total heat transfer rate"
End

"Obtain temperature distribution"
T_H[1]=T_H_in "hot-side inlet temperature"
T_C[1]=T_C_out "cold-side outlet temperature"
i_H[1]=i_H_in "hot_side inlet enthalpy"
i_C[1]=i_C_out "cold-side outlet enthalpy"

"----------------------------------------------
END IF GAS COOLER
----------------------------------------------"

"----------------------------------------------
IF GAS HEATER
----------------------------------------------"

"----------------------------------------------
SUPERCRITICAL GAS HEATER
Hot – air
Cold - refrigerant
----------------------------------------------"
```

```
 "Inputs"
"Inputs"
W=0.6[m] "Gas heater width"
L=2.25[m] "Guessed length of gas heater"
N_ch=130 [-] "Number of channel pairs"
th_H=2[mm]*convert(mm,m) "Width of hot-side channel"
th_C=3[mm]*convert(mm,m) "Width of cold-side channel "
th_m=0.6[mm]*convert(mm,m) "Plate thickness "
p_H=1[atm]*convert(atm,Pa) "Air pressure"
p_C=2e6[Pa] "CO2 pressure"
m_dot_H=2.7[kg/s] "Air mass flow rate"
m_dot_C=3.02[kg/s] "CO2 mass flow rate"
H$='R744' "Air as the working fluid, "
C$='Air_ha' "CO2  cold-side fluid"
T_H_in=493.15 [K] "Inlet temperature of Air "
T_C_in=288.15[K] "Inlet temperature of CO2"
T_C_out=473.15 [K] "Outlet temperature of CO2 "


i_H_in=enthalpy(H$,T=T_H_in,P=p_H) "enthalpy of hot inlet fluid"
i_H_out=enthalpy(H$,T=T_H_out,P=p_H) "enthalpy of hot outlet fluid"
q_dot=m_dot_H*(i_H_in-i_H_out) "total heat transfer rate"

i_C_out=enthalpy(C$,T=T_C_out,P=p_C) "enthalpy of cold inlet fluid"
i_C_in=q_dot/m_dot_C-i_C_in"enthalpy of cold outlet fluid"
T_C_in=temperature(C$,h=i_C_in,P=p_C) "temperature of cold outlet fluid"

N=15 [-] "number of sub-heat exchangers"
Duplicate i=1,N
q_dot[i]=i*q_dot/N "total heat transfer rate"
End

"Obtain temperature distribution"
T_H[1]=T_H_in "hot-side inlet temperature"
T_C[1]=T_C_out "cold-side outlet temperature"
i_H[1]=i_H_in "hot_side inlet enthalpy"
i_C[1]=i_C_out "cold-side outlet enthalpy"

"-----------------------------------------------
END IF GAS HEATER
-----------------------------------------------"

"-----------------------------------------------
HEAT EXCHAGER CALCULATIONS USED FOR BOTH SIMULATIONS
-----------------------------------------------"

N=15 [-] "number of sub-heat exchangers"
Duplicate i=1,N
q_dot[i]=i*q_dot/N "total heat transfer rate"
End

"Obtain temperature distribution"
T_H[1]=T_H_in "hot-side inlet temperature"
T_C[1]=T_C_out "cold-side outlet temperature"
i_H[1]=i_H_in "hot_side inlet enthalpy"
i_C[1]=i_C_out "cold-side outlet enthalpy"

Duplicate i=2,(N+1)
i_H[i]=i_H[i-1]-q_dot/(N*m_dot_H) "energy balance on hot-side of each sub-heat exchanger"
T_H[i]=temperature(H$,h=i_H[i],P=p_H) "temperature leaving hot-side of each sub-heat exchanger"
End

Duplicate i=2,(N+1)
i_C[i]=i_C[i-1]-q_dot/(N*m_dot_C) "energy balance on cold-side of each sub-heat exchanger"
T_C[i]=temperature(C$,h=i_C[i],P=p_C) "temperature leaving cold-side of each sub-heat exchanger"
End
```

```
"Apply effectiveness-NTU solution"
Duplicate i=1,N
C_dot_H[i]=m_dot_H*(i_H[i]-i_H[i+1])/(T_H[i]-T_H[i+1]) "hot-side capacitance rate"
C_dot_C[i]=m_dot_C*(i_C[i]-i_C[i+1])/(T_C[i]-T_C[i+1]) "cold-side capacitance rate"
End


Duplicate i=1,N
eff[i]=q_dot/(N*min(C_dot_H[i],C_dot_C[i])*(T_H[i]-T_C[i+1])) "effectiveness of sub-heat exchanger"
NTU[i]=hx('counterflow', eff[i], C_dot_H[i], C_dot_C[i], 'NTU') "NTU required by sub-heat exchanger"
UA[i]=NTU[i]*min(C_dot_H[i],C_dot_C[i]) "conductance in sub-heat exchanger"
End

"determine length of each sub-heat exchanger"
x[1]=0 [m] "starting position of 1st sub-heat exchanger"
Duplicate i=1,N
Call ductflow_local(H$,(T_H[i]+T_C[i])/2,p_H,m_dot_H/N_ch,th_H,W,x[i]+0.001 [m],0[-]:h_H[i], h_H_H[i], dPHdx[i]) "hot-
side local heat transfer coefficient"
Call ductflow_local(C$,(T_H[i]+T_C[i])/2,p_C,m_dot_C/N_ch,th_C,W,x[N+1]-x[i]+0.001[m],0[-]:h_C[i], h_C_H[i], dPCdx[i]) "
cold-side local heat transfer coefficient"
k_m[i]=k_('Aluminum', (T_H[i]+T_C[i])/2) "metal conductivity at local average temperature"
DELTAx[i]=UA[i]*(1/h_H[i]+th_m/k_m[i]+1/h_C[i])/(2*N_ch*W) "length of sub-heat exchanger"
x[i+1]=x[i]+DELTAx[i]
End


Duplicate i=1,(N-1)
delta_T_C[i]=T_C[i+1]-T_C[i]
delta_T_H[i]=T_H[i+1]-T_H[i]
End

Duplicate i=2,N
A_x[i]=2*W*x[i]
U[i]=UA[i]/A_x[i]
End


err=abs(x[N+1]-L)/L "objective function"
```

Liv Irene Korstad

Energy-efficient High Temperature Heat Pump Systems for a Spray-Dryer

NTNU
Norwegian University of
Science and Technology